PBAD-223936

Publication No. R80-25 Order No. 677

MIT

Seismic Behavior and Design of Buildings

Report No. 4

THE EFFECT OF CONNECTION FLEXIBILITY ON THE SEISMIC RESPONSE OF WELDED OPEN STEEL FRAMES

by

ROGER W. GRAVES

Supervised by

JOHN M. BIGGS

and

H. MAX IRVINE

DEPARTMENT OF CIVIL ENGINEERING

SCHOOL OF ENGINEERING
MASSACHUSETTS INSTITUTE OF TECHNOLOGY
Cambridge, Massachusetts 02139

June 1980

Sponsored by the
National Science Foundation
Division of Problem-Focused Research
Grant ENV-7714174

Additional Copies May Be Obtained from

National Technical Information Service
U.S. Department of Commerce
5285 Port Royal Road
Springfield, Virginia 22161

50272-101

REPORT DOCUMENTATION PAGE	1. REPORT NO. NSF/RA-800122	2.	3. Recipient's Accession No. PB80 223936

4. Title and Subtitle
The Effect of Connection Flexibility on the Seismic Response of Welded Open Steel Frames, Report No. 4

5. Report Date June 1980

6.

7. Author(s)
R. W. Graves

8. Performing Organization Rept. No. R80-25

9. Performing Organization Name and Address
Massachusetts Institute of Technology
School of Engineering
Department of Civil Engineering
Cambridge, MA 02139

10. Project/Task/Work Unit No. Order No. 677

11. Contract(C) or Grant(G) No.
(C)
(G) ENV7714174

12. Sponsoring Organization Name and Address
Engineering and Applied Science (EAS)
National Science Foundation
1800 G Street, N.W.
Washington, D.C. 20550

13. Type of Report & Period Covered

14.

15. Supplementary Notes

16. Abstract (Limit: 200 words)
An analytical investigation of the effect of panel zone flexibility on the seismic response of typical welded open steel frames is described. The study covered three broad areas: (1) analytical development of the panel zone shear mechanism and its incorporation into the stiffness matrix of a general movement-resisting steel frame; (2) investigation of the effect this incorporation has on both the elastic and inelastic seismic response of the structure; and (3) consideration of the implications these results have on the future analysis and design of open steel frames. Incorporation of connection behavior into the stiffness matrix requires that four degrees of freedom (DOFs) be provided at each nodal point, and that these DOFs be transformed geometrically to properly model the connection size. Model analysis results illustrate that connection flexibility significantly affects a structure's vibrational properties, and that under certain circumstances common analysis procedures lead to an inaccurate prediction of vibration frequencies. Inelastic response analysis results indicate that connection behavior directly affects the frame's energy-dissipating mechanism, and that less beam/column damage occurs when more flexible connections are employed.

17. Document Analysis a. Descriptors
Dynamic structural analysis
Frames
Shear properties
Deformation
Earthquake resistant structures
Mathematical models
Steel structures

b. Identifiers/Open-Ended Terms
Seismic response

Earthquake Hazards Mitigation

c. COSATI Field/Group

18. Availability Statement	19. Security Class (This Report)	21. No. of Pages
NTIS	20. Security Class (This Page)	22. Price

(See ANSI-Z39.18) See Instructions on Reverse OPTIONAL FORM 272 (4-77) (Formerly NTIS-35) Department of Commerce

I

Massachusetts Institute of Technology
Department of Civil Engineering
Constructed Facilities Division
Cambridge, Massachusetts 02139

Seismic Behavior and Design of Buildings

Report No. 4

THE EFFECT OF CONNECTION FLEXIBILITY ON THE SEISMIC RESPONSE OF WELDED OPEN STEEL FRAMES

by

ROGER W. GRAVES

supervised by

John M. Biggs
and
H. Max Irvine

June 1980

Sponsored by the

National Science Foundation
Division of Problem-Focused Research
Grant ENV-7714174

Publication No. R80-25 Order No. 677

ABSTRACT

The following report describes an analytical investigation into the effect panel zone flexibility has on the seismic response of typical welded open steel frames. General methods for incorporating the connection behavior, assumed to be a tri-linear shear mechanism, into a structure's stiffness matrix are developed. This incorporation requires that four degrees of freedom be provided at each nodal point, and that these DOF's be geometrically transformed so that connection size is properly modeled.

Modal analysis results illustrate that connection flexibility significantly affects a structure's vibrational properties, and that under certain circumstances common analysis procedures lead to an inaccurate prediction of the frequencies of vibration.

Inelastic analysis results indicate that connection behavior directly affects the frame's energy-dissipating mechanism, and that less beam/column damage will occur when more flexible connections are employed.

PREFACE

This is the fourth report prepared under the research project entitled "Seismic Behavior and Design of Buildings," supported by the National Science Foundation under Grant ENV-7714174. It is also the thesis submitted by Roger Graves in partial fulfillment of the requirements for the degree of Master of Science in the Department of Civil Engineering at M.I.T.

The general purposes of the project are:

To perform a more comprehensive evaluation of various definitions of ductility used at present in dynamic analysis programs, assessing their physical meaning and their relation to expected structural damage; and

to evaluate different design procedures in terms of the behavior of the resulting frames and the expected level of damage during earthquake motions.

The first three reports of the project were:

No. 1 Biggs, John M., Lau, Wai K., and Persinko, Drew, "Seismic Design Procedures for Reinforced Concrete Frames," M.I.T. Department of Civil Engineering, Publication No. R79-21, July 1979.

No. 2 Irvine, H. M., and Kountouris, G.E., "Inelastic Seismic Response of a Torsionally Unbalanced Single-Story Building Model," M.I.T. Department of Civil Engineering, Publication No. R79-31, July 1979.

No. 3 Banon, Hooshang, "Prediction of Seismic Damage in Reinforced Concrete Frames," M.I.T. Department of Civil Engineering, Publication No. R80-16, May 1980.

The project was initiated by Professor José M. Roesset and is supervised by Professors John M. Biggs and H. Max Irvine. Dr. John B. Scalzi is the cognizant NSF Program Officer.

TABLE OF CONTENTS

LIST OF FIGURES

LIST OF TABLES

CHAPTER 1 - INTRODUCTION

1.1 General Background

Dynamic analysis of moment-resisting steel frames is generally performed without consideration of connection flexibility. This assumption naturally simplifies the constitutive relations involved, and permits well-known matrix formulations to be used directly in the analysis. It is conceded, however, that connections do not behave in a rigid fashion with unlimited strength. The assumption of infinitely strong rigid connections is a particularly poor one for frames subjected to lateral earthquake forces, as antisymmetrical bending of the frame has a tendency to exploit both connection flexibility and strength. Specifically, a welded connection can be expected to develop significant internal elastic shear deformation that will influence the overall response of the frame to small ground accelerations. Larger ground motions can force an underdesigned connection into premature yielding and prevent surrounding beam and column elements from participating in the energy-dissipating mechanism.

The purpose of this study is to develop the stiffness equations of a general welded steel frame with shear deformation in the connections, and to determine the connection's influence on the overall elastic and inelastic seismic response of the frame by investigating several design examples.

1.2 Previous Investigations

Shear deformation in a beam-to-column connection, often called panel zone (PZ) distortion, has been well documented in pseudo-static cyclic tests of beam-column subassemblages (5,6,16,19,28,29,30,31,33). These studies demonstrate that typical beam-column panel zones are capable of developing extremely stable hysteretic load-deformation curves with ductilities sometimes in excess of 100. Kato and Nakao (16) have suggested an empirically derived tri-linear model of the PZ hysteretic behavior based upon tests of Japanese H-shapes. Krawinkler, et al. (18,19) have also modeled the PZ behavior as trilinear, but have considered the elastic framing action of the column flanges in determining the second slope, and have allowed a strain-hardening term to replace the zero slope in the Kato model. The Krawinkler model was justified experimentally with a variety of wide flange shapes. In addition, Pinkney (25) has compared Krawinkler's formulation with an elaborate finite element representation of the joint, and found reasonable agreement between the two.

Several research investigations (12,20,21,22,41,44) have demonstrated that connection behavior can significantly alter the stiffness and strength characteristics of open steel frames. Lionberger and Weaver (20, 21) considered the flexibility of bolted connections in the formulation of the structure's stiffness matrix, but ignored PZ deformation. Fielding and Chen (12) modified the general slope-deflection equations to include both PZ shear deformation and finite connection size in the formulation. They concluded that the elastic lateral stiffness of a three-bay frame with rigid panel zones can be up to 78 percent greater than that of the frame with unstiffened PZ's. Doubling the panel zone thickness was found to double the lateral strength of the frame, although this was a result of the author's assumption that the panel zones were the only elements in the frame of limited strength. Naka, et al. (22,41), developed a similar formulation, but employed the Airy stress function in determining the stress-strain relationship of the panel zone. These results were found to agree well with the Fielding formulation, particularly in the elastic range.

Vasquez, Popov, and Bertero (44) have illustrated how a structure's stiffness matrix can be modified to account for panel zone flexibility. This presentation, however, failed to develop the general matrix transformations that are required to include the effect of finite connection size. Using a bi-linear stress-strain relationship for the panel zone, they subjected a ten-story four-bay frame to a base excitation of 1.5 times the NS component of the 1940 El Centro earthquake. The maximum story sway of the frame with rigid joints was found to vary from 1.79 to 0.674 times the sway resulting from the use of unreinforced PZ's.

The dynamic analysis computer program DRAIN-2D (15), developed by Kanaan and Powell, is capable of modeling PZ deformation by connecting intersecting beams and columns through a bi-linear rotational spring. The rotational spring is the physical analog of the matrix formulation presented in ref. 44, and hence is not capable of modeling the physical side of the connection. Some attempts (40) have been made to model connection size by adding rigid links to the rotational springs and thus improve the analysis, but this procedure is not entirely satisfactory, as it implies a deformed shape of the connection which is not physically possible. Full-scale tests (9,40) have been analytically modeled with reasonable accuracy using this technique, however.

1.3 Scope and Organization

The scope of this report may be divided into three general categories:

1) Analytical development of the panel zone shear mechanism, and its incorporation into the stiffness matrix of a general moment-resisting steel frame.

2) An investigation of the effect this incorporation has on both the elastic and inelastic seismic response of the structure.

3) A discussion of the implications these results have on the future analysis and design of open steel frames.

Chapter two is devoted to the analytical development of the connection model, such that, in contrast to earlier works, both connection size and PZ shear deformation are included in a more rational way in the formulation. Chapter three describes the frames on which this model was employed, and discusses their design rationale. Included are four- and ten-story three-bay frames with various connection properties. The lateral stiffness matrix of these frames is formed directly using the model developed in chapter two, allowing modal analysis results to be compared in chapter four. Although the connection model is fully applicable in the inelastic range of the structure, it was not considered feasible at present to incorporate the formulation directly in an inelastic dynamic analysis program. A single four-node finite element placed at each connection and constrained to have only shear deformation provides an equivalent model, however. This is an excellent alternative to the complex and costly substructuring required by the Pinkney (25) formulation. The four-story frame was analyzed using this technique, and the results are elucidated in chapter five, showing that beam and column damage is highly sensitive to connection properties. Chapter six summarizes the report's findings, discusses the implications of ignoring connection deformation in a dynamic analysis, and provides suggestions for future research.

CHAPTER TWO - ANALYTICAL DEVELOPMENT

2.1 Connection Deformation

2.1.1 Connection Behavior

The true load-deformation relationship of a welded beam-to-column connection cannot be determined in closed form due to the complexity of the continuum. However, numerous experimental studies (5,6,16,19,28,29, 30,31,33) have demonstrated that shear distortion of the column web (Fig. 2.1) is the predominate form of deformation, implying that a simple shear model can accurately represent the connection behavior. Connections subjected to antisymmetric moments generate shear forces in the panel zone which are largely responsible for this shear distortion (Fig. 2.2). Since lateral earthquake or wind loads produce antisymmetric bending of the frame elements, this type of loading can greatly accentuate PZ distortion.

2.1.2 Tri-linear Connection Model

Krawinkler, et al. (18,19) developed an empirically verified tri-linear model of the full-range hysteretic PZ behavior. This model is considered the most realistic developed to date of the true curvilinear relationship, and hence is adopted for use in this study. A chief advantage of this formulation is the ease with which it may be incorporated into a piece-wise linear inelastic dynamic analysis program. As with most connection models, the Krawinkler formulation is facilitated by assuming the beam/column flanges transmit all the moment to the connection, while their webs transmit the shear.

Ignoring the influence of axial load in the beams, the shear force at the top of the panel zone (Fig. 2.2) is given by:

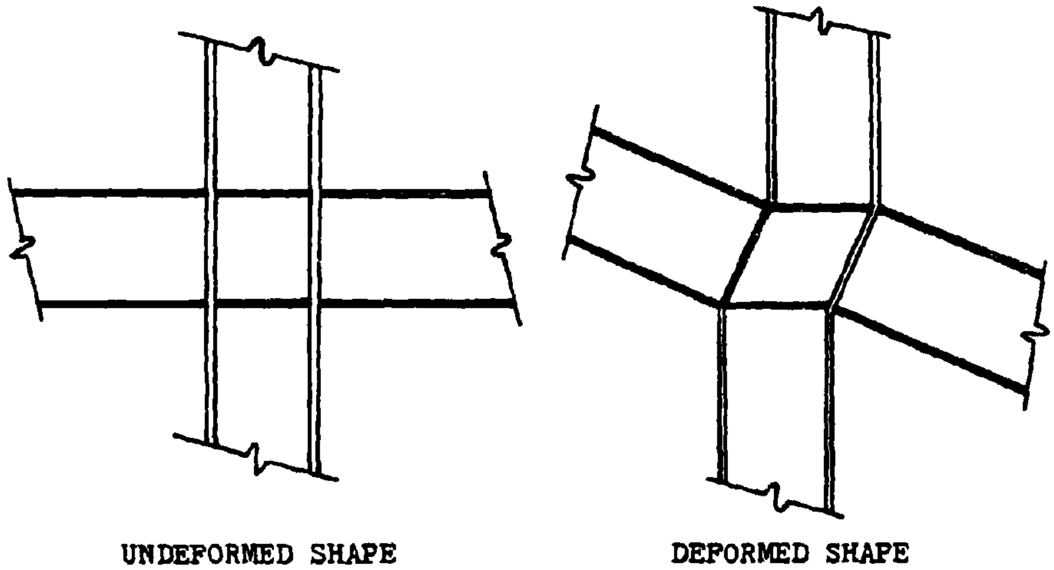

FIGURE 2.1- SHEAR DEFORMATION IN CONNECTION

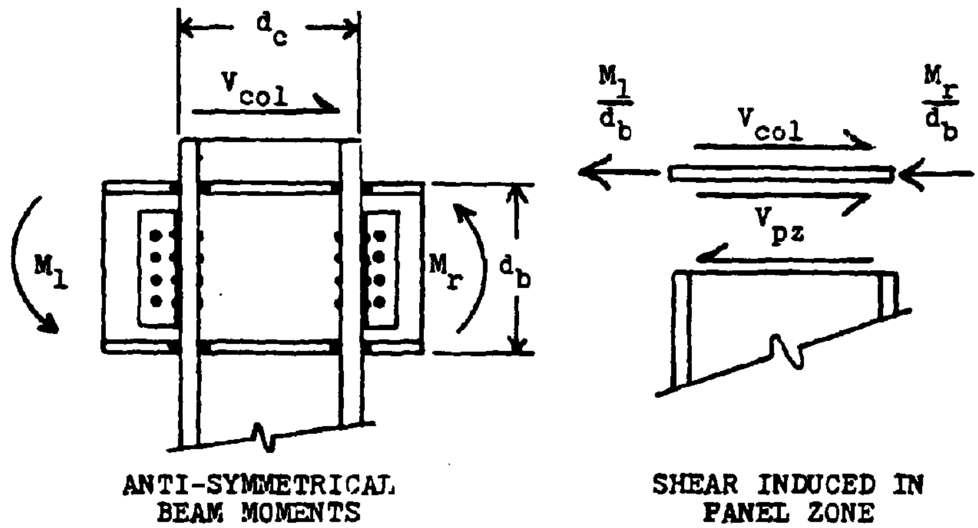

FIGURE 2.2- KRAWINKLER FORCE CONVENTION

$$V_{pz} = \frac{M_r + M_l}{d_b} - V_{col} \tag{2.1}$$

where:

V_{pz} = shear at top of the PZ

M_r, M_l = beam moments to the right and left of the connection, respectively

d_b = beam depth

V_{col} = column shear force

When the frame is subjected to lateral forces, the stress induced in the panel zone by the column shear, V_{col}, will be opposite in direction to that induced by the beam moments; hence a negative sign appears in Eq. (2.1). Column shear force, therefore, is considered a beneficial effect.

The shear force given by Eq. (2.1) is assumed to be uniformly distributed over an effective shear area of $(d_c - t_c^f)t$ (Fig. 2.3), resulting in an average shear stress of:

$$\tau = \frac{V_{pz}}{(d_c - t_c^f)t} = \frac{\Delta M(1 - \rho)}{(d_c - t_c^f)td_b} \tag{2.2}$$

where:

τ = PZ shear stress

d_c = column depth

t_c^f = thickness of a single column flange

t = thickness of column web (PZ)

ΔM = sum of beam moments, $M_r + M_l$

$\rho = V_{col}d_b/\Delta M$.

The PZ shear stiffness is defined in terms of the beam moments and the PZ shear distortion, γ. For a connection behaving elastically, this

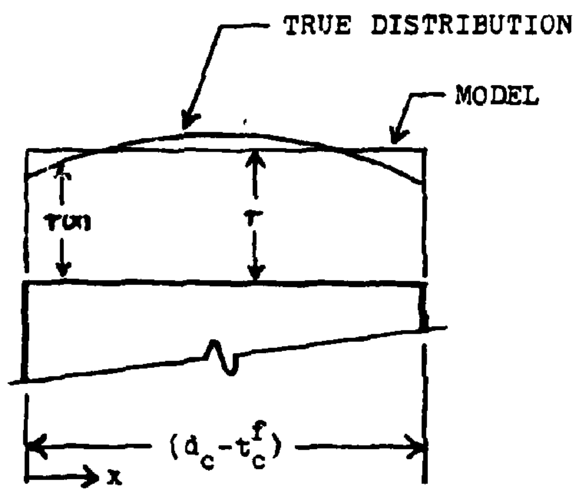

FIGURE 2.3- SHEAR STRESS DISTRIBUTION IN PANEL ZONE

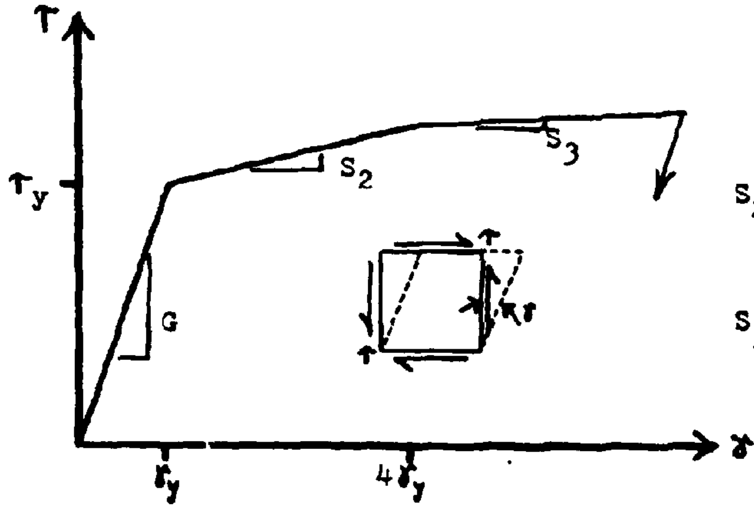

$$S_2 = \frac{12.5\ GI_c^f}{(d_c-t_c^f)t_c^f t d_b}$$

$$S_3 = \frac{GE_s}{E}$$

FIGURE 2.4- TRI-LINEAR STRESS-STRAIN BEHAVIOR OF PANEL ZONE

stiffness is found by solving Eq. (2.2) for ΔM and dividing the result by τ/G:

$$K_e^m = \frac{\Delta M}{\gamma} = \frac{G(d_c - t_c^f)td_b}{(1 - \rho)} \tag{2.3}$$

where G is the shear modulus of steel. Ignored in the equation is the elastic framing action of the surrounding connection stiffeners, an effect which is normally quite small (19).

This elastic stiffness remains valid until the panel zone reaches a state of general shear yielding, which is affected by column axial load and may be determined through the octahedral shear stress failure criteria:

$$\tau_y = \sigma_y \sqrt{\frac{1 - (N/N_y)^2}{3}} \tag{2.4}$$

where:
- τ_y = yield stress in shear of the PZ
- σ_y = yield stress in tension of steel
- N/N_y = ratio of the column axial load to the column yield load.

Normally, N/N_y is small enough so that the yield stress in shear is simply given by $\sigma_y/\sqrt{3}$.

Once the panel zone has yielded, the elastic framing action of the surrounding column flanges and horizontal stiffeners is assumed to carry any additional connection load. An approximate expression for this tangent stiffness was found from a finite element analysis to be:

$$K_t^m = \frac{\Delta M - \Delta M_y}{\Delta \gamma} = \frac{12.5G}{1 - \rho} \frac{I_c^f}{t_c^f} \tag{2.5}$$

where: M_y = beam moments creating shear yielding in the panel zone

I_c^f = moment of inertia of a single column flange.

This stiffness is assumed valid until a ductility of four is reached, at which time the connection resists additional loads with a strain-hardening stiffness given by:

$$K_s^m = \frac{\Delta M - \Delta M_{4\gamma_y}}{\Delta\gamma} = K_e^m \frac{E_s}{E} \tag{2.6}$$

where: $\Delta M_{4\gamma_y}$ = beam moments at four times the yield strain

E_s = strain hardening modulus of steel

E = elastic modulus of steel.

Since the aforementioned experimental studies show that panel zones are capable of generating extremely stable hysteretic loops with very large ductilities, no upper-bound strain is given for Eq. (2.6).

2.1.3 Model Conversion to Stress-Strain

To facilitate incorporation of Krawinkler's model into a general matrix formulation, it is convenient to express the connection stiffness in terms of the PZ shear stress. In the elastic range this is accomplished by solving Eq. (2.2) for ΔM and substituting the result into Eq. (2.2), which after rearranging simply results in:

$$\tau = G\gamma \quad , \qquad 0 \leq |\tau| \leq \tau_y \tag{2.7}$$

Equations (2.2) and (2.5) are used to determine the secondary slope:

$$\frac{\tau - \tau_y}{\Delta\gamma} = \frac{12.5\ GI_c^f}{(d_c - t_c^f)t_c^f\ td_b} \quad , \quad \gamma_y < |\gamma| \leq 4\gamma_y \qquad (2.8)$$

where γ_y is determined from Eqs. (2.4) and (2.7). The tertiary slope is found from Eqs. (2.2) and (2.6):

$$\frac{\tau - \tau_{4\gamma_y}}{\Delta\gamma} = G\frac{E_s}{E} \quad , \quad |\gamma| > 4\gamma_y \qquad (2.9)$$

Graphically, this tri-linear model is illustrated in Fig. 2.4.

At this stage it is useful to introduce an adjusted panel zone thickness:

$$t_{adj} \equiv t(d_c - t_c^f)/d_c \qquad (2.10)$$

which will simplify the notation in the forthcoming matrix formulation. Essentially this adjustment is used to compensate for the overestimation of the effective shear area by using the full column and beam depths in the analysis. The ratio $(d_c - t_c^f)/d_c$ is simply taken as 0.95 in the AISC specification (1), but here it is included for completeness.

2.2 Matrix Formulation

2.2.1 Transformation of PZ Degrees of Freedom

Four degrees of freedom (Fig. 2.5) are needed at each connection to describe the PZ model presented in section 2.1. These DOF's provide the three required rigid-body modes of translation and rotation plus a single shear deformation mode determined by the difference of the beam and column rotations (θ_b and θ_c, respectively). These degrees of freedom

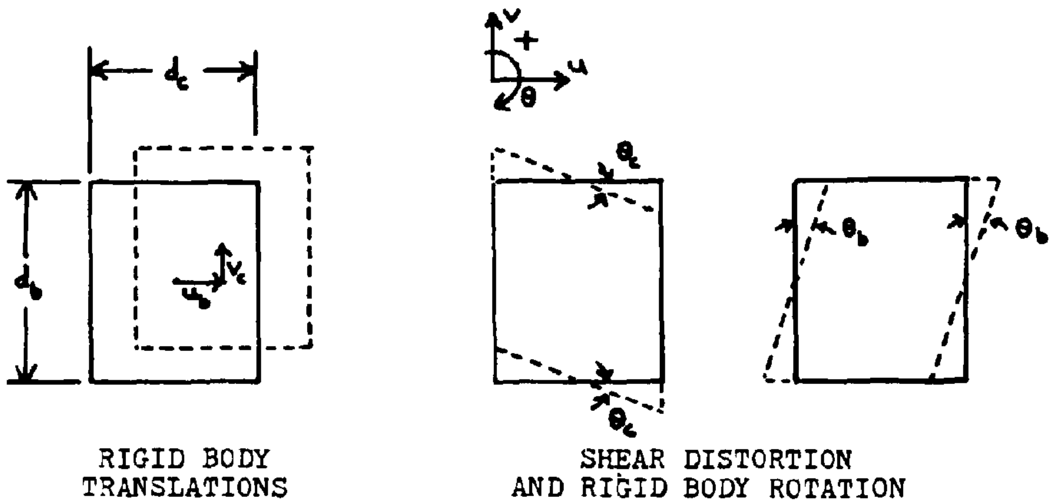

FIGURE 2.5- PANEL ZONE DEGREES OF FREEDOM, $\underset{\sim}{u}_i$

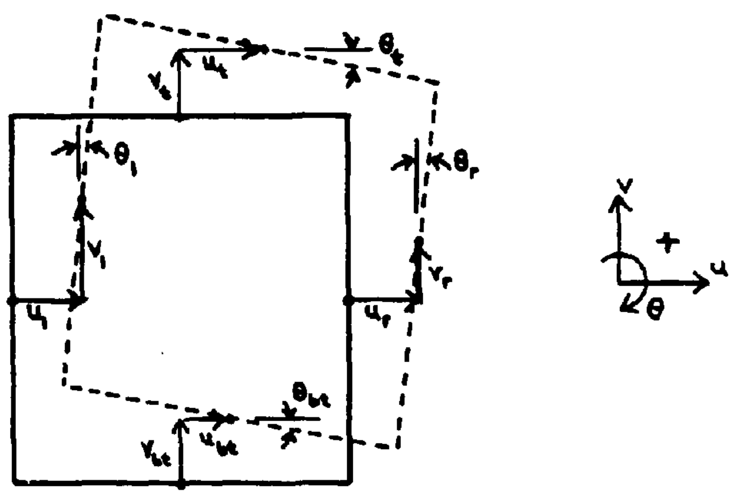

FIGURE 2.6- DISPLACEMENTS AT BEAM/COLUMN CONNECTION INTERFACE

imply displacements at the beam/column connection interface (Fig. 2.6) which can be determined through the transformations:

$$\begin{aligned} \underset{\sim}{u}_{ir} &= \underline{T}_{ir}\, \underset{\sim}{u}_{i} \\ \underset{\sim}{u}_{it} &= \underline{T}_{it}\, \underset{\sim}{u}_{i} \\ \underset{\sim}{u}_{il} &= \underline{T}_{il}\, \underset{\sim}{u}_{i} \\ \underset{\sim}{u}_{ib} &= \underline{T}_{ib}\, \underset{\sim}{u}_{i} \end{aligned} \tag{2.11}$$

where $\underset{\sim}{u}_{ir}$, $\underset{\sim}{u}_{it}$, $\underset{\sim}{u}_{il}$, $\underset{\sim}{u}_{ib}$ are the displacements on the right, top, left and bottom of connection i; $\underline{T}_{ir}$, $\underline{T}_{it}$, $\underline{T}_{il}$, $\underline{T}_{ib}$, are the corresponding transformation matrices; and $\underset{\sim}{u}_{i}$ is the vector of the four panel zone displacements. The displacement vectors take the form:

$$\begin{aligned} \underset{\sim}{u}_{i} &= (u_b \;\; v_c \;\; \theta_c \;\; \theta_b)_i^T \\ \underset{\sim}{u}_{ir} &= (u_r \;\; v_r \;\; \theta_r)_i^T \\ \underset{\sim}{u}_{it} &= (u_t \;\; v_t \;\; \theta_t)_i^T \\ \underset{\sim}{u}_{it} &= (u_l \;\; v_l \;\; \theta_l)_i^T \\ \underset{\sim}{u}_{ib} &= (u_{bt} \;\; v_{bt} \;\; \theta_{bt})_i^T \end{aligned}$$

while the transformation matrices become:

$$\underline{T}_{ir} = \begin{bmatrix} 1 & 0 & 0 & 0 \\ 0 & 1 & \frac{-d_c}{2} & 0 \\ 0 & 0 & 0 & 1 \end{bmatrix}_i$$

$$\underline{T}_{it} = \begin{bmatrix} 1 & 0 & 0 & \frac{d_b}{2} \\ 0 & 1 & 0 & 0 \\ 0 & 0 & 1 & 0 \end{bmatrix}_i$$

$$\underline{T}_{i1} = \begin{bmatrix} 1 & 0 & 0 & 0 \\ 0 & 1 & \frac{d_c}{2} & 0 \\ 0 & 0 & 0 & 1 \end{bmatrix}_i$$

$$\underline{T}_{ib} = \begin{bmatrix} 1 & 0 & 0 & \frac{-d_b}{2} \\ 0 & 1 & 0 & 0 \\ 0 & 0 & 1 & 0 \end{bmatrix}_i$$

2.2.2 PZ Stiffness Relations

The incremental shear stress in the panel zone is related to the incremental shear deformation through the relations developed in section 2.1.3:

$$d\tau = \alpha_i \, G d\gamma \tag{2.12}$$

where α_i is the tri-linear stiffness coefficient taken to satisfy Eqs. (2.8), (2.8) and (2.9), such that:

$$\alpha_i = \begin{cases} 1 & 0 \leq |\gamma| \leq \gamma_y \\ \left. \dfrac{12.5\ I_c^f}{(d_c - t_c^f)t_c^f t d_b} \right|_i & \gamma_y < |\gamma| \leq 4\gamma_y \\ E_s/E & |\gamma| > 4\gamma_y \end{cases}$$

The incremental shear force at the top of the panel zone, dQ_t, may be written in terms of the incremental beam and column rotations using Eqs. (2.10) and (2.12):

$$d\tau = \frac{dQ_t}{t_{adj}\, d_c} = \alpha_i G \, d\gamma = \alpha_i G(d\theta_b - d\theta_c)$$

Solving for dQ_t,

$$dQ_t = \alpha_i \; G \; t_{adj} \; d_c(d\theta_b - d\theta_c) \quad .$$

The remaining incremental PZ shears (Fig. 2.7) can be found in a similar way and assembled into matrix form:

$$d\underset{\sim}{Q}_i = \hat{\underline{K}}_i \; d\underset{\sim}{u}_i \tag{2.13}$$

where: $\qquad \underset{\sim}{Q}_i = (Q_r, \;\; Q_l, \;\; Q_b, \;\; Q_t)_i^T$

$$\hat{\underline{K}}_i = \alpha G t_{adj} \begin{bmatrix} 0 & 0 & -d_b & d_b \\ 0 & 0 & d_b & -d_b \\ 0 & 0 & d_c & -d_c \\ 0 & 0 & -d_c & d_c \end{bmatrix}_i$$

Note that the panel zone shears are not related to the translational degrees of freedom, and that $\hat{\underline{K}}_i$ is rank deficient by three, suggesting that the PZ is totally unconstrained and has only one deformable mode.

2.2.3 Equilibrium Requirements of Surrounding Elements

Referring to Figs. 2.7 and 2.8, the shear force at the top of the panel zone, Q_t can be written in terms of the surrounding beam/column element forces:

$$Q_t = - N_{rf} - \frac{M_r}{d_b} - S_t - N_{lf} - \frac{M_l}{d_b} + \frac{M_v}{d_b}$$

The remaining PZ shears follow from equilibrium considerations on the other sides of the connection. In matrix form,

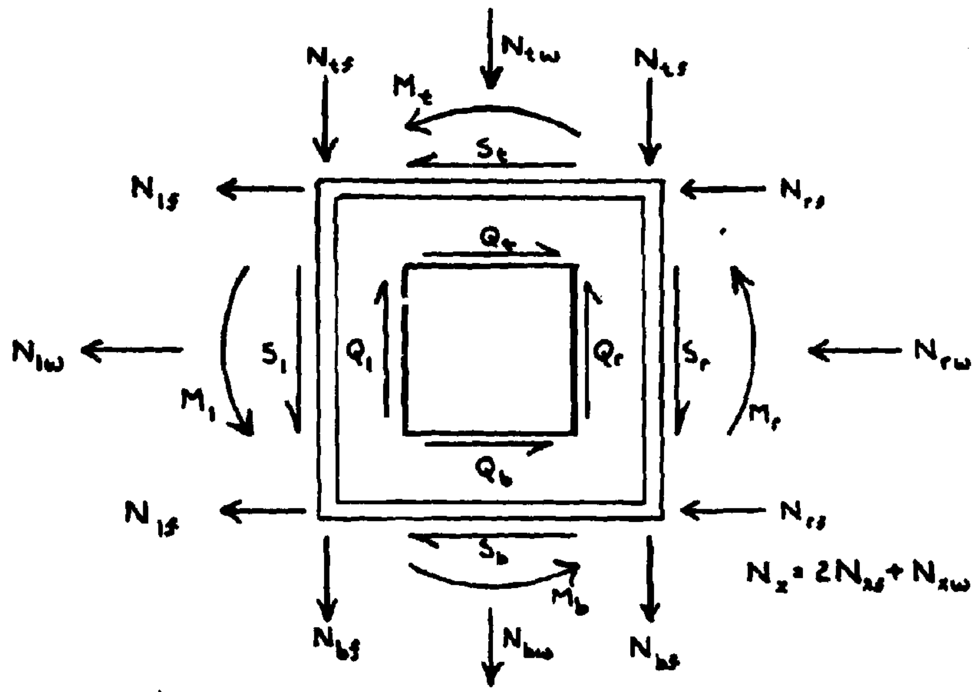

FIGURE 2.7- POSTIVE Q_i, Q_i^s, Q_i^{sr}, Q_i' FORCES FOR CONNECTION

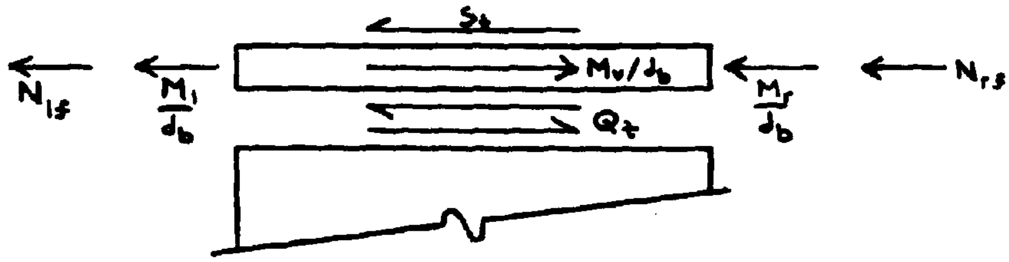

$$Q_t = -N_{lf} - \frac{M_l}{d_b} - S_t + \frac{M_v}{d_b} - \frac{M_r}{d_b} - N_{rf}$$

FIGURE 2.8- HORIZONTAL EQUILIBRIUM OF TOP STIFFENER

$$d\underset{\sim}{Q}_i = \underline{B}_i \, d\underset{\sim}{Q}_i^s - d\underset{\sim}{M}_{ti} \tag{2.14}$$

where:

$$\underline{B}_i = \begin{bmatrix} 0 & -1 & 0 & 0 & -1 & 1/d_c & 0 & 0 & 0 & 0 & -1 & 1/d_c \\ 0 & 0 & 0 & 0 & -1 & -1/d_c & 0 & -1 & 0 & 0 & -1 & -1/d_c \\ -1 & 0 & 1/d_b & 0 & 0 & 0 & -1 & 0 & 1/d_b & -1 & 0 & 0 \\ -1 & 0 & -1/d_b & -1 & 0 & 0 & -1 & 0 & -1/d_b & 0 & 0 & 0 \end{bmatrix}_i$$

$$\underset{\sim}{Q}_i^s = (N_{rf} \;\; S_r \;\; M_r \;\; S_t \;\; N_{tf} \;\; M_t \;\; N_{lf} \;\; S_l \;\; M_l \;\; S_b \;\; N_{bf} \;\; M_b)_i^T$$

$$M_{ti} = \left(\frac{M_u}{d_c} \;\; \frac{-M_u}{d_c} \;\; \frac{M_v}{d_b} \;\; \frac{-M_v}{d_b}\right)_i^T$$

Here, $\underset{\sim}{Q}_i^s$ is the vector of loads at connection i induced by the surrounding beams and columns. N_{xf} is that portion of the axial load in a single beam/column flange to the "x" side of connection i. $\underset{\sim}{M}_{ti}$ is the vector of torsional moments of beams framing into connection i such that their axis of bending is parallel to the main frame. M_u and M_v are the torsional moments of beams framing into the connection so that their webs are parallel to the u and v axes, respectively. For an accurate representation of each torsional moment, the depth of the beam by which it is carried must be approximately the size of the connection; that is, the depth of the beam inducing M_u or M_v must be approximately equal to d_c or d_b, respectively.

Equation (2.14) is not valid for beams with unsymmetrical cross-sections. The $\underline{B}_i$ matrix can be modified to account for this, but any manipulation should be undertaken with caution, as the PZ model is based upon experimental work that did not consider this effect.

At this stage it is convenient to define two moments that correspond to the PZ rotational degrees of freedom, θ_{bi} and θ_{ci}. They are, respectively:

$$M_{bm\ i} = (Q_b - Q_t)\frac{d_b}{2}$$
$$M_{cl\ i} = (Q_r - Q_l)\frac{d_c}{2} \qquad (2.15)$$

Equations (2.13) and (2.14) can be expressed in terms of Eq. (2.15) and equated, thus reducing to:

$$d\underset{\sim}{M}^r_{ti} = \underline{B}^r_i\, d\underset{\sim}{Q}^{sr}_i + \underline{K}^r_i\, d\underset{\sim}{u}_i \quad , \qquad (2.16)$$

in which $\underset{\sim}{M}^r_{ti}$ is the reduced external moment vector; $\underline{B}^r_i$ is the reduced equilibrium matrix; $\underset{\sim}{Q}^{sr}_i$ is the reduced beam/column force vector; and $\underline{K}^r_i$ is the reduced PZ stiffness matrix; and where

$$\underset{\sim}{M}^r_{ti} = (M_u \quad M_v)^T_i$$

$$\underset{\sim}{Q}^{sr}_i = (S_r \quad M_r \quad S_t \quad M_t \quad S_l \quad M_l \quad S_b \quad M_b)^T_i$$

$$\underline{B}^r_i = \begin{bmatrix} -\frac{d_c}{2} & 0 & 0 & 1 & \frac{d_c}{2} & 0 & 0 & 1 \\ 0 & 1 & \frac{d_b}{2} & 0 & 0 & 1 & -\frac{d_b}{2} & 0 \end{bmatrix}_i$$

$$\underline{K}^r_i = \alpha G d_b d_c t_{adj} \begin{bmatrix} 0 & 0 & 1 & -1 \\ 0 & 0 & -1 & 1 \end{bmatrix}_i$$

Hence the beam/column axial flange forces drop out of the formulation, suggesting, as should be expected for symmetrical cross-sections, that they play no role in the shearing distortion of the panel zone. Equation (2.16) is the statement of panel zone rotational equilibrium and compatibility.

2.2.4 Incorporation into Structure's Stiffness Matrix

The four degrees of freedom needed to model the PZ behavior of each connection require that four displacements be provided at each node in a structure's stiffness matrix, rather than the customary three. Figure 2.9 illustrates a substructure in a general moment-resisting steel frame. Equation (2.14) can be combined with expressions of horizontal and vertical equilibrium at node i to give the total equilibrium expression for this node in terms of panel zone displacements, surrounding element forces, and external loads:

$$d\underset{\sim}{F}_i = \underline{B}_i' \, d\underset{\sim}{Q}_i' + \underline{K}_i \, d\underset{\sim}{u}_i \tag{2.17}$$

where

$$\underset{\sim}{F}_i = (H \quad V \quad M_u \quad M_v)_i^T$$

H = external horizontal load at node

V = external vertical load at node

$$\underline{B}_i' = \begin{bmatrix} 1 & 0 & 0 & 1 & 0 & 0 & 1 & 0 & 0 & 1 & 0 & 0 \\ 0 & 1 & 0 & 0 & 1 & 0 & 0 & 1 & 0 & 0 & 1 & 0 \\ 0 & -\frac{d_c}{2} & 0 & 0 & 0 & 1 & 0 & \frac{d_c}{2} & 0 & 0 & 0 & 1 \\ 0 & 0 & 1 & \frac{d_b}{2} & 0 & 0 & 0 & 0 & 1 & -\frac{d_b}{2} & 0 & 0 \end{bmatrix}_i$$

$$\underset{\sim}{Q}_i' = (N_r \quad S_r \quad M_r \quad S_t \quad N_t \quad M_t \quad N_l \quad S_l \quad M_l \quad S_b \quad N_b \quad M_b)_i^T$$

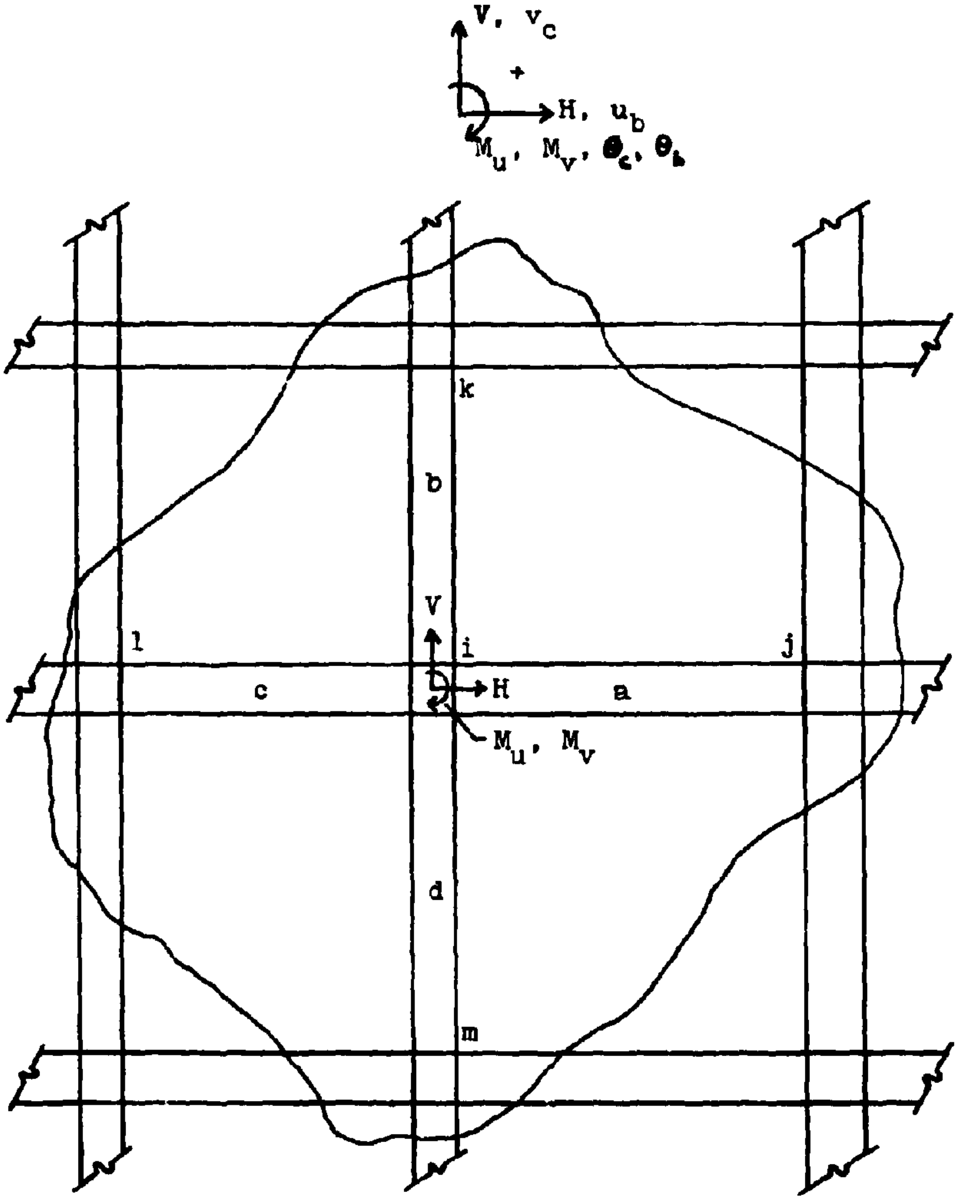

FIGURE 2.9- FRAME SUBSTRUCTURE

$$\underline{K}_i = \alpha G d_b d_c t_{adj} \begin{bmatrix} 0 & 0 & 0 & 0 \\ 0 & 0 & 0 & 0 \\ 0 & 0 & 1 & -1 \\ 0 & 0 & -1 & 1 \end{bmatrix}_i$$

It can be seen from Eq. (2.11) that $\underline{B}_i'$ is simply a matrix of transposed PZ transformations; that is,

$$\underline{B}_i' = (\underline{T}_{ir}^T \;\; \underline{T}_{it}^T \;\; \underline{T}_{il}^T \;\; \underline{T}_{ib}^T)$$

The beam/column forces, $\underset{\sim}{Q}_i'$, can be expressed in terms of the PZ displacements at node i and the surrounding nodes j, k, l, m, by using Eq. (2.11) and well-known stiffness relations:

$$d\underset{\sim}{Q}_i' = \underline{C}_{ii}\, d\underset{\sim}{u}_i + \underline{C}_{i\eta}\, d\underset{\sim}{u}_\eta \tag{2.18}$$

where:

$$\underline{C}_{ii} = \begin{bmatrix} \underline{K}_{ii}^a \; \underline{T}_{ir} \\ \underline{K}_{ii}^b \; \underline{T}_{it} \\ \underline{K}_{ii}^c \; \underline{T}_{il} \\ \underline{K}_{ii}^d \; \underline{T}_{ib} \end{bmatrix}$$

$$\underline{C}_{i\eta} = \begin{bmatrix} \underline{K}_{ij}^a \; \underline{T}_{jl} & \underline{0} & \underline{0} & \underline{0} \\ \underline{0} & \underline{K}_{ik}^b \; T_{kb} & \underline{0} & \underline{0} \\ \underline{0} & \underline{0} & \underline{K}_{il}^c \; \underline{T}_{lr} & \underline{0} \\ \underline{0} & \underline{0} & \underline{0} & \underline{K}_{im}^d \; \underline{T}_{mt} \end{bmatrix}$$

$$d\underset{\sim}{u}_\eta = (d\underset{\sim}{u}_j \;\; d\underset{\sim}{u}_k \;\; d\underset{\sim}{u}_l \;\; d\underset{\sim}{u}_m)^T$$

$\underline{K}^n_{xy}$ is the incremental stiffness matrix of beam n rotated into global coordinates, representing forces at node x resulting from displacements at node y

$\underline{0}$ is a 3 x 4 null matrix .

Equation (2.18) can thus be substituted into Eq. (2.17) yielding:

$$d\underset{\sim}{F}_i = (\underline{B}_i' \, \underline{C}_{ii} + \underline{K}_i) \, d\underset{\sim}{u}_i + \underline{B}_i' \, \underline{C}_{in} \, d\underset{\sim}{u}_n \tag{2.19}$$

which completes the stiffness equations representing node i. This expression can be expanded:

$$\begin{aligned} d\underset{\sim}{F}_i = \; & (\underline{T}^T_{ir} \, \underline{K}^a_{ii} \, \underline{T}_{ir} + \underline{T}^T_{it} \, \underline{K}^b_{ii} \, \underline{T}_{it} + \underline{T}^T_{il} \, K^c_{ii} \, \underline{T}_{il} \\ & + \underline{T}^T_{ib} \, \underline{K}^d_{ii} \, \underline{T}_{ib} + \underline{K}_i) \, d\underset{\sim}{u}_i + \underline{T}^T_{ir} \, \underline{K}^a_{ij} \, \underline{T}_{jl} \, d\underset{\sim}{u}_j \\ & + \underline{T}^T{}_{it} \, \underline{K}^b_{ik} \, \underline{T}_{kb} \, d\underset{\sim}{u}_k + \underline{T}^T_{il} \, \underline{K}^c_{il} \, \underline{T}_{lr} \, d\underset{\sim}{u}_l \\ & + \underline{T}^T_{ib} \, \underline{K}^d_{im} \, \underline{T}_{mt} \, d\underset{\sim}{u}_m \end{aligned}$$

For exterior connections in the frame, Eq. (2.19) still applies, but the stiffness submatrices, $\underline{K}^n_{xy}$, are taken as zero matrices for the beams and/or columns that no longer frame into the node. The procedure for assembling Eq. (2.19) into a structure's stiffness matrix is illustrated by Fig. 2.10 and Eq. (2.20).

The computer program JAN, prsented in Appendix A, assembles the stiffness matrix of frames with finite connection size and PZ shear deformation automatically, and will condense out any degrees of freedom specified by the user. Rigid connections of finite size can also be handled by specifying the two rotational degrees of freedom at each node to be identical through the Equal Displacement Command. This allows quick comparison of the lateral stiffness properties of typical building frames with different connection properties, as is done in chapter four.

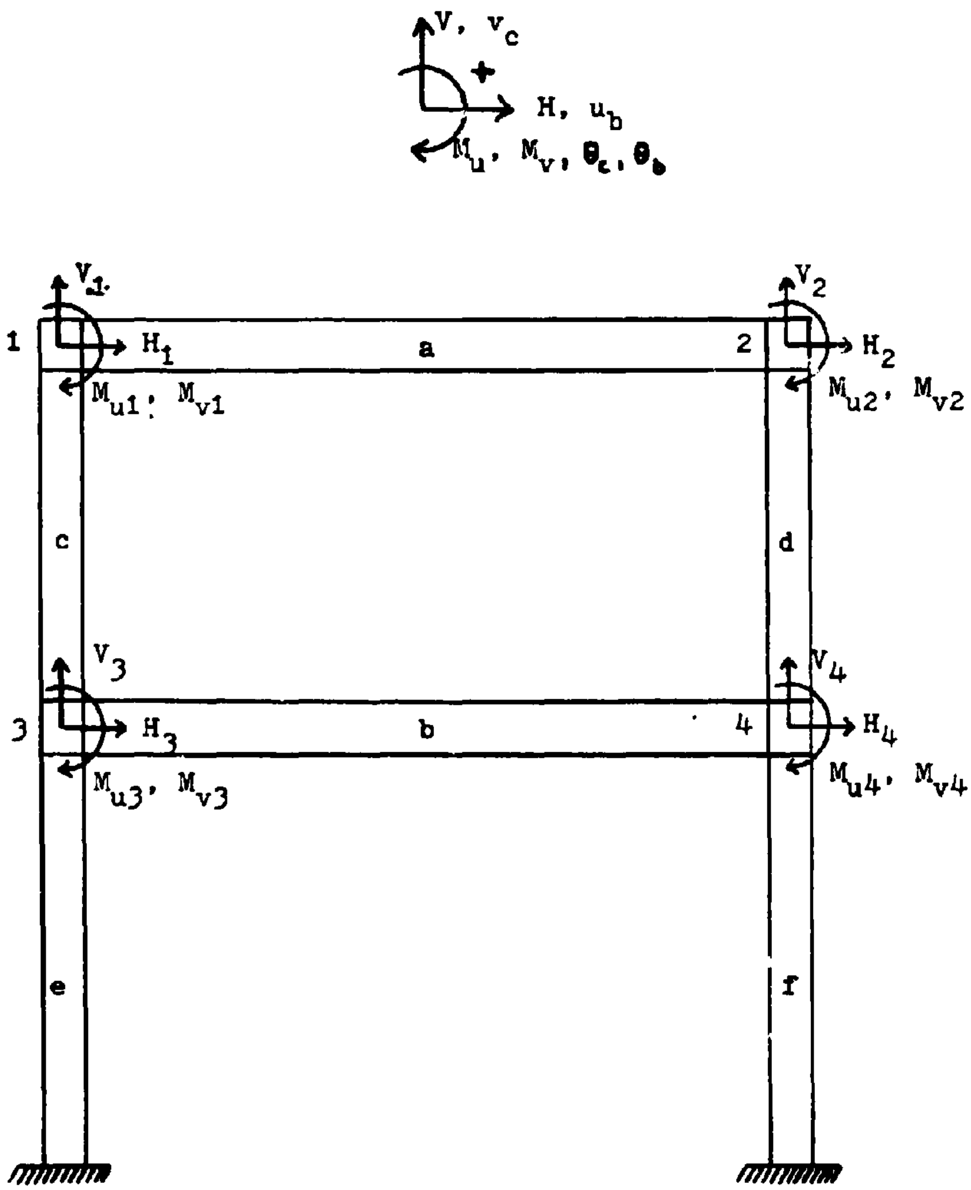

FIGURE 2.10- EXAMPLE FRAME FOR EQ. (2.20)

$$
\left[\begin{array}{c|c|c|c}
\begin{array}{l} \underline{T}_{1r}^{T}\,\underline{K}_{11}^{a}\,\underline{T}_{1r} \\ \quad + \underline{T}_{1b}^{T}\,\underline{K}_{11}^{c}\,\underline{T}_{1b} \\ \quad\quad + \underline{K}_{1} \end{array} & \underline{T}_{1r}^{T}\,\underline{K}_{12}^{a}\,\underline{T}_{2L} & \underline{T}_{1b}^{T}\,\underline{K}_{13}^{c}\,\underline{T}_{3t} & \underline{0} \\
\hline
\underline{T}_{2L}^{T}\,\underline{K}_{21}^{a}\,T_{1r} & \begin{array}{l} \underline{T}_{2L}^{T}\,\underline{K}_{22}^{a}\,\underline{T}_{2L} \\ \quad + \underline{T}_{2b}^{T}\,\underline{K}_{22}^{d}\,\underline{T}_{2b} \\ \quad\quad + \underline{K}_{2} \end{array} & \underline{0} & \underline{T}_{2b}^{T}\,\underline{K}_{24}^{d}\,\underline{T}_{4t} \\
\hline
\underline{T}_{3t}^{T}\,\underline{K}_{31}^{c}\,\underline{T}_{1b} & \underline{0} & \begin{array}{l} \underline{T}_{3r}^{T}\,\underline{K}_{33}^{b}\,\underline{T}_{3r} \\ \quad + \underline{T}_{3t}^{T}\,\underline{K}_{33}^{c}\,\underline{T}_{3t} \\ \quad + \underline{T}_{3b}^{T}\,\underline{K}_{33}^{e}\,\underline{T}_{3b} \\ \quad\quad + \underline{K}_{3} \end{array} & \underline{T}_{3r}^{T}\,\underline{K}_{34}^{b}\,\underline{T}_{4L} \\
\hline
\underline{0} & \underline{T}_{4t}^{T}\,\underline{K}_{42}^{d}\,\underline{T}_{2b} & \underline{T}_{4L}^{T}\,\underline{K}_{43}^{b}\,\underline{T}_{3r} & \begin{array}{l} T_{4t}^{T}\,\underline{K}_{44}^{d}\,T_{4t} \\ \quad + \underline{T}_{4L}^{T}\,\underline{K}_{44}^{b}\,\underline{T}_{4L} \\ \quad + \underline{T}_{4b}^{T}\,\underline{K}_{44}^{f}\,\underline{T}_{4b} \\ \quad\quad + \underline{K}_{4} \end{array}
\end{array}\right]
\left[\begin{array}{c} u_{b1} \\ v_{c1} \\ \theta_{c1} \\ \theta_{b1} \\ \hline u_{b2} \\ u_{c2} \\ \theta_{c2} \\ \theta_{b2} \\ \hline u_{b3} \\ v_{c3} \\ \theta_{c3} \\ \theta_{b3} \\ \hline u_{b4} \\ v_{c4} \\ \theta_{c4} \\ \theta_{b4} \end{array}\right]
=
\left[\begin{array}{c} H_{1} \\ V_{1} \\ M_{u1} \\ M_{v1} \\ \hline H_{2} \\ V_{2} \\ M_{u2} \\ M_{v2} \\ \hline H_{3} \\ V_{3} \\ M_{u3} \\ M_{v3} \\ \hline M_{4} \\ V_{4} \\ M_{u4} \\ M_{v4} \end{array}\right]
$$

2.3 Effect of PZ Reinforcement

2.3.1 Elastic Properties

2.3.1.1 Doubler Plates

The addition of plate stiffeners to a panel zone will increase both the strength and stiffness of the connection. The magnitude of this increase depends on the size of the stiffeners, their yield strength, their physical placement in the connection, and how effectively they are welded. The upper bound of the increase is found by assuming the doubler plates are simply an extra thickness of column web. The connection behavior can be modeled in this fashion, as is done in refs. 17 and 19, and adjusted with an effectiveness factor, k_1, to correct for any over-estimation of strength and stiffness that the assumption implies. For plate stiffeners welded directly to the column web, k_1 is close to unity. Ignoring the influence of beam/column axial load on the strength of the connection, the model can be expressed:

$$\Delta V_{ps} = k_1 t_{ps}(d_c - t_c^f)\tau_{ps} \tag{2.21}$$

$$\Delta K_{ps}^s = \frac{\Delta V_{ps}}{\gamma} = k_1 t_{ps} G(d_c - t_c^f) \tag{2.22}$$

$$\Delta V_{ps}^y = k_1 t_{ps}(d_c - t_c^f)\sigma_y/\sqrt{3} \tag{2.23}$$

where:
- ΔV_{ps} = shear resisted by plate stiffeners
- k_1 = plate stiffener effectiveness factor ≤ 1.0
- t_{ps} = total thickness of plate stiffeners
- τ_{ps} = shear stress in plate stiffeners

ΔK^s_{ps} = additional shear stiffness, defined in terms of the PZ shear, provided by the plate stiffeners.

ΔV^y_{ps} = additional shear strength provided by the plate stiffeners.

2.3.1.2 Diagonal Stiffeners

A second common method of connection reinforcement is the use of diagonal stiffeners, a model of which is shown in Fig. 2.11. Consistent with the assumption that the connection undergoes only shear deformation, the column flanges and horizontal stiffeners are considered to be rigid to axial loads. Once again, the elastic framing action of these elements is ignored. Diagonal stiffeners carrying a total force F_d can be expected to resist a connection shear force above that carried by the panel zone of:

$$\Delta V_{ds} = \frac{k_2\, F_d\, d_c}{\sqrt{d_c^2 + d_b^2}} \tag{2.24}$$

with a stiffness equal to:

$$\Delta K^s_{ds} = \frac{\Delta V_{ds}}{\gamma} = \frac{k_2 A_s\, E\, d_b d_c^2}{(d_c^2 + d_b^2)^{3/2}} \tag{2.25}$$

where:

ΔV_{ds} = shear resisted by diagonal stiffeners

k_2 = diagonal stiffener effectiveness factor ≤ 1.0

F_d = total axial load in diagonal stiffeners

ΔK^s_{ds} = additional shear stiffness providea by diagonal stiffeners

A_s = total area of shear stiffeners.

Ignoring the influence axial load has on the strength of the connection, and assuming elasto-plastic behavior of the diagonal stiffener, the

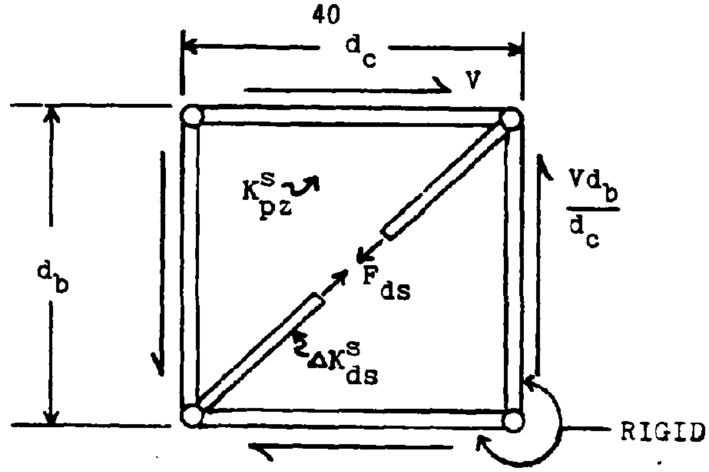

TOTAL CONNECTION SHEAR STIFFNESS = $V/\gamma = K^s_{pz} + K^s_{ds}$

FIGURE 2.11- CONNECTION MODEL WITH DIAGONAL STIFFENER

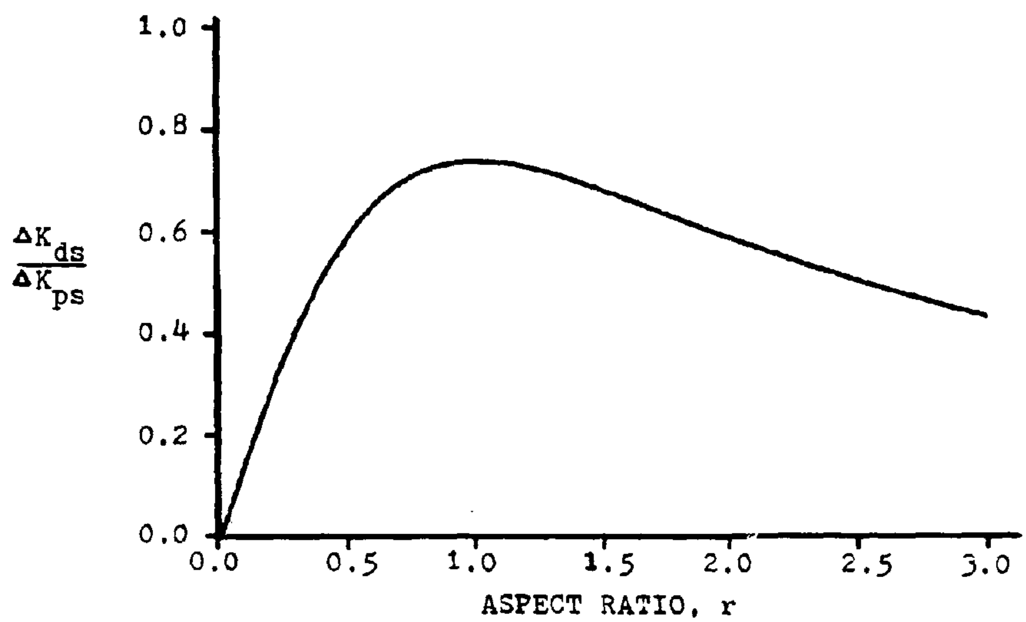

FIGURE 2.12- RELATIVE ADDITIONAL STIFFNESS
OF REINFORCEMENT OPTIONS

maximum additional shear the connection can carry as a result of reinforcement is:

$$\Delta V^{y}_{ds} = \frac{k_2\ \sigma_y\ A_s\ d_c}{\sqrt{d_c^2 + d_b^2}} \tag{2.26}$$

Should the connection be designed upon a strength criteria, the use of diagonal stiffeners will always produce a more flexible connection than the use of doubler plates. Consider a connection subjected to an additional shear force, ΔV, above that causing yield in the column web. The required doubler plate thickness is given by Eq. (2.23):

$$t^{r}_{ps} = \frac{\Delta V\ \sqrt{3}}{k_1(d_c - t^{f}_{c})\sigma_y} \tag{2.23a}$$

while the same connection reinforced with diagonal stiffeners would require a stiffener area as given by Eq. (2.26):

$$A^{r}_{s} = \frac{\Delta V\sqrt{d_c^2 + d_b^2}}{k_2 d_c \sigma_y} \tag{2.26a}$$

Substituting these values into Eqs. (2.22) and (2.25) permits calculation of the additional stiffness provided by the two options:

$$\Delta K_{ps} = \frac{\Delta V\ G\sqrt{3}}{\sigma_y} \tag{2.27}$$

and

$$\Delta K_{ds} = \frac{\Delta V E\, d_b\ d_c}{(d_c^2 + d_b^2)\sigma_y} \tag{2.28}$$

Hence the relative additional stiffness of the two designs becomes:

$$\frac{\Delta K_{ds}}{\Delta K_{ps}} = \frac{2(1+\mu)}{\sqrt{3}}\ \frac{r}{1+r^2} \tag{2.29}$$

where: μ = Poisson's ratio

$r = d_b/d_c$ = aspect ratio of the PZ .

For steel, this reduces to:

$$\frac{\Delta K_{ds}}{\Delta K_{ps}} = 1.5 \frac{r}{1 + r^2} \quad . \tag{2.29a}$$

The relative total stiffness of the two design options is found by adding Eqs. (2.27) and (2.28) to the elastic shear stiffness of the column web, $Gd_c t_{adj}$, and dividing the result. For steel this ratio becomes:

$$\frac{K_{pz} + \Delta K_{ds}}{K_{pz} + \Delta K_{ps}} = \frac{1 + 1.5S \dfrac{r}{(1 + r^2)}}{1 + S} \tag{2.30}$$

where: $S = V/V_y$ = increase in shear strength over unreinforced connection .

Equations (2.29a) and (2.30) are plotted in Figs. 2.12 and 2.13, respectively, and illustrate that a connection reinforced with diagonal stiffeners reaches its maximum stiffness with an aspect ratio of one. Equation (2.29a) has a maximum value of 75%, suggesting the additional stiffness provided by diagonal stiffeners will be at least 25% less than that provided by doubler plates. The total relative stiffness of the two options depends on additional strength that the connection is expected to develop, as shown in Fig. 2.13. These figures also imply that if the two designs are based upon an equal stiffness criteria, the design with the diagonal stiffeners will always be the stronger.

The elastic stiffness of a connection reinforced with diagonal stiffeners can be defined in terms of a PZ with an equivalent thickness

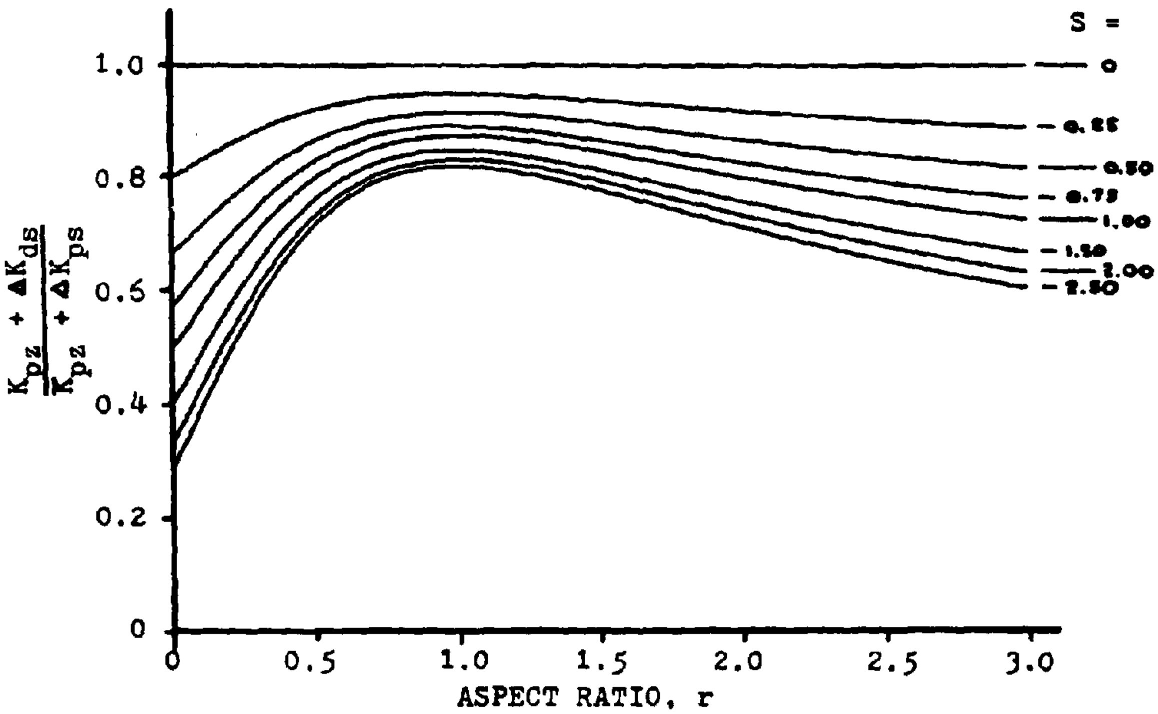

FIGURE 2.13- RELATIVE TOTAL STIFFNESS
OF REINFORCEMENT OPTIONS

found by equating:

$$K_{eqv} = Gd_c t_{eqv} = K_{pz} + \Delta K^s_{ds} \tag{2.31}$$

For steel:

$$t_{eqv} = t_{adj} + \frac{2.6\ A_s k_2 d_b d_c}{(d_c^2 + d_b^2)^{3/2}} \tag{2.32}$$

2.3.2 Inelastic Properties

References 17 ahd 19 suggest that the analytical tri-linear model presented in section 2.1.2 is applicable in the inelastic range of connections reinforced with doubler plates, and experimental work presented in those references justifies this to some extent. It is felt, however, that the model may prove inaccurate for connections with shear stiffeners placed a distance away from the column web, as the web and stiffener may not yield simultaneously (as implied by $k_1 < 1$).

The yield behavior of a connection reinforced with diagonal stiffeners is also uncertain, and it would be presumptuous to extend the results presented in section 2.3.1.2 into the inelastic range without experimental justification. It must be noted, however, that a reinforced connection will normally be designed not to yield, making the post-yield behavior only of academic concern, although there may be some advantage to inelastic energy dissipation occurring within the connection. This topic will be addressed further in chapter five.

CHAPTER THREE - FRAME SELECTION AND DESIGN

3.1 Frame Design

In order to establish the role panel zone flexibility and strength characteristics play on the seismic response of typical building structures, two illustrative frames—with three sets of connection properties—were considered in this study. Both of the frames were designed according to 1973 Uniform Building Code (UBC) standards by Piqué (26), and were presented as part of his doctoral dissertation. These same frames were later used in a study by Robinson (35). The connection properties of the example frames ranged from totally rigid to completely unreinforced, with one case considering the behavior of a reinforced connection, the design of which is presented in sec. 3.2.

Considered here are four- and ten-story three-bay frames (Figs. 3.1 and 3.2), as it was felt that their dynamic behavior would be fairly typical of most modern open steel frames. The four-story frame (4UBC) was designed for a typical floor live load of 40 psf, while the ten-story frame (10 UBC) was designed for a floor live load of 50 psf. Both frames were designed for roof live loads of 20 psf and for dead loads of 80 psf. The earthquake loads on the structures were taken as those satisfying U.B.C. zone 3 requirements. Wind loads were taken as a uniform 20 psf over the height of both structures. Only in-plane effects were considered in the design of the frames, and each frame was considered responsible for carrying loads twenty feet perpendicular to the frame itself.

Standard elastic analysis procedures were used to design the frames, such that the connections were considered infinitely small with no flexibility. The frame elements were designed for the most severe of:

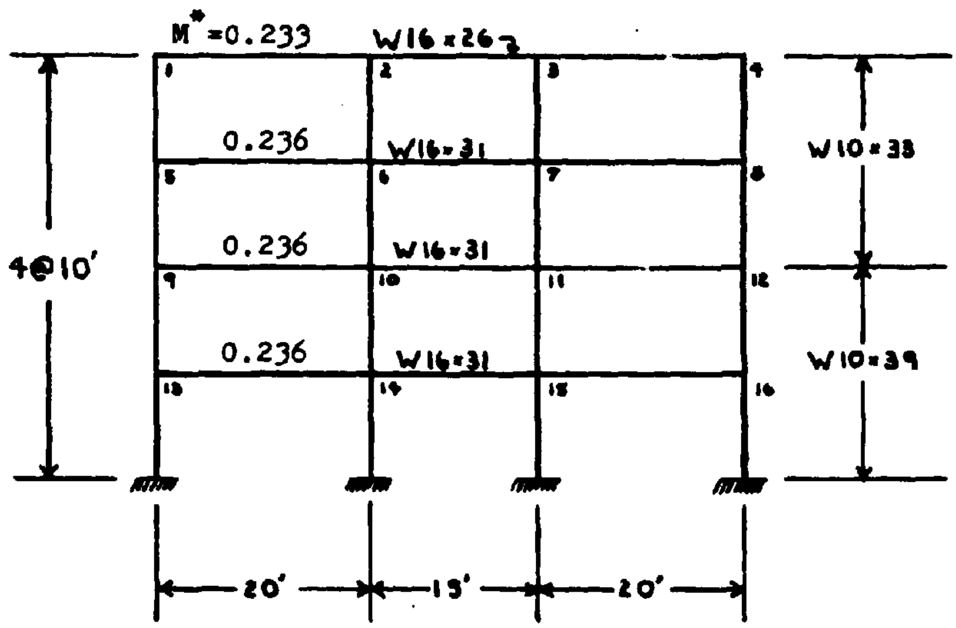

* Story mass in k-s^2/in

FIGURE 3.1- FOUR STORY FRAME (4-UBC)

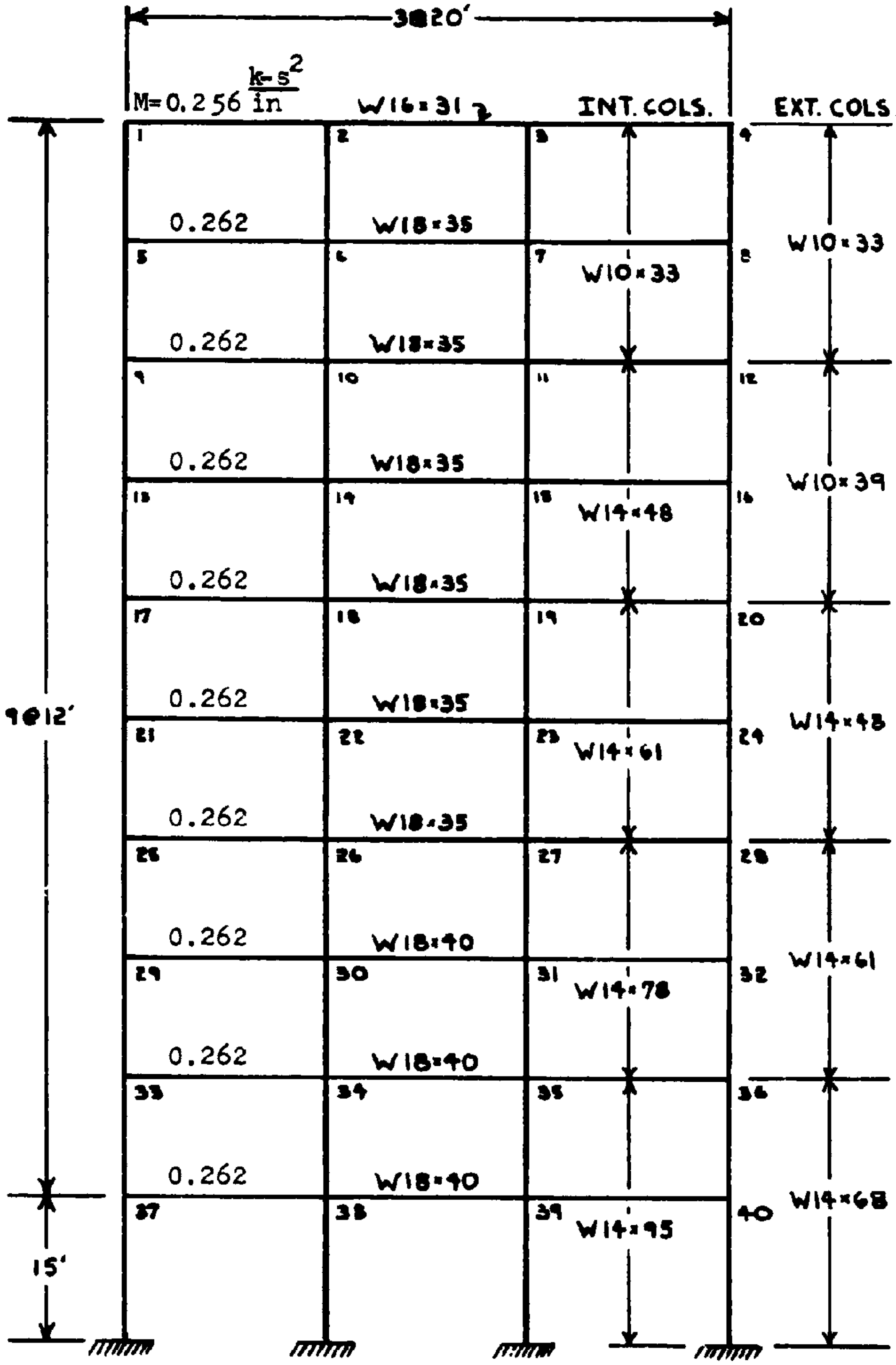

FIGURE 3.2- TEN STORY FRAME (10-UBC)

1) Dead plus live load (D+L) combinations,
2) Dead, live, and wind load (D+L+W) effects,
or 3) Dead, live, and earthquake load (D+L+Q) effects.

Interstory drift limitations were taken as 1/350 and 1/500 for wind and earthquake loadings, respectively. The section properties of the frames' beams and columns varied at story intervals in a way that was felt to reflect current economic practice.

3.2 Connection Design

Typical frame analysis procedures do not consider beam-to-column connections as structural elements—they are designed only after the frame analysis is complete. This somewhat erroneous, albeit convenient, procedure creates an inaccurate design on two fronts. Firstly, the beams and columns are not designed for the proper distribution of forces throughout the structure, and secondly, since the connection design is dependent upon these forces, they too may become improperly proportioned.

Conventional design of horizontal connection stiffeners is straightforward and is aimed at prevention of column flange bending and beam flange weld fracture that can occur under the intense localized beam flange forces at the beam/column interface. AISC specification sec. 1.15.5 and ASCE Manual 41 art. 8.6 provide the appropriate design criteria.

In addition to the horizontal stiffeners, shear reinforcement is required, according to AISC specification, whenever antisymmetric connection moments induce a connection shear force greater than (17):

$$V_{max} = 0.40\ \sigma_y\ d_c\ t \tag{3.1}$$

for working stress design, and

$$V_{max} = 0.55\ \sigma_y\ d_c\ t \tag{3.2}$$

for plastic design.

The ASCE plastic design manual 41 states that connection shear reinforcement is required when the connection shear is greater than:

$$V_{max} = \frac{\sigma_y}{\sqrt{3}}\ d_c\ t\ . \tag{3.3}$$

All three equations ignore the influence of column axial load, and assume that the column web can generate its allowable shear without buckling. Implicit in Eq. (3.2) is an effective P7 shear area of 0.95 $d_c t$; the other equations assume an unreduced shear area of $d_c t$.

The connection shear force is determined by:

$$V = \frac{\Delta M}{\beta d_b} - V_{col}\ , \tag{3.4}$$

where $\beta = 0.95$ if designing in accord with AISC specification or $\beta = 1$ if designing with regard to ASCE 41. Should Eq. (3.4) exceed Eq. (3.1), (3.2), or (3.3), as appropriate, connection reinforcement is required.

As was mentioned in section 2.3, connection reinforcement may take the form of either doubler plates or diagonal stiffeners. Plastic design equations (2.23a) and (2.26a) can be used to determine the required doubler plate and diagonal stiffener dimensions, respectively. These equations are believed to be more realistic than those suggested in AISC Commentary sec. 2.5 and ASCE 41 arts. 8.2 and 8.6, which differ in how they treat the effective PZ shear area, and simply assume k_1 and k_2 to be unity. It should be noted, however, that these effectiveness factors are uncertain quantities, and furtner research is needed to determine appropriate values for their use in design.

The philosophy of the codes is to produce a connection that will remain elastic, forcing the beams and columns into the role of energy dissipators. Conversely, it is possible to underdesign a connection so that all the energy dissipation will occur within the panel zone. It is difficult to achieve both effects, however, as plastic behavior in a given element necessarily limits the forces that can be transferred to adjacent elements. Nevertheless, Krawinkler (17) has suggested that the secondary slope of the PZ stress-strain behavior be taken advantage of in the design of doubler plates, and has proposed that the connection shear strength be taken as that value of shear corresponding to four times the yield strain of the tri-linear model presented in section 2.1. This procedure will theoretically force the panel zones to be the first elements of the frame to yield and relies upon their secondary hardening slopes to eventually yield the beams and/or columns, thus creating as many energy-dissipating mechanisms as possible. To fully achieve this effect, the beam/column forces and PZ thickness must be delicately balanced during the frame design, and approach requiring nonlinear dynamic analysis with connection behavior considered in the formulation. Even with this sophistication, it would be difficult to obtain reliable values of the design moments and shears, since they would be earthquake dependent and also quite sensitive to the assumed hysteretic behavior—a relationship that is not known with confidence.

In any event, localized inelastic deformation can occur even in a connection designed to remain elastic, since the true shear stress at the center of the panel zone sides is somewhat higher than the constant-stress model implies (Fig. 2.3).

For purposes of this study, reinforced connections were proportioned to remain elastic according to the following simplified criterion for determining the connection design moment, M_d:

$$M_{di} = \min\left(\Sigma M_p^b,\ \Sigma M_p^c\right)_i \tag{3.5}$$

where: M_{di} = Design moment at connection i;

M_{pi}^b, M_{pi}^c = Plastic moment capacity of beams and columns framing into connection i.

The influence of beam/column shear is conservatively ignored, and hence the required doubler plate thickness follows from Eq. (2.23a),

$$t_{ps\ i}^r = \left.\frac{\sqrt{3}\ M_d}{(d_c - t_c^f)\ d_b \sigma_y}\right|_i - t_i \tag{3.6}$$

Here is has been assumed that the plate stiffeners are welded directly to the column web, and thus k_1 was taken as unity. It was also assumed that $d_b(d_c - t_c^f) \approx d_c(d_b - t_b^f)$, as was done implicitly in the matrix formulation of section 2.2. Initially the panel zone yield stress was determined considering the interaction of column gravity loads, but the effect was small enough that the shear yield stress was taken as $\sigma_y/\sqrt{3}$. The results of the connection design for the four- and ten-story frames are summarized in Tables 3.1 and 3.2. Although the connections were reinforced with doubler plates, the equivalent elastic stiffness of connections designed with diagonal stiffeners would be somewhat less, and may be determined by referring to Figs. 2.12 and 2.13.

Connection	Beam Depth d_b(in)	Column Depth d_c(in)	Design Moment M_d(k-in)	Col. Flange Thickness t_c^f (in)	Col. Web Thickness t(in)	P.S. Thickness Req. t_{ps}^r (in)	P.S. Thickness Used** t_{ps} (in)
1,2,3,4	15.65	9.75	1397	0.433	0.292	0.169	1/4
5,8	15.84	9.75	1944	0.433	0.292	0.342	3/8
6,7	15.84	9.75	2794	0.433	0.292	0.619	5/8
9,12*	15.84	9.94	1944	0.528	0.318	0.309	3/8
10,11*	15.84	9.94	3085	0.528	0.318	0.678	3/4
13,16	15.84	9.94	1944	0.528	0.318	0.309	3/8
14,15	15.84	9.94	3377	0.528	0.318	0.772	7/8

* Column splice occurs directly above connection.

** PZ's symmetrically reinforced; plate stiffeners available in 1/16" increments; A36 steel used throughout.

TABLE 3.1 - FOUR-STORY (4 UBC) PLATE STIFFENER DESIGN

Connection	Beam Depth d_b(in)	Column Depth d_c(in)	Design Moment M_d(k-in)	Col. Flange Thickness t_c^f(in)	Column Web Thickness t(in)	P.S. Thickness Req. t_{ps}^r(in)	P.S. thickness Used** t_{ps} (in)
1,2,3,4	15.84	9.75	1397	0.433	0.292	0.163	1/4
5,8	17.71	9.75	2405	0.433	0.292	0.409	1/2
6,7	17.71	9.75	2794	0.433	0.292	0.523	5/8
9,12*	17.71	9.94	2405	0.528	0.318	0.376	1/2
10,11*	17.71	13.81	4218	0.593	0.339	0.528	5/8
13,16	17.71	9.94	2405	0.588	0.318	0.381	1/2
14,15	17.71	13.81	4810	0.593	0.339	0.650	3/4
17,20*	17.71	13.81	2405	0.593	0.339	0.155	1/4
18,19*	17.71	13.91	4810	0.643	0.378	0.607	3/4
21,24	17.71	13.81	2405	0.593	0.339	0.155	1/4
22,23	17.71	13.91	4810	0.643	0.378	0.607	3/4
25,28*	17.71	13.91	2405	0.643	0.378	0.114	1/4

* Column splice occurs directly above connection.

** PZ's symmetrically reinforced; plate stiffeners available in 1/16" increments; A36 steel used throughout.

TABLE 3.2 - TEN-STORY (10 UBC) PLATE STIFFENER DESIGN

Connection	Beam Depth d_b(in)	Column Depth d_c(in)	Design Moment M_d(k-in)	Col. Flange Thickness t_c^t(in)	Column Web Thickness t(in)	P.S. Thickness Req. t_{ps}^r(in)	P.S. Thickness Used** t_{ps}(in)
26,27*	17.71	14.06	4810	0.718	0.428	0.551	5/8
29,32	17.90	13.91	2822	0.643	0.378	0.194	1/4
30,31	17.90	14.06	5645	0.718	0.428	0.709	3/4
33,36*	17.90	14.06	2822	0.718	0.418	0.151	1/4
34,35*	17.90	14.12	5645	0.748	0.465	0.670	3/4
37,40	17.90	14.06	2822	0.718	0.418	0.151	1/4
38,39	17.90	14.12	5645	0.748	0.465	0.670	3/4

*Column splice occurs directly above connecti-n.

** PZ's symmetrically reinforced; plate stiffeners available in 1/16" increments; A36 steel used throughout.

TABLE 3.2 - TEN-STORY (10 UBC) PLATE STIFFENER DESIGN (Continued).

CHAPTER FOUR - MODAL ANALYSIS

4.1 Implementation of Elastic Connection Model

The four- and ten-story frames discussed in Chapter Three were analyzed with three different connection properties, as follows:

1) Assuming that the PZ's were totally rigid but of finite size;

2) Designing the PZ's to remain elastic according to Eqs. (3.5) and (3.6);

3) Using unreinforced connections with shear stiffness provided solely by the column web.

These three cases were also compared with an analysis performed by Robinson (35) on the same frames in which the connections were assumed totally inflexible and of no physical dimensions. The Robinson analysis, therefore, overestimates the flexibility of the beams and columns by using center-to-center connection distances in calculation of the beam/column lengths, and ignores the flexibility of the connection itself. With regard to lateral frame stiffness, the errors produced by this simplified analysis can, in some cases, be self-compensating.

The lateral stiffness matrix of the frames representing the three cases were assembled using the program JAN (Appendix A), which takes into account finite connection size, PZ shear distortion, and beam/column flexural, axial and shear deformation. This program was developed directly from the matrix formulation presented in section 2.2. For consistency with the Robinson analysis, only horizontal dynamic degrees of freedom at each story level were considered, and axial beam deformation was assumed negligible—as will be the case when rigid floor diaphragms are present in the frame. For cases 2) and 3), the panel zone thicknesses as shown in Tables 3.1 and 3.2 were adjusted according to Eq. (2.10) before being input to the program, thus correcting for overestimation of the effective shear area implied by using the full column and beam depths in the analysis. Case 1) was implemented by constraining the column and beam rotations to be identical at each connection by using the Equal Displacement Command.

Once the lateral stiffness matrix representing horizontal floor displacements was obtained, the program STRUDL (38) performed a standard eigenvalue/eigenvector analysis to determine the first four mode shapes and periods of the three cases. This was accomplished by iterating to find non-trivial solutions of:

$$\underset{\sim}{K_L}\, \underset{\sim}{\phi_i} = \omega_i^2\, \underline{M}\, \underset{\sim}{\phi_i} \tag{4.1}$$

where: $\underset{\sim}{K_L}$ = Lateral stiffness matrix of frame, obtained from program JAN

$\underset{\sim}{\phi_i}$ = Mode shape vector corresponding to mode i

ω_i = Frequency of mode i

$\underline{M}$ = Diagonal mass matrix corresponding to horizontal floor masses.

Following this analysis, the modal participation factors were calculated for synchronous horizontal base excitation:

$$\Gamma_i = \frac{\underset{\sim}{\phi_i}^T\ \underline{M}\ \underset{\sim}{(1)}}{\underset{\sim}{\phi_i}^T\ \underline{M}\ \underset{\sim}{\phi_i}} \tag{4.2}$$

Since $\underset{\sim}{\phi_i}$ was normalized for a unit mass matrix, this becomes:

$$\Gamma_i = \underset{\sim}{\phi_i}^T\ \underline{M}\ \underset{\sim}{(1)} \tag{4.2a}$$

where Γ_i = Participation factor of mode i

$\underset{\sim}{(1)}$ = Column vector of unity corresponding to the dimension of $\underline{M}$.

Hence the quantity $\frac{-\Gamma_i}{\omega_i^2} \underset{\sim}{\phi}_i$ becomes the equivalent relative static displacement of mode i corresponding to a constant unit horizontal ground acceleration.

The results of the modal analysis are presented in Figs. 4.1 through 4.8 and in Tables 4.1 and 4.2. In order to illustrate the relative lateral stiffness properties of the frames, the mode shapes for graphing purposes were normalized with respect to the maximum equivalent static displacement occurring in the frame with unreinforced connections; that is:

$$\text{Normalized Static Displacement} = \frac{\Gamma_i \, \underset{\sim}{\phi}_i \, \omega_{i\,ur}^2}{\omega_i^2 \, (\Gamma_i \, \phi_{i\,max})_{ur}}$$

where: $\Gamma_{i\,ur}$ = Participation factor of mode i for the frame with unreinforced connections

$\phi_{i\,max\,ur}$ = Maximum eigenvector entry of mode i for the frame with unreinforced connections

$\omega_{i\,ur}$ = Frequency of mode i for the frame with unreinforced connections.

The relative participation of higher modes, as expressed in Tables 4.1 and 4.2, is defined as:

$$\text{Relative Participation} = 100\left|\frac{\Gamma_i}{\Gamma_1}\right|. \tag{4.4}$$

4.2 Discussion of Results

4.2.1 Four-Story Frame

Table 4.1 illustrates that the mode shapes of the various design options are roughly equivalent. The differences in lateral stiffness and vibrational period, as shown in Figs. 4.1 through 4.4, are more significant, with variations as much as 23% and 12%, respectively. For the lowest modes, as expected, the use of unreinforced connections produces the most flexible frame, while the use of rigid PZ's creates the stiffest. For the fundamental mode, reinforcing the connections with doubler plates produces a frame with lateral stiffness characteristics between these two extremes, and almost identical to that found by Robinson. The reason for this similarity is that Robinson's overestimation of the true beam/column lengths implied an extra lateral frame flexibility, fictitious in nature, that was very close to the true additional flexibility provided by panel zone shear deformation.

During higher modes of vibration, the frames of finite connection size had a tendency to merge to a common vibrational period and stiffness, while the Robinson analysis diverged to have the longest period and the most lateral flexibility. This result is explained by the realization that PZ shear deformation is largely induced by antisymmetrical bending of the frame elements. Since higher modes create less antisymmetrical bending, the PZ shear flexibility is not of great concern in determining the lateral frame stiffness, but rather, this stiffness is controlled by the beam and column elements themselves. Because Robinson significantly overestimates the flexibility of these controlling elements, the result is an analysis that significantly overestimates the highest period of vibration.

4.2.2 Ten-Story Frame

Similar results were found for the ten-story frame, but since only the first four modes of vibration were obtained, the divergence of the Robinson analysis was not found. Presumably, this effect would have appeared if the highest modes of 10 UBC were calculated.

Again, in the fundamental mode, the use of reinforcement produced a frame stiffness almost identical to that found by Robinson. The results of the ten-story frame analysis are illustrated in Figs. 4.5 through 4.8 and in Table 4.2.

4.2.3 General Interpretation

For structures with heavily reinforced connections, a good approximation of the lowest mode shapes and periods can be obtained by ignoring the size of the connection and its flexibility, and by using center-to-center connection distances in calculation of the beam and column lengths. For structures left without connection reinforcement, or reinforced less heavily with either thinner plate stiffeners or by using more flexible diagonal stiffeners, a standard analysis such as that performed by Robinson can lead to an overestimation of the frame stiffness by 14%, and an underestimation of the period by 7%. Assuming that the connection is totally rigid but of finite size, as is sometimes done in a frame analysis, leads to an unrealistically stiff structure in the fundamental mode of vibration.

Conversely, for an accurate analysis of the highest modes, it is not necessary to model carefully the panel zone shear stiffness, but it is necessary to account for the physical connection size so that the true beam and column lengths are used in the analysis.

More substantial variations in the response of structure are found when the inelastic behavior of the frame is investigated, as in this case the full-range load-deflection behavior of the connection and beam/column elements become a factor. This topic will be addressed in Chapter Five.

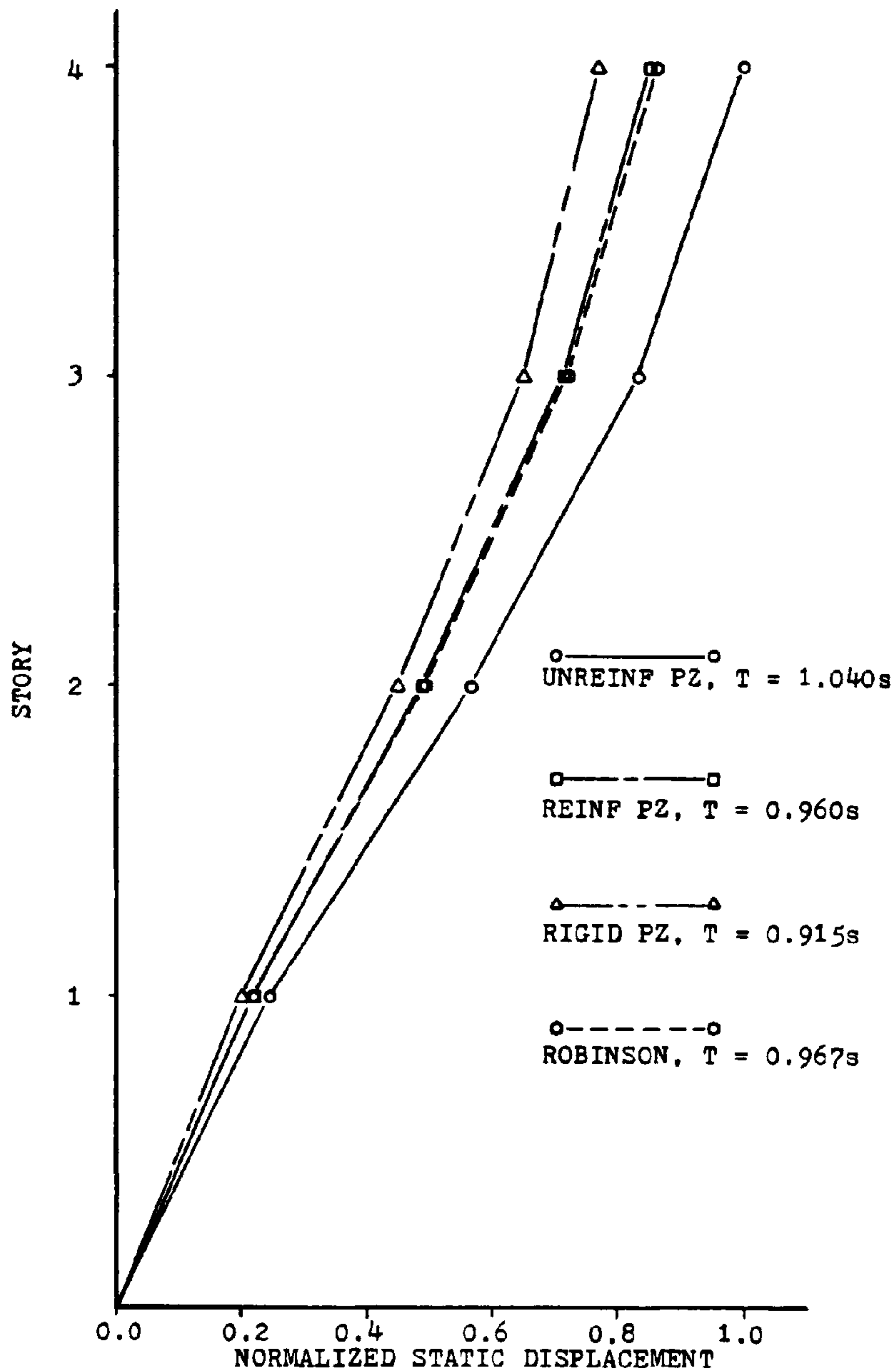

FIGURE 4.1- 4 UBC, FIRST MODE

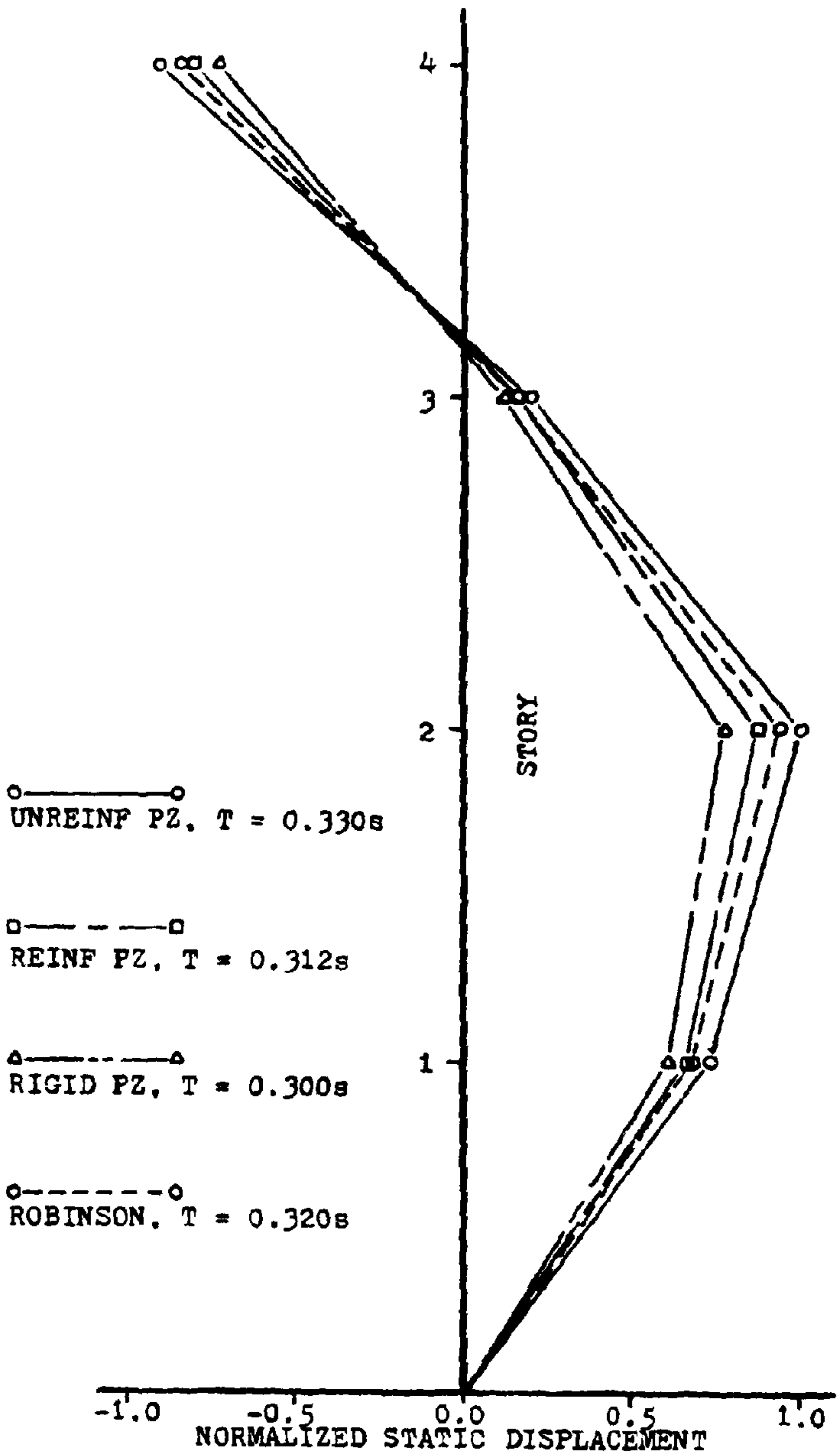

FIGURE 4.2- 4 UBC, SECOND MODE

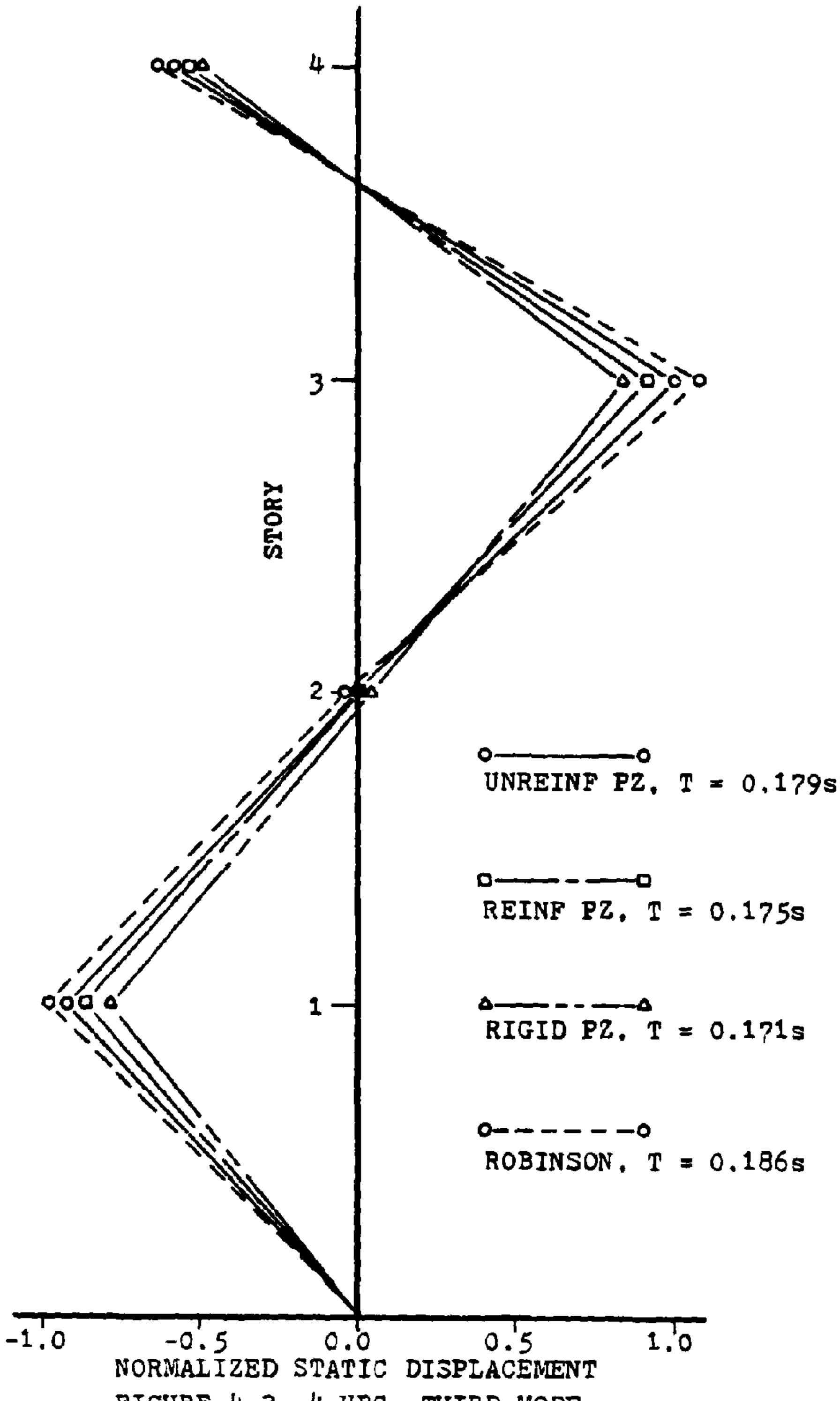

FIGURE 4.3- 4 UBC, THIRD MODE

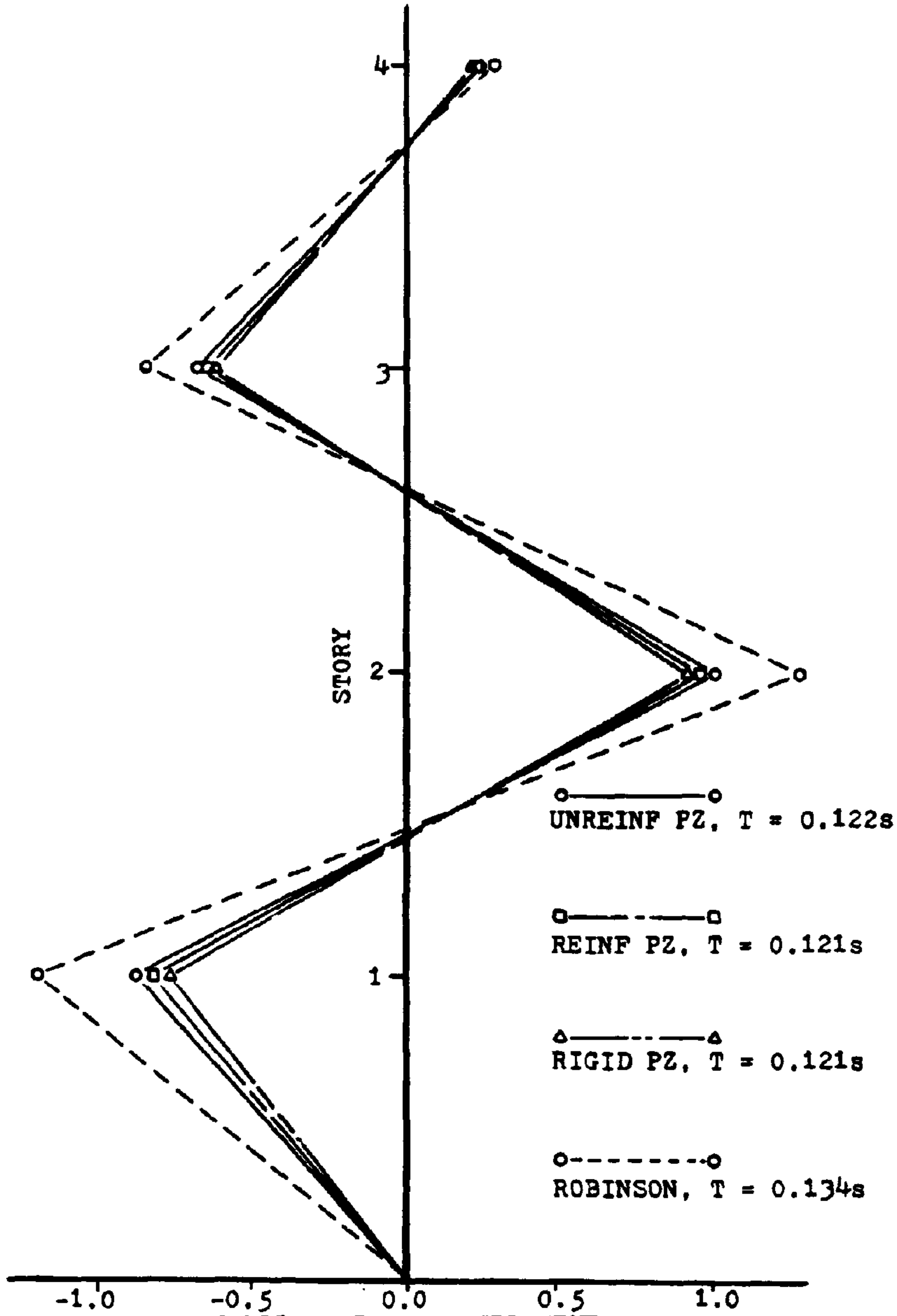

NORMALIZED STATIC DISPLACEMENT

FIGURE 4.4- 4 UBC, FOURTH MODE

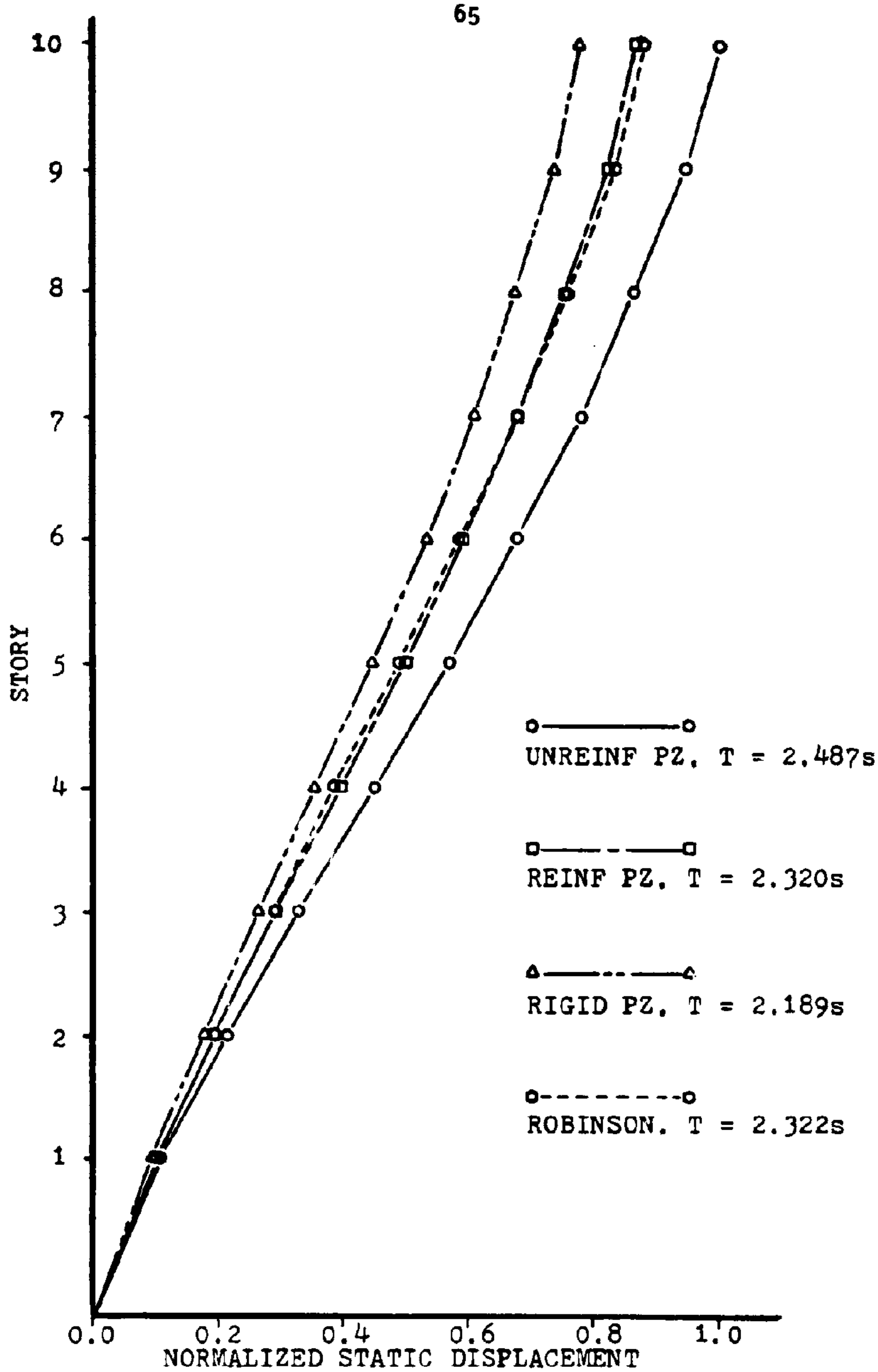

FIGURE 4.5- 10 UBC, FIRST MODE

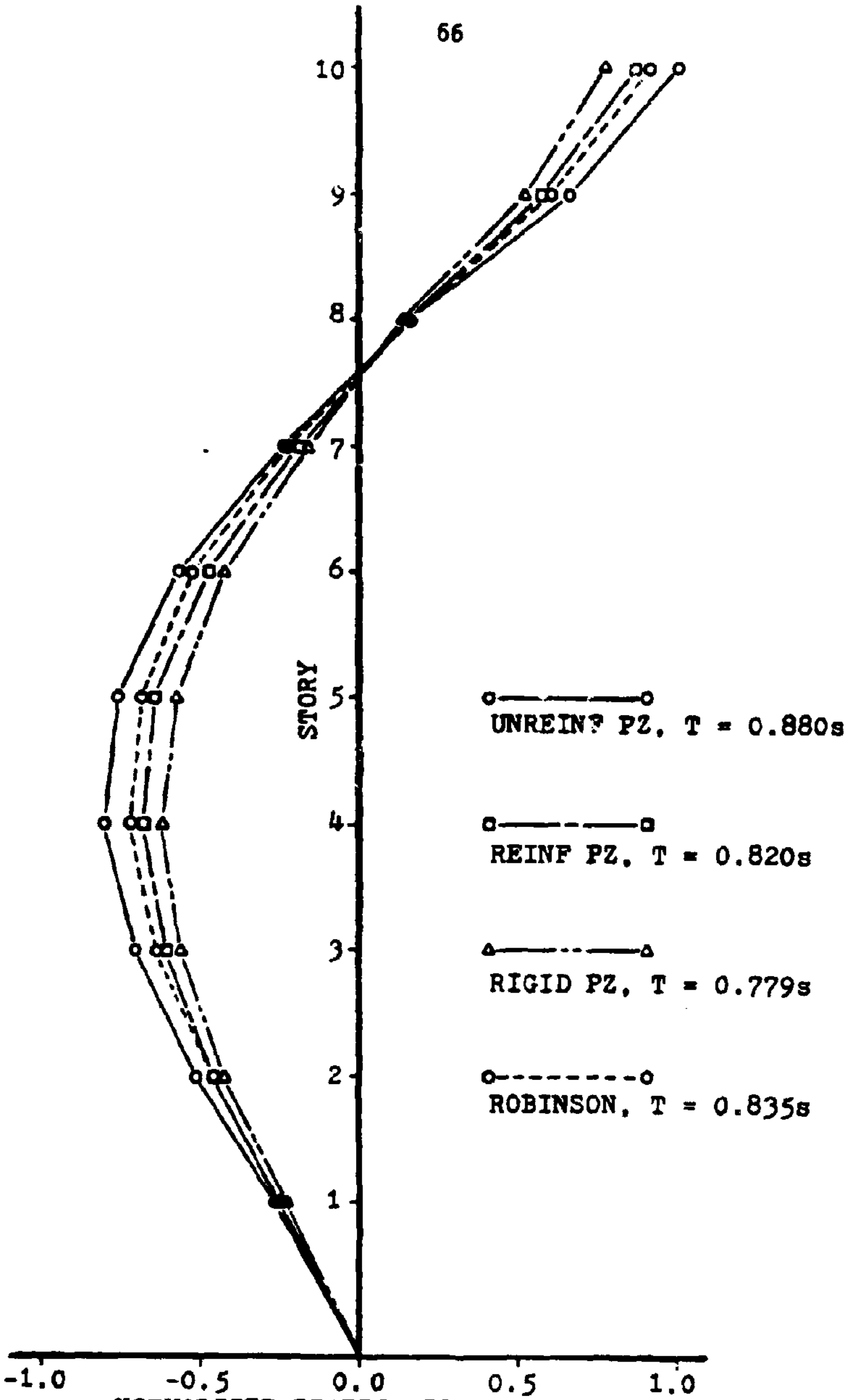

FIGURE 4.6- 10 UBC, SECOND MODE

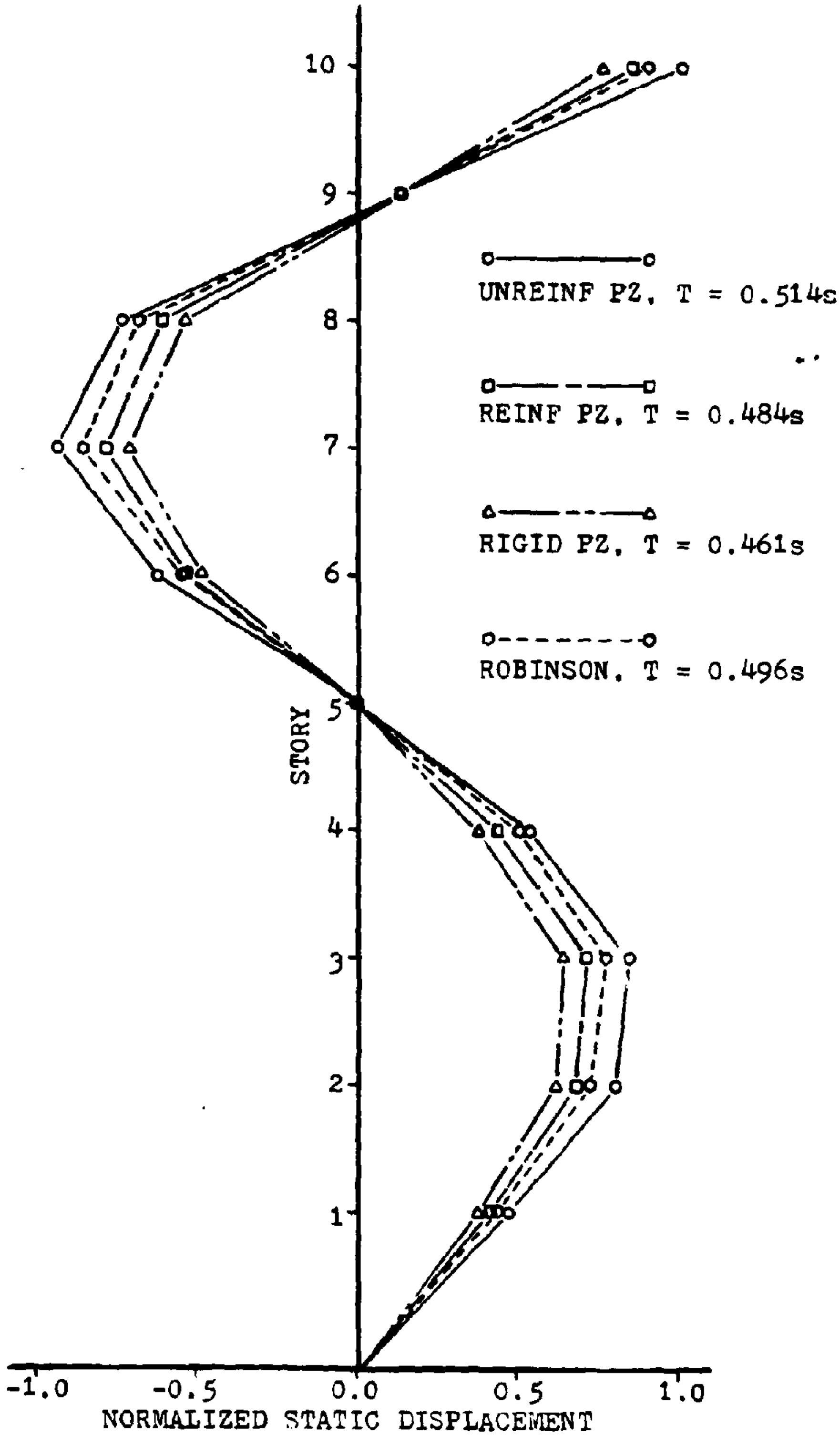

FIGURE 4.7- 10 UBC, THIRD MODE

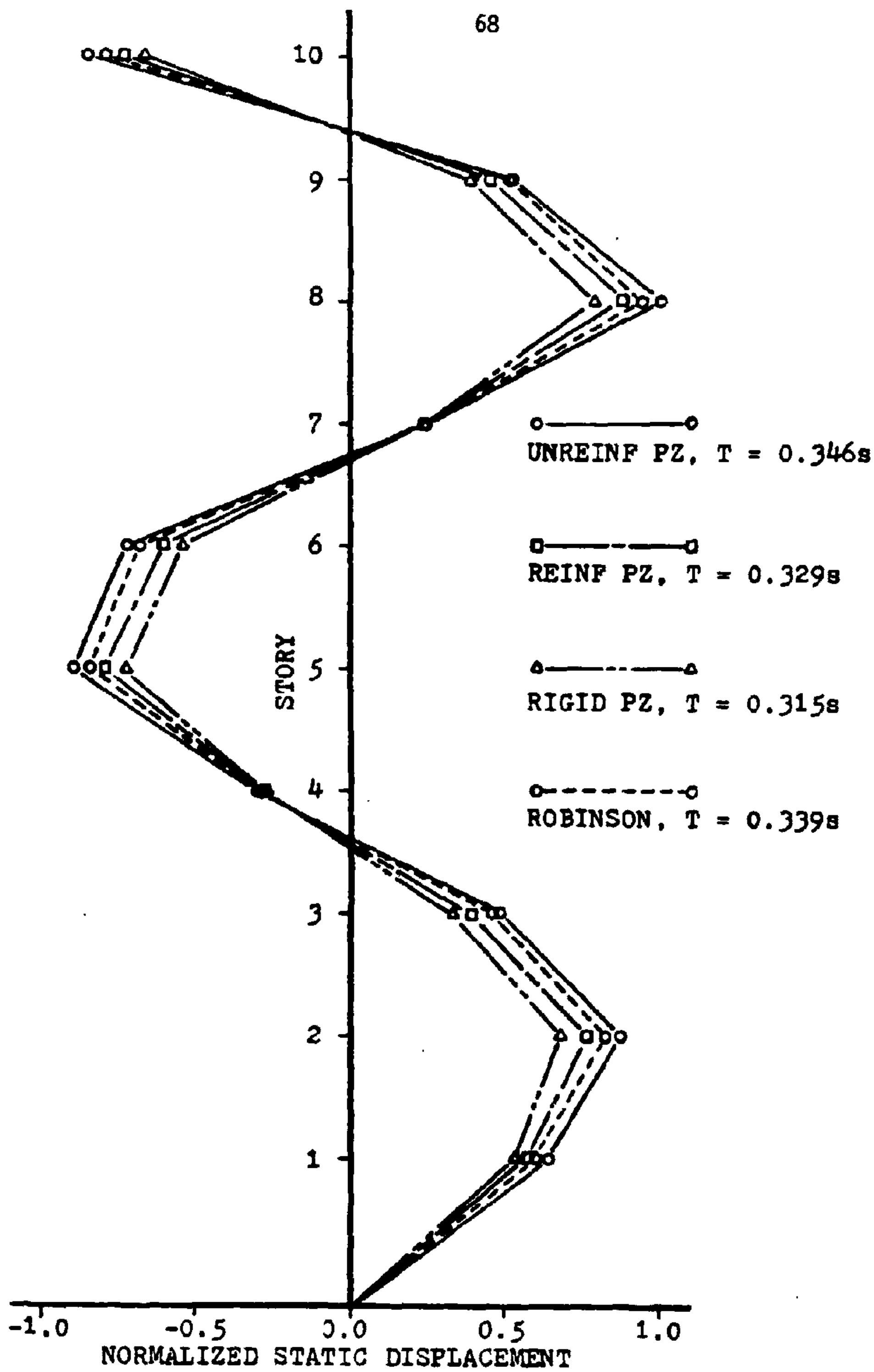

FIGURE 4.8- 10 UBC, FOURTH MODE

FIRST MODE

Case	Unreinforced	Reinforced	Rigid	Robinson
Period (sec)	1.040	0.960	0.915	0.967
Participation Factor	0.886	0.894	0.897	0.890
Relative Participation (%)	100	100	100	100

Story	Mode Shape			
4	1.4351	1.4262	1.4153	1.4311
3	1.1962	1.1952	1.1969	1.2008
2	0.8051	0.8145	0.8246	0.8061
1	0.3523	0.3694	0.3829	0.3517

SECOND MODE

Period (sec)	0.330	0.312	0.300	0.320
Participation Factor	-0.321	-0.317	-0.311	-0.319
Relative Participation (%)	36.2	35.5	34.7	35.8

Story	Mode Shape			
4	1.2158	1.2193	1.2154	1.2121
3	-0.2640	-0.2386	-0.1986	-0.2455
2	-1.3245	-1.3091	-1.2996	-1.3347
1	-0.9769	-0.9996	-1.0252	-0.9721

TABLE 4.1 - 4 UBC MODAL PROPERTIES

THIRD MODE

Case	Unreinforced	Reinforced	Rigid	Robinson
Period (sec.)	0.179	0.175	0.171	0.186
Participation Factor	0.184	0.175	0.168	0.181
Relative Participation (5)	20.8	19.6	18.7	20.3

Story	Mode Shape			
4	0.8052	0.8162	0.8370	0.8278
3	-1.3652	-1.3706	-1.3670	-1.3965
2	0.0319	0.0054	-0.0386	0.0766
1	1.3171	1.3051	1.2953	1.2667

FOURTH MODE

Period (sec)	0.122	0.121	0.121	0.134
Participation Factor	-0.109	-0.105	-0.100	-0.118
Relative Participation (%)	12.3	11.7	11.2	13.3

Story	Mode Shape			
4	0.3166	0.3151	0.3252	0.2987
3	-0.9363	-0.9365	-0.9488	-0.8859
2	1.3555	1.3652	1.3677	1.3417
1	-1.1949	-1.1840	-1.1685	-1.2507

TABLE 4.1 - 4 UBC MODAL PROPERTIES
(Continued)

FIRST MODE

Case	Unreinforced	Reinforced	Rigid	Robinson
Period (sec)	2.487	2.320	2.189	2.322
Participation Factor	1.444	1.450	1.452	1.492
Relative Participation (%)	100	100	100	100
Story	Mode Shape			
10	0.9335	0.9274	0.9284	0.9393
9	0.8864	0.8817	0.8828	0.8913
8	0.8107	0.8077	0.8071	0.8094
7	0.7292	0.7299	0.7289	0.7280
6	0.6301	0.6334	0.6316	0.6262
5	0.5276	0.5331	0.5317	0.5239
4	0.4159	0.4220	0.4212	0.4108
3	0.3066	0.3133	0.3146	0.3034
2	0.1981	0.2049	0.2083	0.1966
1	0.0956	0.1013	0.1054	0.0954

TABLE 4.2 - 10 UBC MODAL PROPERTIES

SECOND MODE

Case	Unreinforced	Reinforced	Rigid	Robinson
Period (sec)	0.880	0.820	0.779	0.835
Participation Factor	-0.543	-0.539	-0.544	-0.548
Relative Participation (%)	37.6	37.2	37.5	38.0

Story	Mode Shape			
10	0.9886	0.9860	0.9796	0.9918
9	0.6467	0.6520	0.6551	0.6531
8	0.1604	0.1696	0.1685	0.1359
7	-0.2381	-0.2202	-0.2171	-0.2509
6	-0.5701	-0.5532	-0.5505	-0.5794
5	-0.7519	-0.7420	-0.7386	-0.7521
4	-0.7954	-0.7955	-0.7939	-0.7895
3	-0.7074	-0.7168	-0.7198	-0.7009
2	-0.5160	-0.5312	-0.5398	-0.5112
1	-0.2670	-0.2821	-0.2934	-0.2656

TABLE 4.2 - 10 UBC MODAL PROPERTIES
(Continued)

THIRD MODE

Case	Unreinforced	Reinforced	Rigid	Robinson
Period (sec)	0.514	0.484	0.461	0.496
Participation Factor	0.339	0.323	0.321	0.330
Relative Participation (%)	23.5	22.3	22.1	22.9

Story	Mode Shape			
10	0.9045	0.9039	0.8968	0.8914
9	0.1166	0.1330	0.1475	0.1226
8	-0.6653	-0.6519	-0.6503	-0.6945
7	-0.8538	-0.8520	-0.8544	-0.8586
6	-0.5685	-0.5849	-0.5909	-0.5450
5	-0.0452	-0.0750	-0.0866	-0.0256
4	0.4797	0.4566	0.4467	0.4955
3	0.7579	0.7507	0.7446	0.7592
2	0.7219	0.7309	0.7340	0.7143
1	0.4257	0.4428	0.4548	0.4198

TABLE 4.2 - 10 UBC MODAL PROPERTIES
(Continued)

FOURTH MODE

Case	Unreinforced	Reinforced	Rigid	Robinson
Period (sec)	0.346	0.329	0.315	0.339
Participation Factor	-0.231	-0.224	-0.220	-0.229
Relative Participation (%)	16.0	15.4	15.2	15.9

Story	Mode Shape			
10	0.7521	0.7546	0.7516	0.7442
9	-0.4642	-0.4560	-0.4390	-0.4791
8	-0.8870	-0.8864	-0.8915	-0.8811
7	-0.2156	-0.2459	-0.2623	-0.2007
6	0.6386	0.6180	0.6146	0.6694
5	0.7984	0.8096	0.8154	0.7994
4	0.2743	0.3052	0.3166	0.2444
3	-0.4205	-0.3921	-0.3763	-0.4348
2	-0.7707	-0.7637	-0.7575	-0.7638
1	-0.5693	-0.5820	-0.5917	-0.5568

TABLE 4.2 - 10 UBC MODAL PROPERTIES
(Continued)

CHAPTER FIVE - INELASTIC ANALYSIS

5.1 Implementation of Inelastic Models

5.1.1 Methodology

In order to assess the effect that connection flexibility and strength limitation have on the full-range inelastic seismic response of a typical building frame, the four-story three-bay frame (4 UBC) was analyzed with the three sets of connection properties using two records of artificial horizontal ground acceleration. Both ground motions were of ten-second duration scaled to a peak acceleration of 1/3 g, and were derived from the standard Newmark-Hall response spectrum. Consistent with the previous modal analysis, only horizontal dynamic degrees of freedom at each story level were considered.

Inelastic analysis was accomplished using the program DRAIN-2D (15), fitted with an isoparametric finite element constrained to have only shear deformation to model the individual connection behavior. This finite element representation, rather than the use of infinitesimal rotational springs attached to rigid links as was done by Tang (40), is believed to be a superior model, since it does not imply a deformed shape of the connection that is physically unreasonable.

For comparative purposes, damping was taken as five percent of critical in the first and second modes, and was assumed to be of Rayleigh form:

$$\underline{C}_i = a_0 \, \underline{M} + a_1 \, \underline{K}_{fi} \tag{5.1}$$

where

$$a_0 = \frac{4\pi\lambda \, (T_1 - T_2)}{T_1^2 - T_2^2}$$

$$a_1 = \frac{T_1 T_2 \lambda (T_1 - T_2)}{\pi(T_1^2 - T_2^2)}$$

$\underline{C}_i$ = Incremental viscous damping matrix

$\underline{K}_{fi}$ = Incremental stiffness matrix of frame

$\underline{M}$ = Diagonal Mass Matrix

λ = 0.05, assumed damping of the first and second modes

T_1, T_2 = Periods of vibration of the first and second modes, respectively, as determined in Chapter Four.

This form of damping implies progressively larger dissipation in the higher modes given by:

$$\lambda_i = \frac{a_0 T_i}{4\pi} + \frac{a_1 \pi}{T_i} \quad , \qquad (5.2)$$

where: λ_i = Proportion of damping in mode i

T_i = Period of mode i .

The damping properties of 4 UBC as determined by Eqs. (5.1) and (5.2) are summarized in Table 5.1.

The integration time-step for use in DRAIN-2D was taken as 0.015 sec., a figure believed to be reasonable in view of the natural frequencies of the frame. Robinson (35) had previously obtained good results using a time-step of 0.02 sec. on the same frame; hence no further validation of the chosen increment was felt necessary.

DRAIN-2D incorporates the P-Δ effect by adding linearized geometric stiffness terms to the column shears, but this effect should not be of great importance for a frame the height of 4 UBC.

Case	λ	$a_0(s^{-1})$	$a_1(x10^{-2}s)$	λ_3	λ_4
Unreinforced	0.050	0.459	0.399	0.076	0.107
Reinforced	0.050	0.494	0.375	0.074	0.102
Rigid	0.050	0.517	0.359	0.073	0.099

TABLE 5.1 - 4 UBC DAMPING PROPERTIES

Panel Zone	b_1	b_2	τ_y(ksi)
1, 2, 3, 4	0.0365	0.0233	20.78
5,8	0.0360	0.0233	20.77
6,7	0.0360	0.0233	20.71
9,19	0.0486	0.0233	20.73
10,11	0.0486	0.0233	20.58
13,16	0.0486	0.0233	20.66
14,15	0.0496	0.0233	20.33

TABLE 5.2 - SECONDARY AND TERTIARY SLOPES
OF UNREINFORCED PZ'S

5.1.2 Connection Model

Figure 5.1 illustrates the finite element representation of a typical interior frame connection. Similar models were used throughout the frame, and were given material stress-strain properties according to the tri-linear formulation presented in Sec. 2.1. Since the unreinforced connection was the only connection type found to yield, as might be expected, the secondary and tertiary slopes of the reinforced connections became inconsequential. The shear yield of the unreinforced connections was adjusted for column gravity load interaction through Eq. (2.4).

Standard DRAIN-2D allows material properties to be modeled in a bi-linear fashion; hence two bi-linear finite elements were superimposed to achieve the required tri-linear unreinforced connection behavior, as is shown in Fig. 5.2. Actually, any piece-wise linear relationship of dimension *n* (n-linear) can be expressed through (n-1) bi-linear superpositions, the procedure for which is illustrated in Appendix B.

The tri-linear stress-strain relationships for the unreinforced connection case are summarized in Table 5.2. For reinforced connections, only the elastic shear stress-strain relationship is relevant, and for the rigid connection case all connection constitutive relations are disregarded. Once again, the panel zone thicknesses were adjusted using Eq. (2.10), thus permitting the full column and beam depths to be used in determining the physical connection size.

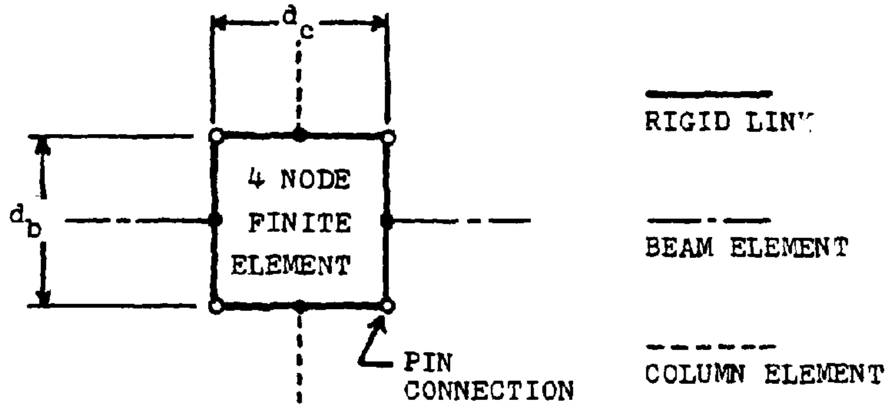

FIGURE 5.1- FINITE ELEMENT MODEL OF CONNECTION
(Element constrained to have only shear deformation)

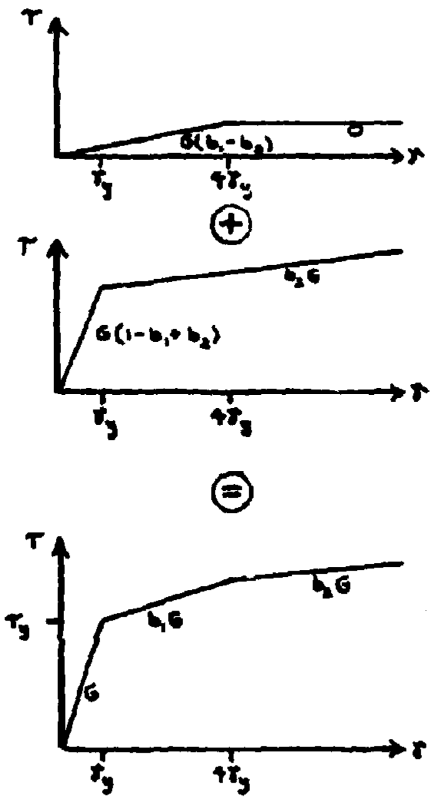

FIGURE 5.2- BI-LINEAR SUPERPOSTION
TO CREATE TRI-LINEAR RESULT

5.1.3 Beam/Column Models

The true hysteretic behavior of steel, as shown by Peterson, Oritz and Popov (23, 32), is quite complex and requires sophisticated mathematical techniques to model even simple tension specimens—techniques well beyond what can be incorporated into present non-linear dynamic analysis programs. Nevertheless, reasonable results can be obtained for purposes of comparison by using a simple bi-linear relationship to represent the plastic hinge moment-rotation behavior. One method of determining the plastic hinge properties is to first determine a suitable bi-linear approximation of the curvilinear moment-curvature relation at the cross-section under consideration. An assumption on the shape of moment diagram in the member then allows calculation of the plastic hinge behavior. This behavior may then, once again, be approximated as bi-linear, allowing easy incorporation into the computer program.

Although it is realized that the virgin moment-curvature relationship is not completely indicative of the full-range hysteretic behavior, it was used as the basis of the bi-linear approximation mentioned above. This virgin curve was determined for a given wide-flange section from the tensile stress-strain diagram of steel, assumed to be tri-linear (Fig. 5.3), by integrating across the cross-section to determine the value of moment corresponding to various values of strain and curvature.

Figure 5.3 illustrates the bi-linear approximation of the moment-curvature relationship. As was done in Ref. 40, the start of the secondary slope was taken as that value of moment corresponding to the yield moment of the cross-section, as this procedure has produced a good match with experimental results of full-scale dynamic frame tests.

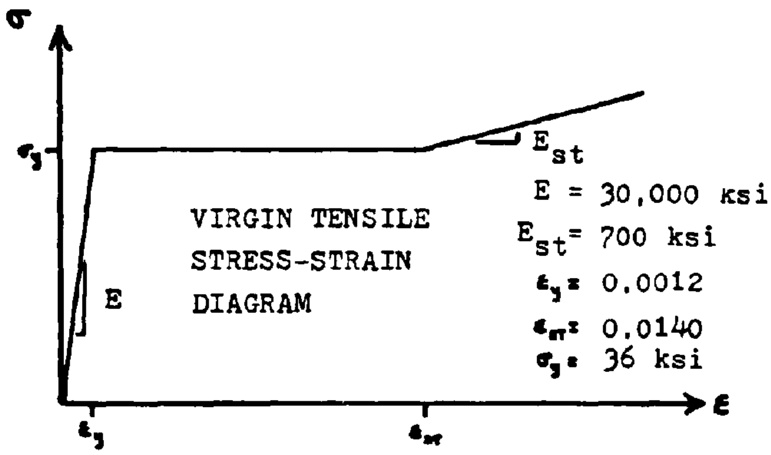

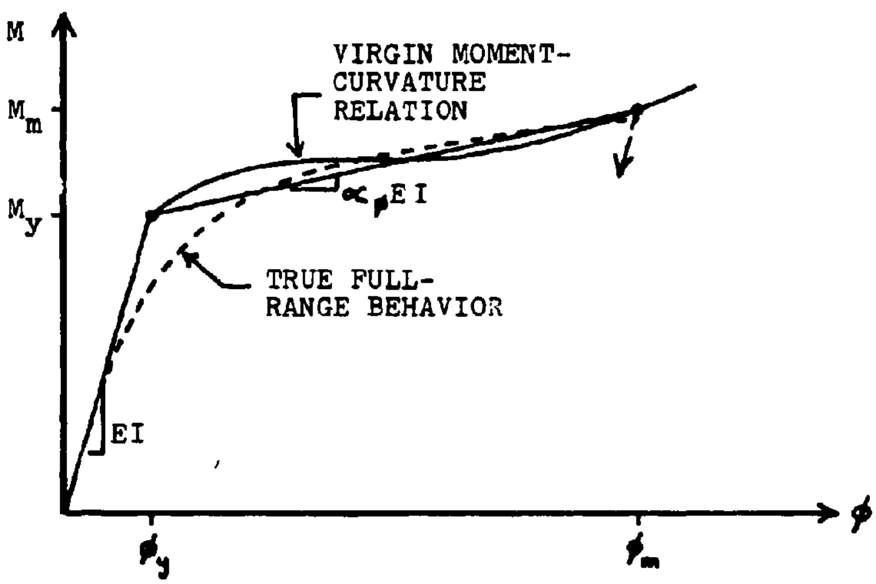

FIGURE 5.3- BI-LINEAR APPROXIMATION
OF MOMENT-CURVATURE RELATIONSHIP

The shape of the moment diagram (for purposes of calculating hinge properties) was assumed to be that of a beam of length L in pure antisymmetrical bending (Fig. 5.4), a reasonable assumption in view of the dominant form of frame deformation. Since this assumption implies a point of contraflexure at mid-span of the beam, a cantilever of length L/2 can be used to calculate the load-deflection properties. A cantilever of this length subjected to a load at the tip will undergo a deflection found by double-integration of the curvature diagram. From the moment-area theorem, the tip deflection is found to be:

$$\delta = \begin{cases} \dfrac{1}{24}\dfrac{PL^3}{EI} & \dfrac{PL}{2} \leq M_y \\ \left[\dfrac{\phi_y^3}{6}\left(\dfrac{EI}{P}\right)^2 - \dfrac{L^2\phi_y}{8}\right]\left(\dfrac{1}{\alpha_\phi} - 1\right) + \dfrac{PL^3}{24EI\alpha_\phi} & \dfrac{PL}{2} > M_y \end{cases} \tag{5.3}$$

where: $\delta = L\theta/2$ = Deflection at cantilever tip

$P = 2M/L$ = Load at cantilever tip

I = Moment of inertia of cross-section, strong axis in bending

$\phi_y = M_y/EI$ = Yield curvature

α_ϕ = Second slope of moment-curvature relation, as proportion of EI.

The load-deflection relationship, as determined by Eq. (5.3), is found to be somewhat curvilinear in the inelastic range (Fig. 5.5), but may be approximated with good accuracy as linear. This linearization assumption implies a tip deflection in the inelastic range given by:

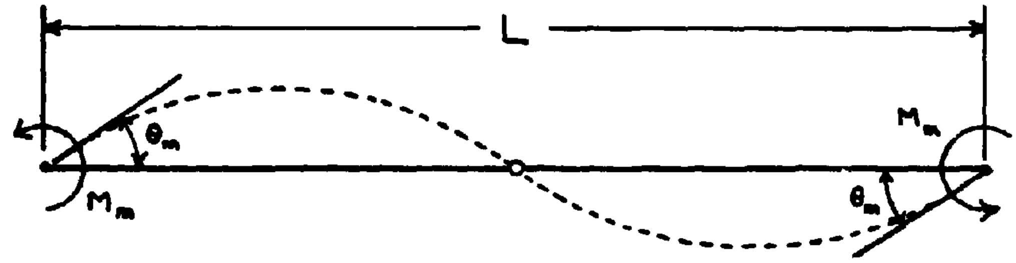

ANTI-SYMMETRICAL BEAM BENDING

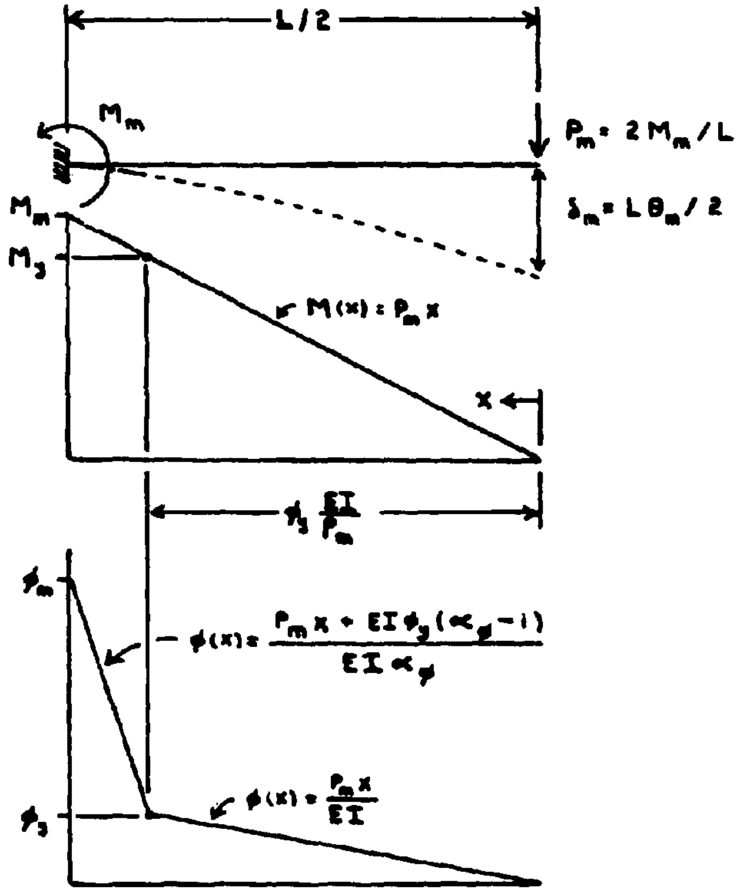

CANTILEVER DEFLECTION

MOMENT DIAGRAM

CURVATURE DIAGRAM

FIGURE 5.4- CALCULATION OF PLASTIC HINGE PROPERTIES

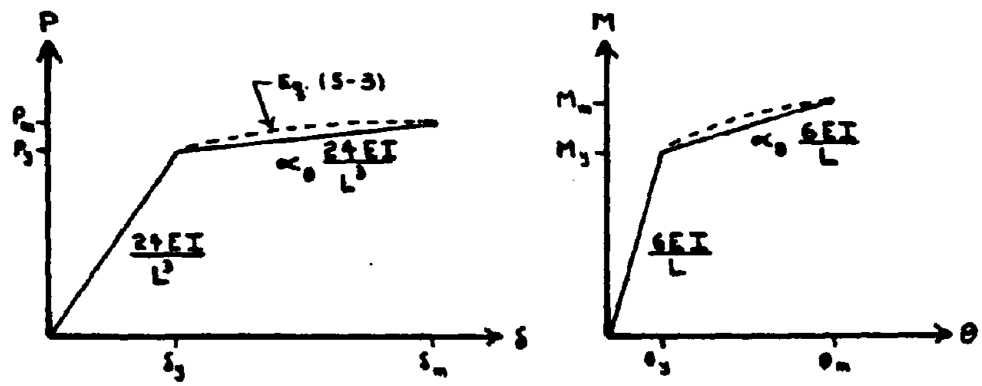

FIGURE 5.5- BI-LINEAR APPROXIMATION OF P-δ AND M-θ RELATIONS

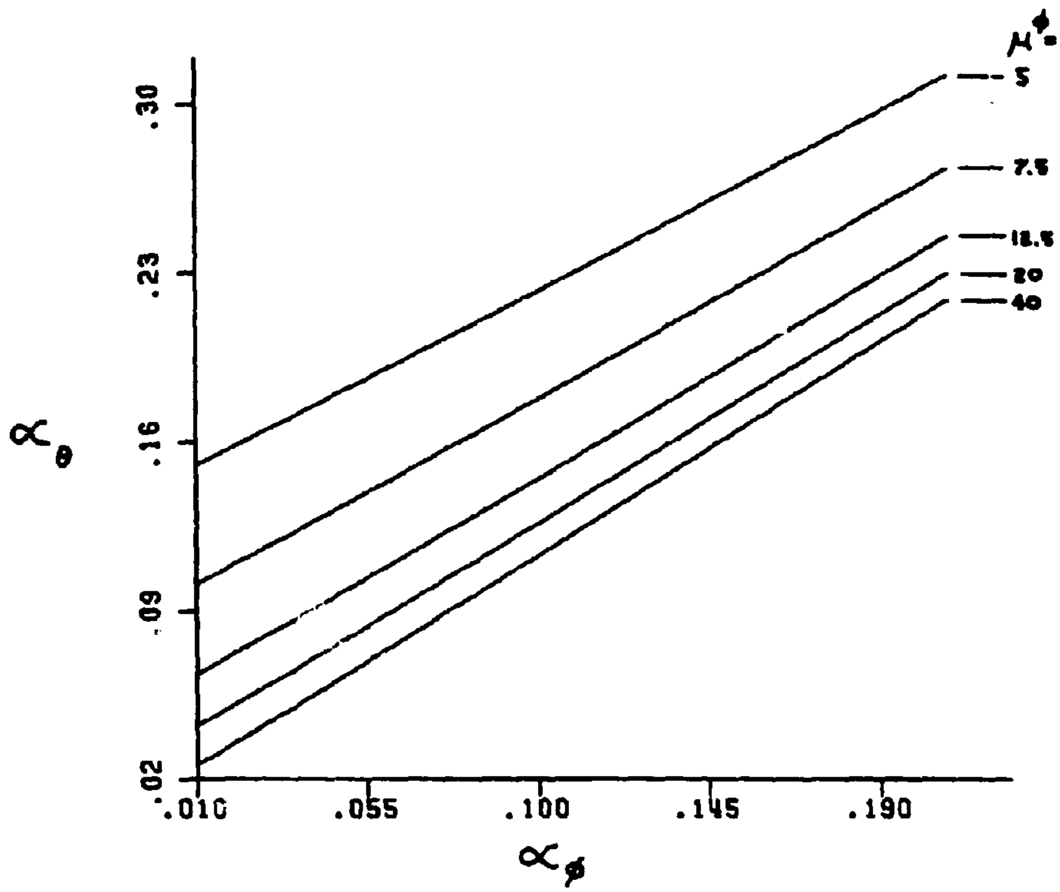

FIGURE 5.6- RELATION OF SECONDARY CURVATURE AND ROTATION SLOPES

$$\delta = \frac{P_y L^3}{24EI} + (P - P_y)\frac{L^3}{24EI\alpha_\theta} \qquad P \geq P_y \qquad (5.4)$$

where: P_y = Tip load corresponding to M_y

α_θ = Secondary secant slope of the load-deflection relation, as proportion of $24EI/L^3$.

Since $P_y L/2 = M_y = EI\phi_y$, this expression reduces to

$$\delta = \frac{\phi_y L^2}{12}(1 - 1/\alpha_\theta) + \frac{PL^3}{24EI\alpha_\theta} \quad .$$

Equating this result with the portion of Eq. (5.3) valid for the inelastic range permits an expression for α_θ to be obtained. After introducing the curvature ductility factor $\mu^\phi = \phi m/\phi_y$, this expression becomes:

$$\alpha_\theta = \frac{2(\alpha_\phi(\mu^\phi - 1) + 1)^2}{(3\mu^\phi - 1) + \alpha_\phi(2\mu^{\phi 2} - 3\mu^\theta + 1)} \quad . \qquad (5.5)$$

This function is plotted in Fig. 5.6, and can be seen to be quite linear over the range of interest. Ideally, the values of μ^ϕ and α_ϕ would be obtained through an iterative process—by first assuming appropriate values and then carrying out the non-linear dynamic analysis to obtain a revised estimate of the curvature ductility demand. This revised value would permit an improved estimate of the bi-linear moment-curvature approximation, and then from Eq. (5.5) a better estimate of α_θ could be obtained for use in the next analysis. This iteration technique, however, could be quite costly in view of the expense of non-linear dynamic analysis. For purposes of this study, the assumed curvature ductility for use in Eq. (5.5) was simply taken as thirty and α_ϕ was found corresponding to

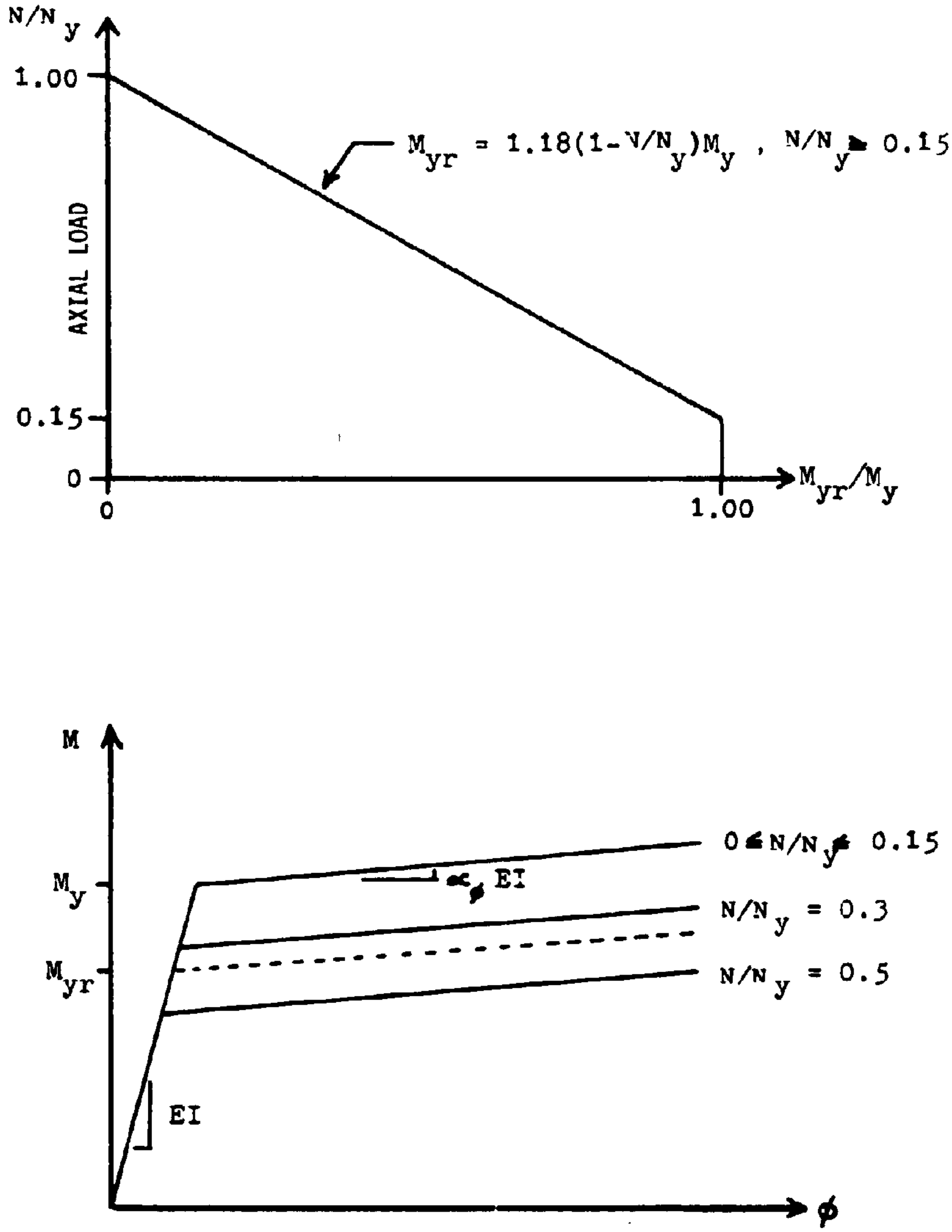

FIGURE 5.7- AXIAL LOAD INTERACTION WITH MOMENT CAPACITY

this ductility from the aforementioned virgin moment-curvature diagram, and no iteration was performed. This simplified procedure will be conservative in the calculation of beam/column ductilities and damage ratios, as α_θ is likely to be underestimated, thus resulting in more inelastic deformation for any required amount of energy dissipation. The bi-linear properties of the beams and columns comprising 4 UBC are summarized in Table 5.3.

The moment capacity of the columns was reduced corresponding to the instantaneous axial load present in them as determined by the ASCE interaction criteria of Art. 7.2 in Ref. 2 (Fig. 5.7). Only axial cross-sectional effects were considered; thus shear interaction and column buckling were ignored. Beams were assumed to have no axial deformation; thus they were permitted to develop their full moment capacity; again, buckling effects were ignored. Plastic hinges were assumed to form only at the beam and column ends, in keeping with the assumptions used to calculate the bi-linear hinge properties.

5.2 Measures of Damage

There is considerable debate over what parameters provide good measures of structural damage. For purposes of this study, however, absolute quantities of damage need not be determined with precision, as only comparative measures are needed. Hence the common definitions of beam and column damage, namely curvature and rotation ductility demand, were adopted:

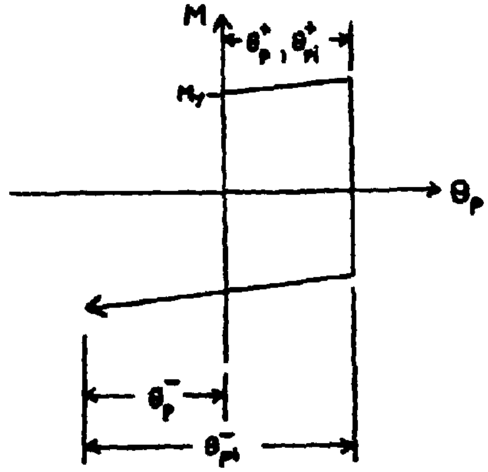

FIGURE 5.8- PLASTIC HINGE BEHAVIOR AND DAMAGE PARAMETERS

Member	M_y(k - in)	α_ϕ	α_θ
10 x 39	1519	0.0167	0.0375
10 x 33	1260	0.0164	0.0372
16 x 31	1699	0.0176	0.0383
16 x 26	1379	0.0173	0.0380

TABLE 5.3 - PLASTIC HINGE PROPERTIES OF BEAMS AND COLUMNS (MATCHED @ μ^ϕ = 30)

$$\mu^{\phi} = \frac{\phi_m}{\phi_y} = \begin{cases} \dfrac{|M_m| - M_y}{\alpha_{\phi} M_y} + 1 & |M_m| \geq M_y \\ |M_m|/M_y & |M_m| \leq M_y \end{cases} \tag{5.6}$$

$$\mu^{\theta} = 1 + \frac{|\theta_{pl}|}{\theta_y} \tag{5.7}$$

where: μ^{ϕ} = Curvature ductility demand

μ^{θ} = Rotation ductility demand

θ_{pl} = Maximum plastic hinge rotation

θ_y = $M_y L/6EI$ = Yield rotation of a member in antisymmetric bending, adjusted for gravity loads via Fig. 5.7

M_m = Maximum end moment.

Values greater than one suggest that inelastic behavior has occurred in the member, with values greater than ten typically considered to imply extensive damage. The yield moments used in these definitions, in the case of column ductility calculations, were adjusted for the presence of axial gravity loads in accordance with Fig. 5.7. This procedure, though debatable, provides an adjustment for the approximate average axial column load experienced during the earthquake excitation.

Two further measures were used to express beam and column damage, those being: Normalized Peak Plastic Rotation (NPPR) and Normalized Cumulative Plastic Rotation (NCPR), where:

$$\text{NPPR} = \frac{\theta_p^+ + |\theta_p^-|}{\theta_y} \tag{5.8}$$

$$NCPR = \frac{\Sigma\theta^{+}_{pi} + |\Sigma\theta^{-}_{pi}|}{\theta_y} \tag{5.9}$$

where: θ^{+}_{p}, θ^{-}_{p} = The maximum positive and negative plastic hinge rotations, respectively

$\Sigma\theta^{+}_{pi}$, $\Sigma\theta^{-}_{pi}$ = Sum of all plastic hinge rotations in the positive and negative directions, respectively.

Any values of NPPR and NCPR greater than zero indicate inelastic behavior, while identical values of NPPR and NCPR suggest that only one inelastic hinge excursion has occurred.

The definitions of panel zone damage are analogous to the beam/column parameters, and take the form:

$$\mu_{pz} = |\gamma_m/\gamma_y| \tag{5.10}$$

$$NPPD = \frac{\gamma^{+}_{p} + |\gamma^{-}_{p}|}{\gamma_y} \tag{5.11}$$

$$NCPD = \frac{\Sigma\gamma^{+}_{pi} + \Sigma\gamma^{-}_{pi}}{\gamma_y} \tag{5.12}$$

where: μ_{PZ} = Panel Zone Ductility Demand

NPPD = Normalized Peak Plastic Deformation

NCPD = Normalized Cumulative Plastic Deformation

γ_m = Maximum shear deformation occurring in the PZ

γ^{+}_{p}, γ^{-}_{p} = The maximum positive and negative plastic panel zone deformation, respectively

$\Sigma\gamma^{+}_{pi}$, $\Sigma\gamma^{-}_{pi}$ = Sum of all plastic PZ deformations in the positive and negative directions, respectively.

Any value of μ_{pz} less than one indicates elastic panel zone behavior, values between one and four imply that the tri-linear stress-strain model reached its secondary slope, while values greater than four suggest that the final tertiary slope was achieved at some point in the earthquake excitation. It should be noted that connections are capable of developing very high ductilities without impairment of their load-carrying capability—values in excess of 100 have been recorded in experimental pseudo-static cyclic tests (16).

5.3 Discussion of Results

5.3.1 General Frame Response

The use of unreinforced panel zones in the connection design produced a frame that dissipated energy through inelastic connection deformation (Figs. 5.9 , 5.12) and prevented plastic hinges from forming in the beams and columns at all locations except at the fixed supports of the frame base. Conversely, reinforced or rigid connections dissipated no energy, thus forcing inelastic behavior to occur in the beams and columns (Figs. 5.10, 5.11, 5.13, 5.14). The greatest number of plastic hinges formed in the frame with rigid connections. Nevertheless, inelastic behavior occurred extensively throughout the frame regardless of the connection properties and earthquake excitation, and was most severe in the first and second stories on the interior of the frame. Somewhat surprisingly, the maximum top story drift (Figs. 5.15, 5.16) was not appreciably affected by the physical behavior of the connection. The computed displacement envelopes illustrate that there is no clear relationship between the lateral stiffness properties of the frames (as determined in Chapter

Four) and their maximum story drifts. The most rigid frame (i.e., with rigid PZ's), for example, exhibited the softest first story of all the cases examined. It is difficult to draw a meaningful conclusion from this, however, as the maximum drifts occurred at different times depending upon the connection design.

Figures 5.17, 5.19, 5.21, 5.23, 5.25, and 5.27 display the time history of the frames' top story horizontal displacement, and suggest that the motion was dominated by the fundamental mode of vibration. The erratic hystereses illustrated in Figs. 5.18, 5.20, 5.22, 5.24, 5.26 and 5.28, however, imply that higher vibrational modes influenced the frames' base shear force.

Typically, in terms of ductility demand and normalized plastic distortion, the frame with unreinforced connections exhibited comparatively higher measures of damage (in th PZ's) than did the frame with reinforced and rigid connections (in the beams and columns). Since panel zones are capable of tolerating extremely large inelastic deformations—much larger than beams or columns—this does not necessarily imply that the frame as a whole was in any more danger when the connections were left unreinforced, however.

5.3.2 Behavior of Frame with Unreinforced PZ's

The behavior of the panel zones for this case is illustrated by Figs. 5.35 and 5.36, for QKE no. 1, and by Figs. 5.49 and 5.50 for QKE no. 2. The results indicate that the panel zones undergo significant inelastic deformation, achieving the tertiary slope of the tri-linear stress-strain model. Hysteresis loops for connections 4, 10 and 14, which are typical of all connections undergoing inelastic deformation, are shown in Figs. 5.29 through 5.34.

Since a connection in a state of shear yield limits the forces that can be transferred to the adjacent beams and columns, these surrounding elements remained elastic during the excitation and thus experienced no permanent damage. The sole exception to this were the plastic hinges that formed at the fixed supports at the frame base, and even at these locations damage was less severe when unreinforced connections were employed. This phenomenon is illustrated in Figs. 5.39, 5.40, 5.43, 5.44, 5.47, 5.48, 5.53, 5.54, 5.57, 5.58, 5.61, and 5.62.

The ductilities and normalized plastic deformations found in the panel zones suggest that for these levels of earthquake excitation, 4 UBC was in no imminent danger when the panel zones were left unreinforced.

5.3.3 Behavior of Frame with Reinforced and Rigid PZ's

The connection design procedure presented in Sec. 3.2, as expected, produced a connection that remained elastic during plastic hinge formation in the surrounding beams and columns. The rigid connection case—a mathematical abstraction that cannot occur in reality—also forced all inelastic behavior to occur in the beams and columns. Figures 5.35 and 5.49 illustrate the effect connection reinforcement has on the stresses induced in the panel zone, and show that Eqs. (3.5) and (3.6) produced a fairly efficient utilization of connection materials throughout the frame.

The ductility requirements of the beams and columns (Figs. 5.37 through 5.44 and 5.51 through 5.58) suggest that only moderate damage at worst, was sustained by these elements. Again, the frame was in no immediate danger of collapse. Figures 5.45 through 5.48 and 5.59 through 5.62 imply that only a few inelastic cycles, often only one, occurred in the beams and columns as suggested by nearly identical or identical values of NPPR and NCPR. This is in contrast to the unreinforced connections that underwent several inelastic cycles.

In all cases, rigid connections induced more damage in the beams and columns that did reinforced connections (Figs. 5.37 through 5.48 and 5.51 through 5.62). This result was also shown experimentally by Bertero et al. (6) in a test of frame subassemblages where beams and columns experienced greater inelastic deformation when more rigid panel zones were used in otherwise identical assemblies. This beneficial effect is believed to be caused by elastic relaxation of the panel zone which better distributes forces around the connection to elements in a better position to carry any excessive loads.

5.3.4 General Interpretation

From the viewpoint of overall seismic structural response, the use of unreinforced connections was not shown to be inherently inferior to the use of reinforced connections in a frame design. The two design options merely provide a choice of the energy dissipating mechanism—either through inelastic deformation in the connection itself or via plastic hinge rotation in the beams and columns. The first option will require comparitively greater inelastic excursions and ductility demands, but since panel zones are by nature capable of tolerating greater demands than beams and columns, this cannot be said to be necessarily bad.

The inelastic analysis has also shown that more elastically rigid connections induce more inelastic deformation in the surrounding beams and columns. This implies that if a non-linear dynamic analysis is performed in which connection flexibility is ignored but the physical connection size is modeled, the result will be a conservative estimation of the beam and column ductility demands. It also implies that for a connection designed to remain elastic, the use of more flexible diagonal stiffeners—as opposed to the use of doubler plates—would produce even fewer demands on the required energy dissipation of the beams and columns.

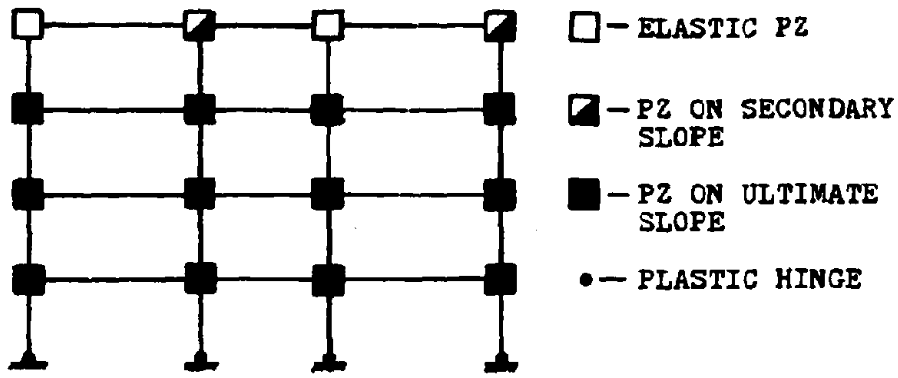

FIGURE 5.9- QKE 1
INELASTIC BEHAVIOR OF FRAME WITH UNREINFORCED PZs

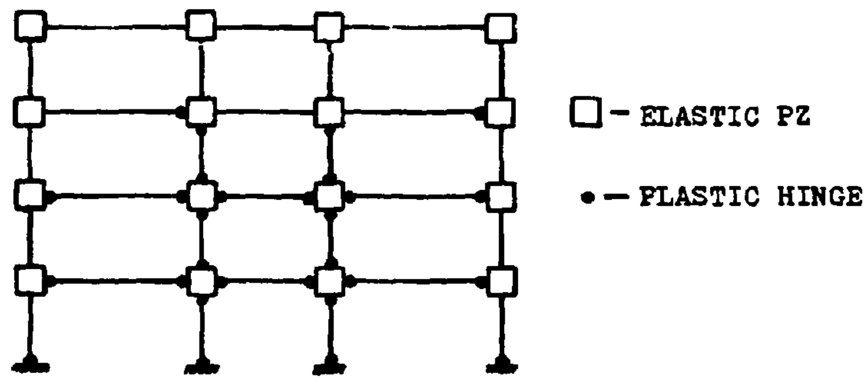

FIGURE 5.10- QKE 1
INELASTIC BEHAVIOR OF FRAME WITH REINFORCED PZs

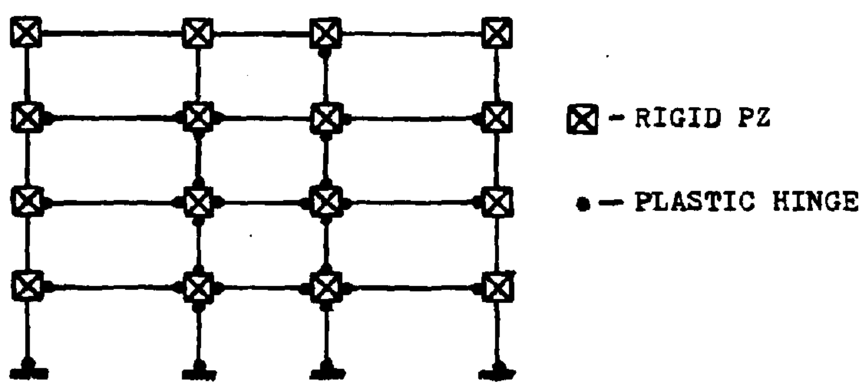

FIGURE 5.11- QKE 1
INELASTIC BEHAVIOR OF FRAME WITH RIGID PZs

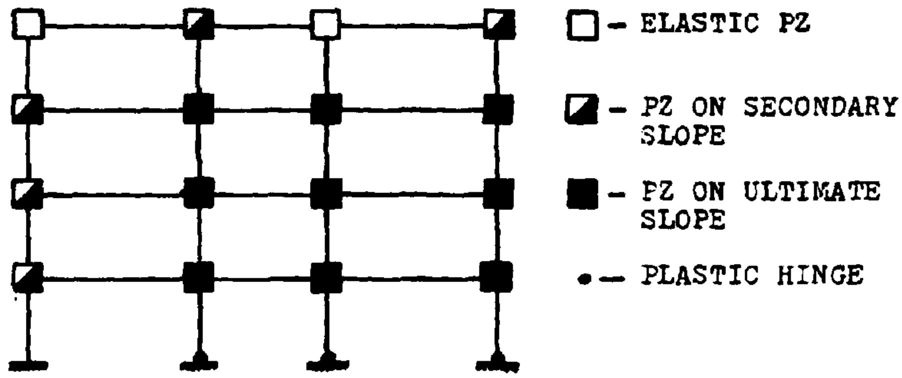

FIGURE 5.12- QKE 2

INELASTIC BEHAVIOR OF FRAME WITH UNREINFORCED PZs

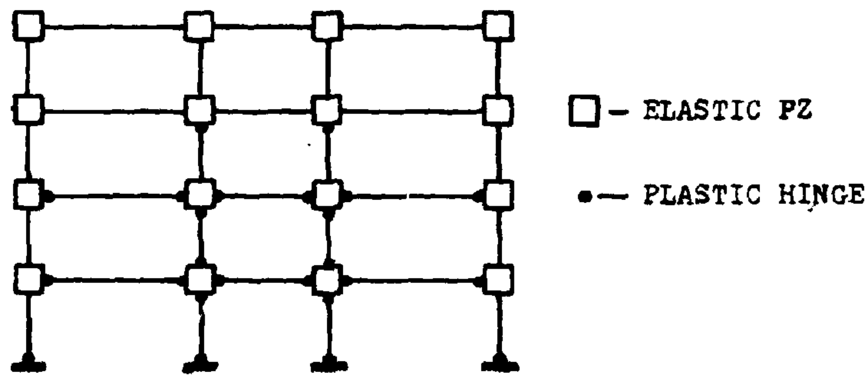

FIGURE 5.13- QKE 2

INELASTIC BEHAVIOR OF FRAME WITH REINFORCED PZs

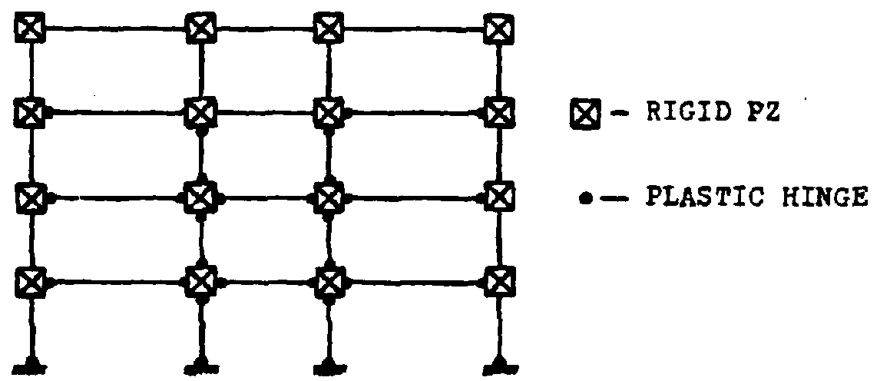

FIGURE 5.14- QKE 2

INELASTIC BEHAVIOR OF FRAME WITH RIGID PZs

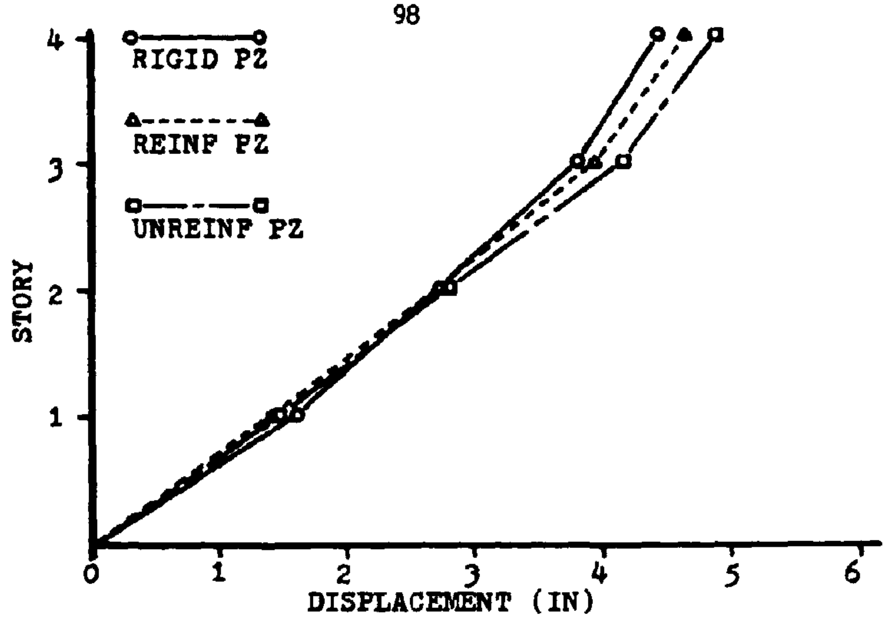

FIGURE 5.15- QKE 1, MAXIMUM STORY DISPLACEMENT ENVELOPES

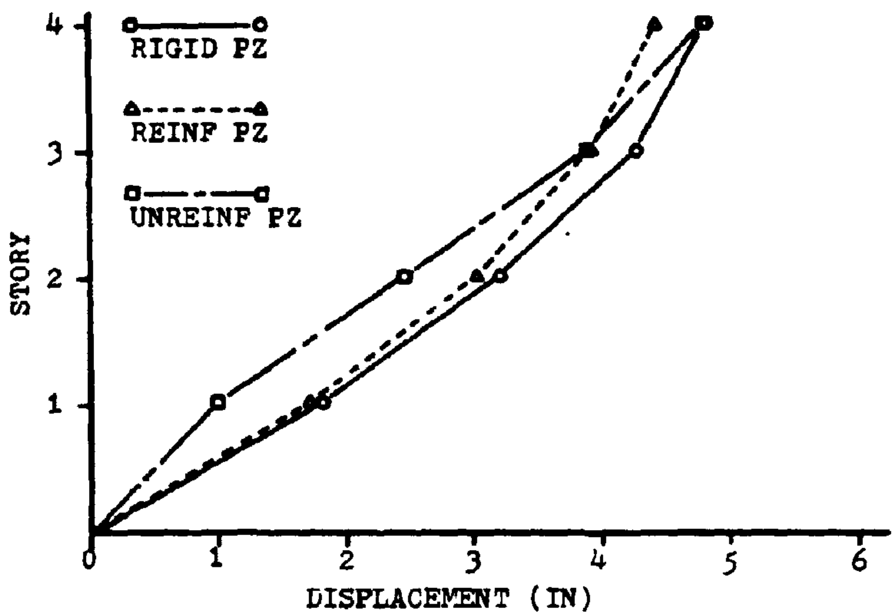

FIGURE 5.16- QKE 2, MAXIMUM STORY DISPLACEMENT ENVELOPES

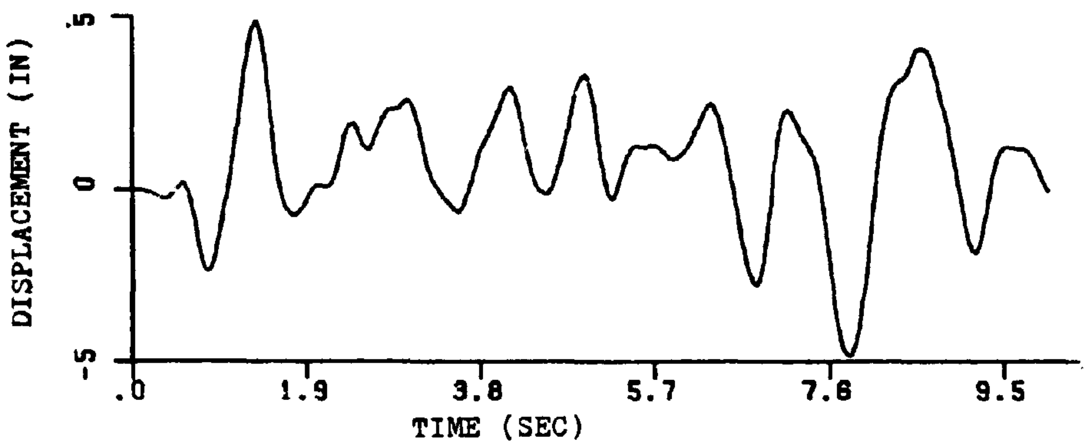

FIGURE 5.17- QKE 1, UNREINFORCED CONNECTION CASE
TOP STORY HORIZONTAL DISPLACEMENT vs TIME

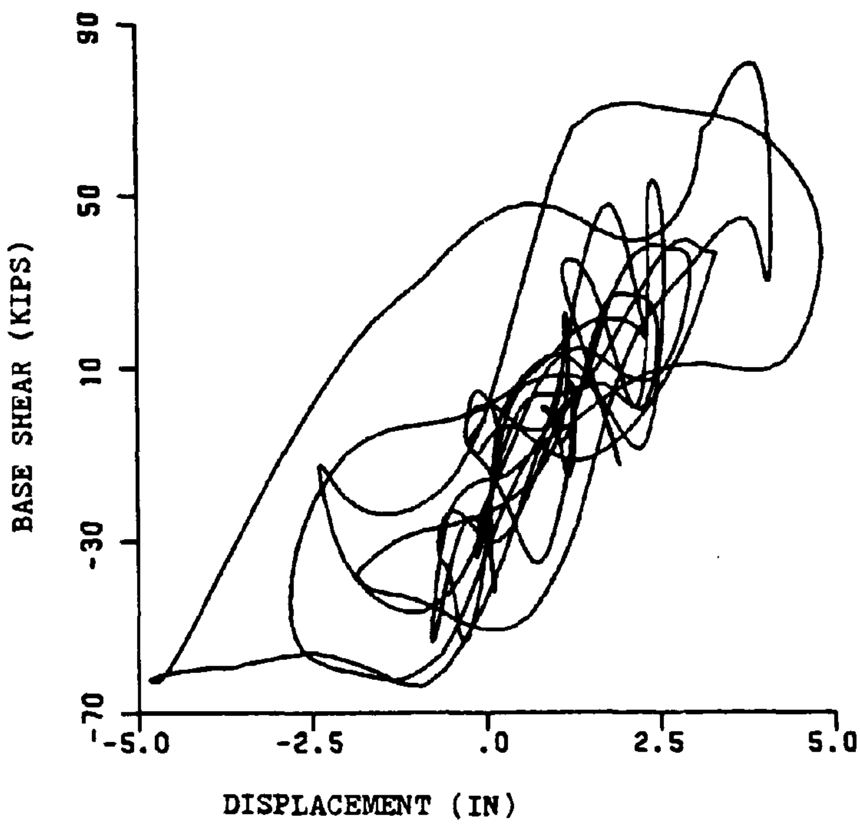

FIGURE 5.18- QKE 1, UNREINFORCED CONNECTION CASE
BASE SHEAR vs TOP STORY HORIZONTAL DISPLACEMENT

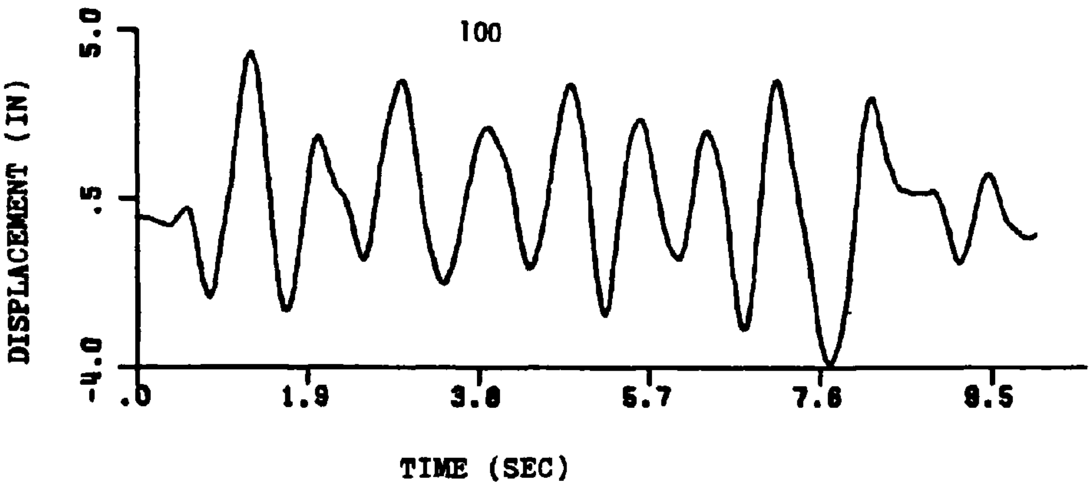

FIGURE 5.19- QKE 1, REINFORCED CONNECTION CASE
TOP STORY HORIZONTAL DISPLACEMENT vs TIME

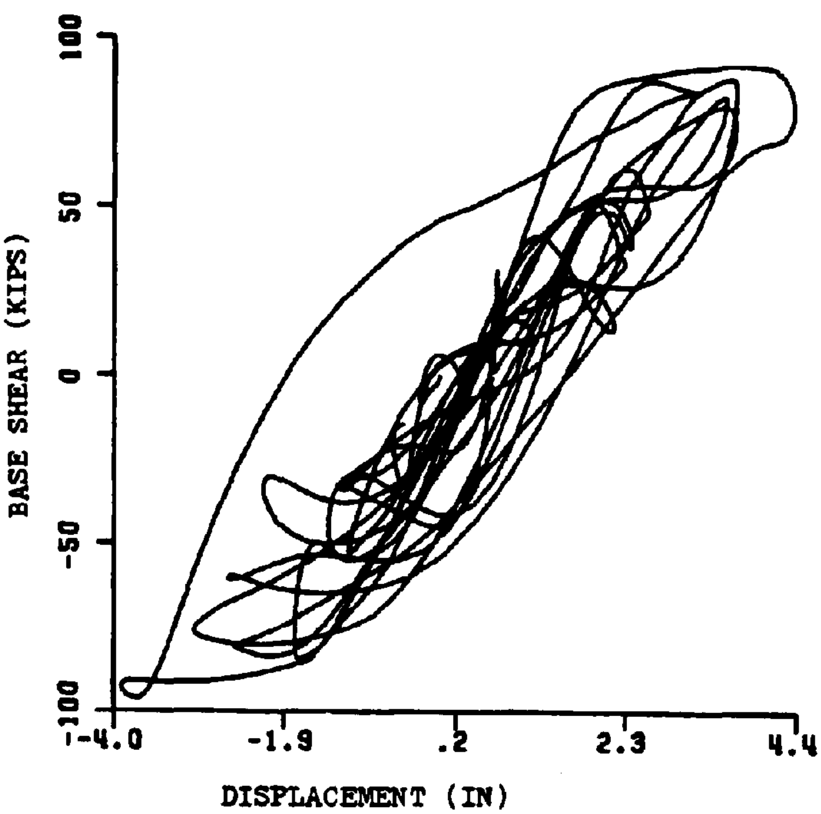

FIGURE 5.20- QKE 1, REINFORCED CONNECTION CASE
BASE SHEAR vs TOP STORY HORIZONTAL DISPLACEMENT

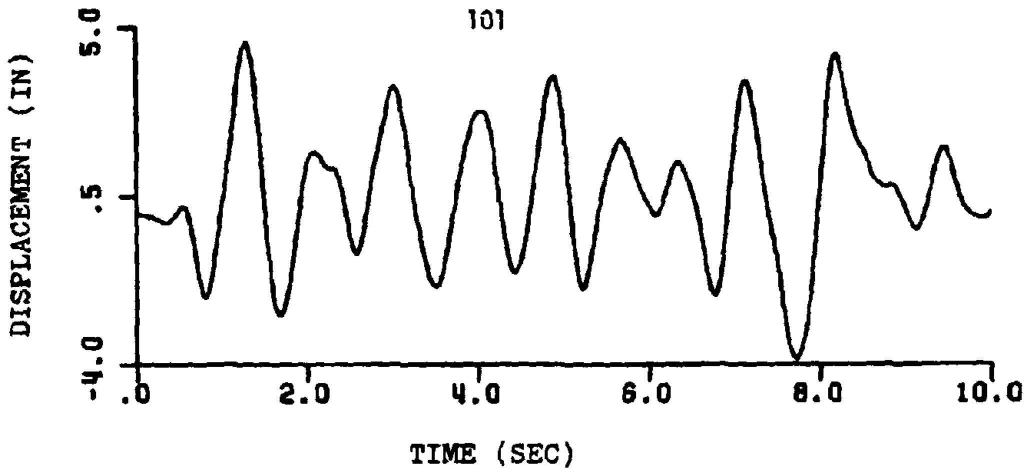

FIGURE 5.21- QKE 1, RIGID CONNECTION CASE
TOP STORY HORIZONTAL DISPLACEMENT vs TIME

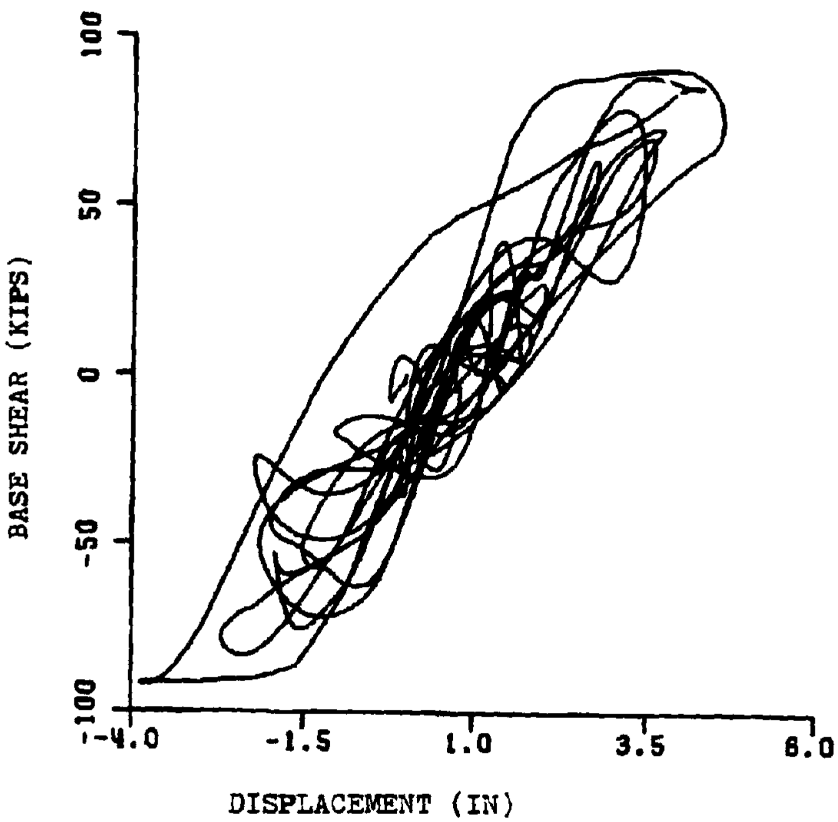

FIGURE 5.22- QKE 1, RIGID CONNECTION CASE
BASE SHEAR vs TOP STORY HORIZONTAL DISPLACEMENT

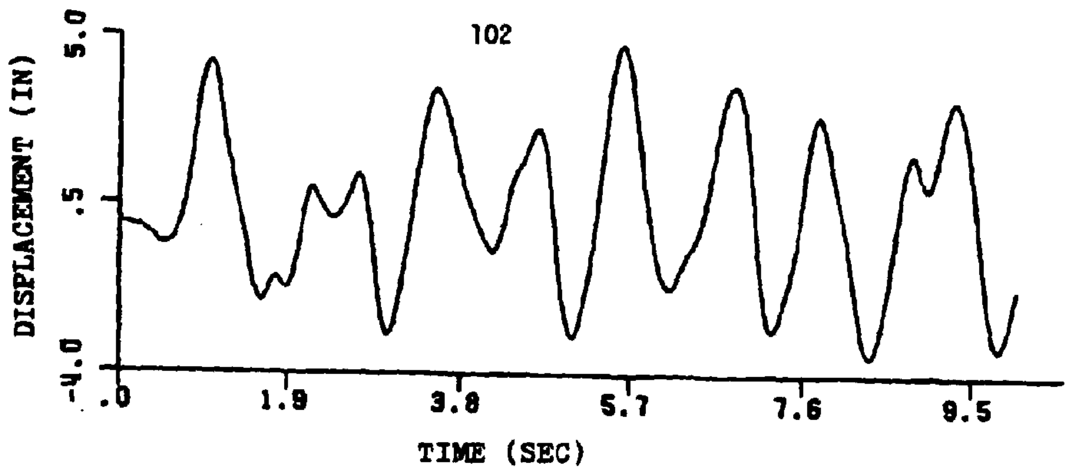

FIGURE 5.23- QKE 2, UNREINFORCED CONNECTION CASE
TOP STORY HORIZONTAL DISPLACEMENT vs TIME

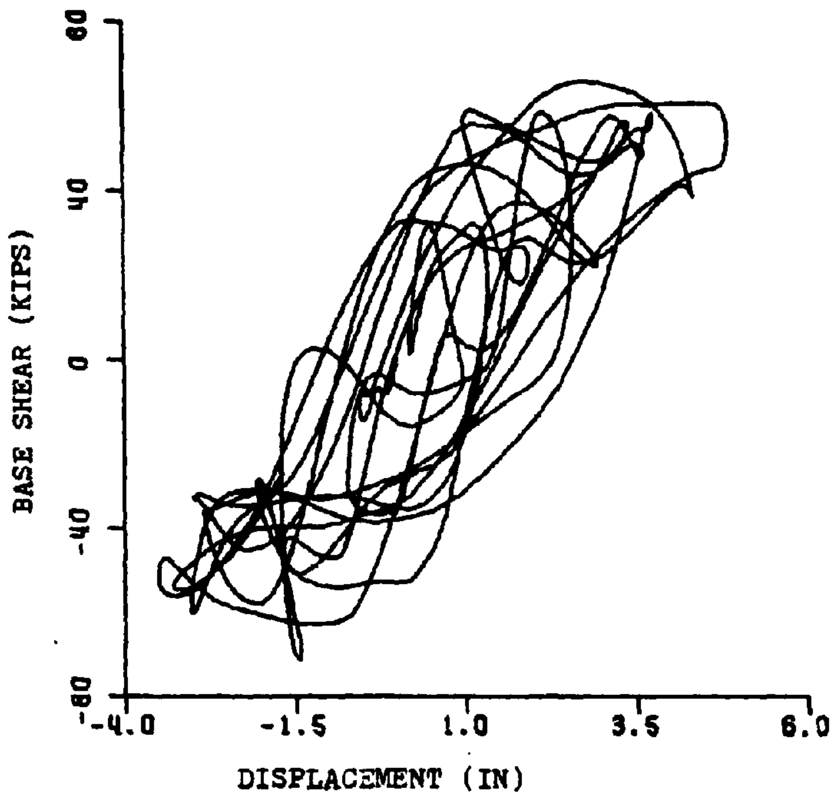

FIGURE 5.24- QKE 2, UNREINFORCED CONNECTION CASE
BASE SHEAR vs TOP STORY HORIZONTAL DISPLACEMENT

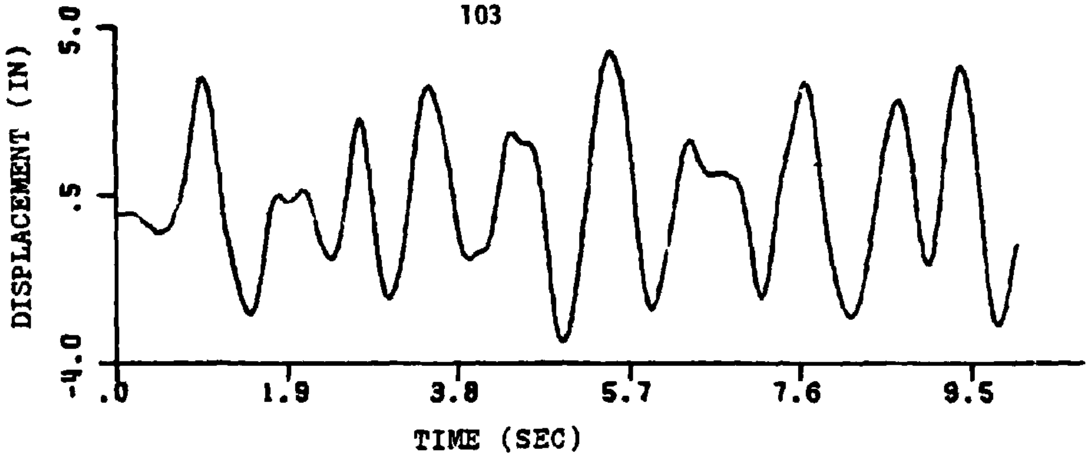

FIGURE 5.25- QKE 2, REINFORCED CONNECTION CASE
TOP STORY HORIZONTAL DISPLACEMENT vs TIME

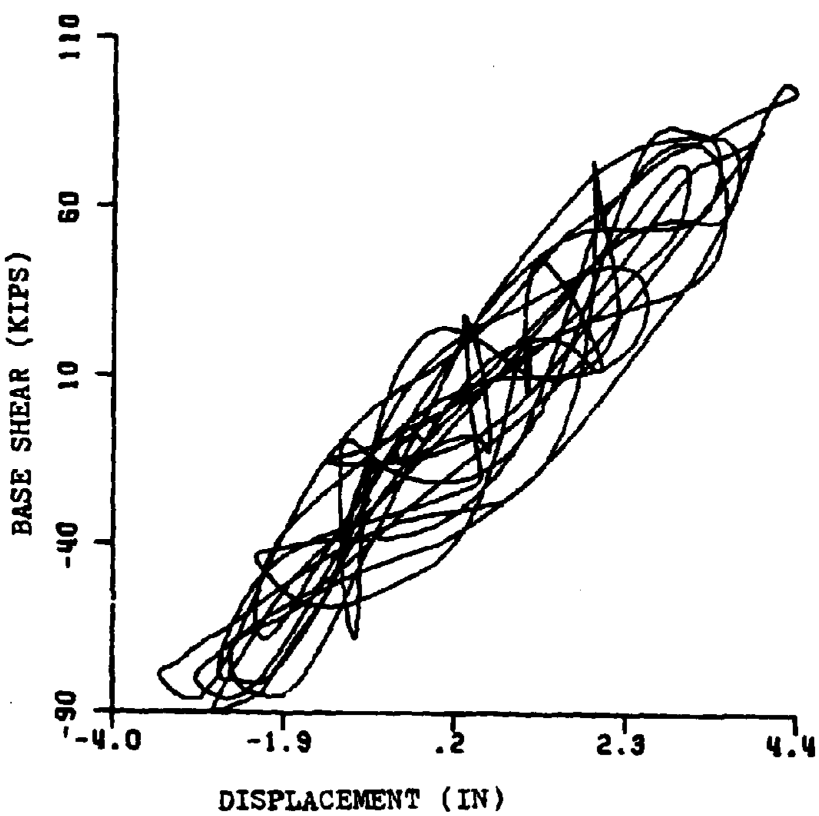

FIGURE 5.26- QKE 2, REINFORCED CONNECTION CASE
BASE SHEAR vs TOP STORY HORIZONTAL DISPLACEMENT

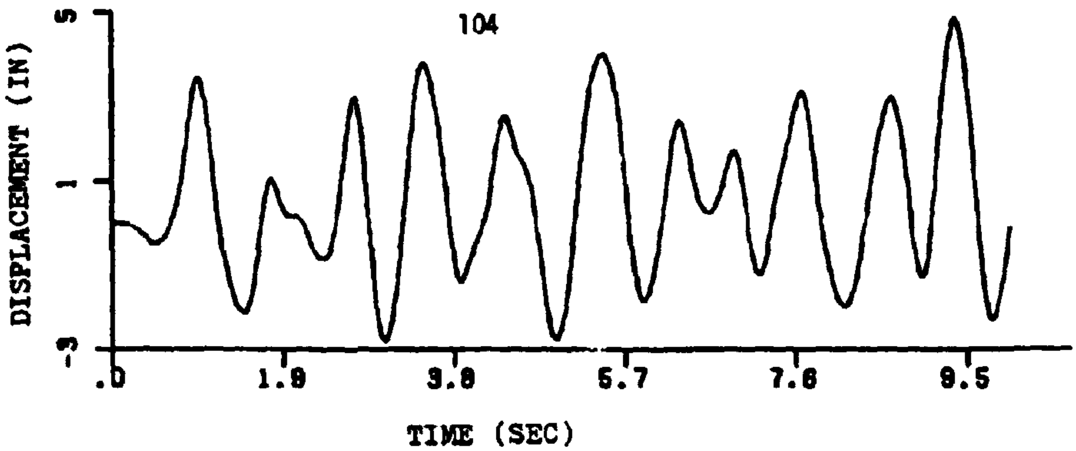

FIGURE 5.27- QKE 2, RIGID CONNECTION CASE
TOP STORY HORIZONTAL DISPLACEMENT vs TIME

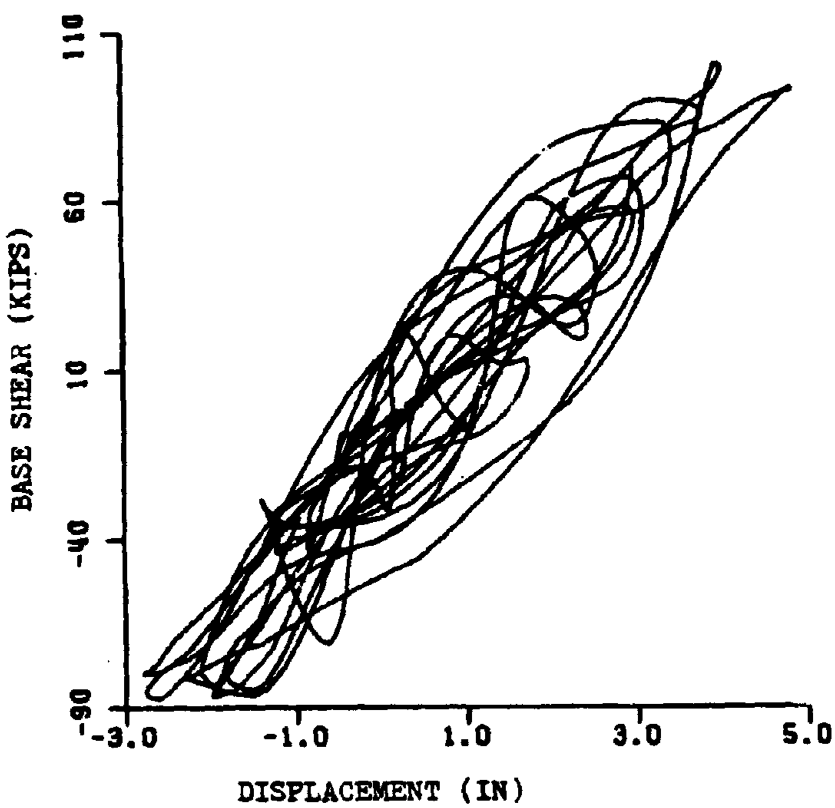

FIGURE 5.28- QKE 2, RIGID CONNECTION CASE
BASE SHEAR vs TOP STORY HORIZONTAL DISPLACEMENT

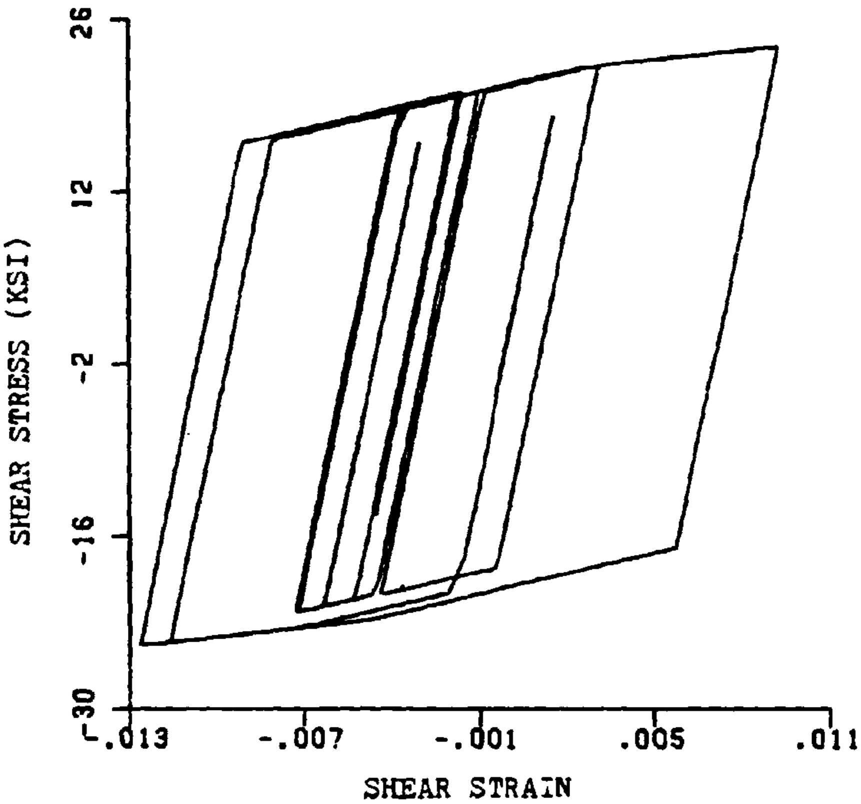

FIGURE 5.29- QKE 1

PANEL ZONE FOURTEEN HYSTERETIC BEHAVIOR

UNREINFORCED CONNECTION CASE

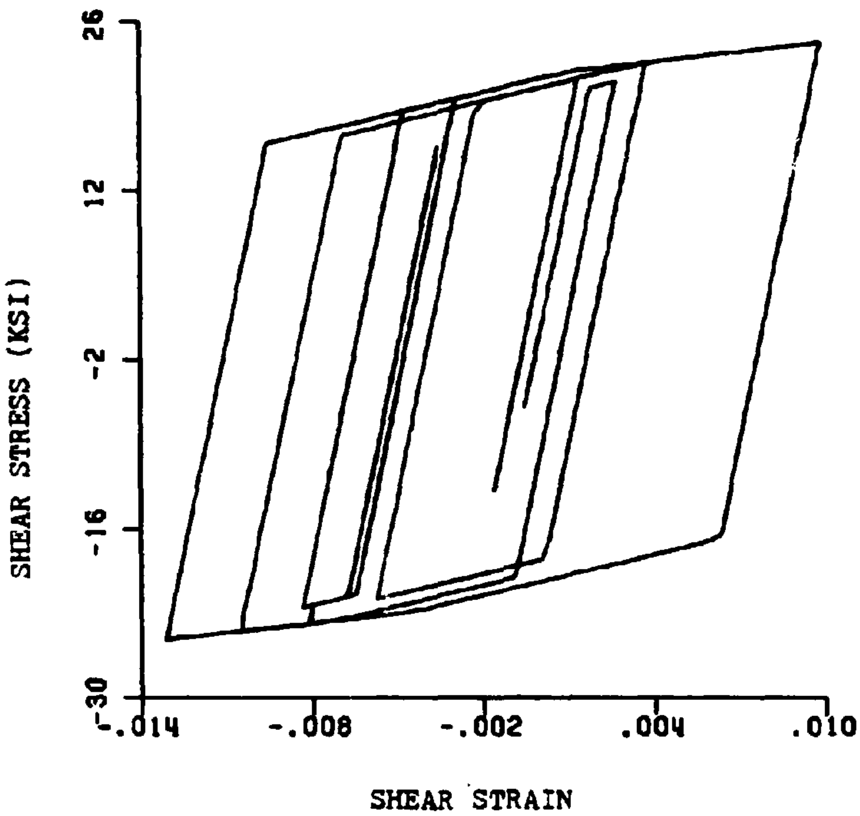

FIGURE 5.30 - QKE 1

PANEL ZONE TEN HYSTERETIC BEHAVIOR
UNREINFORCED CONNECTION CASE

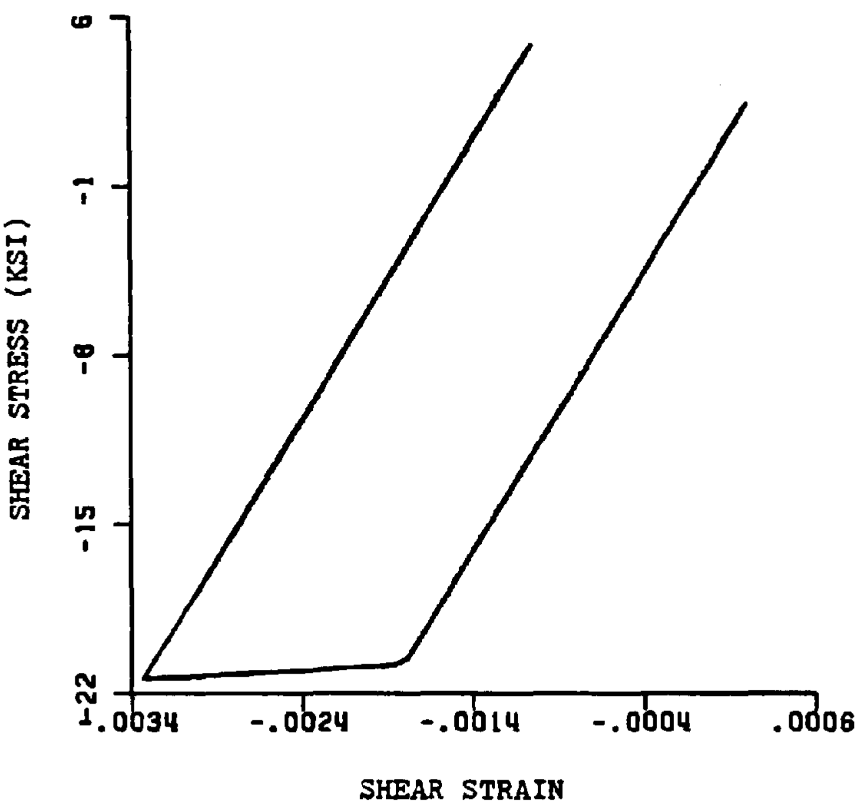

FIGURE 5.31- QKE 1

PANEL ZONE FOUR HYSTERETIC BEHAVIOR

UNREINFORCED CONNECTION CASE

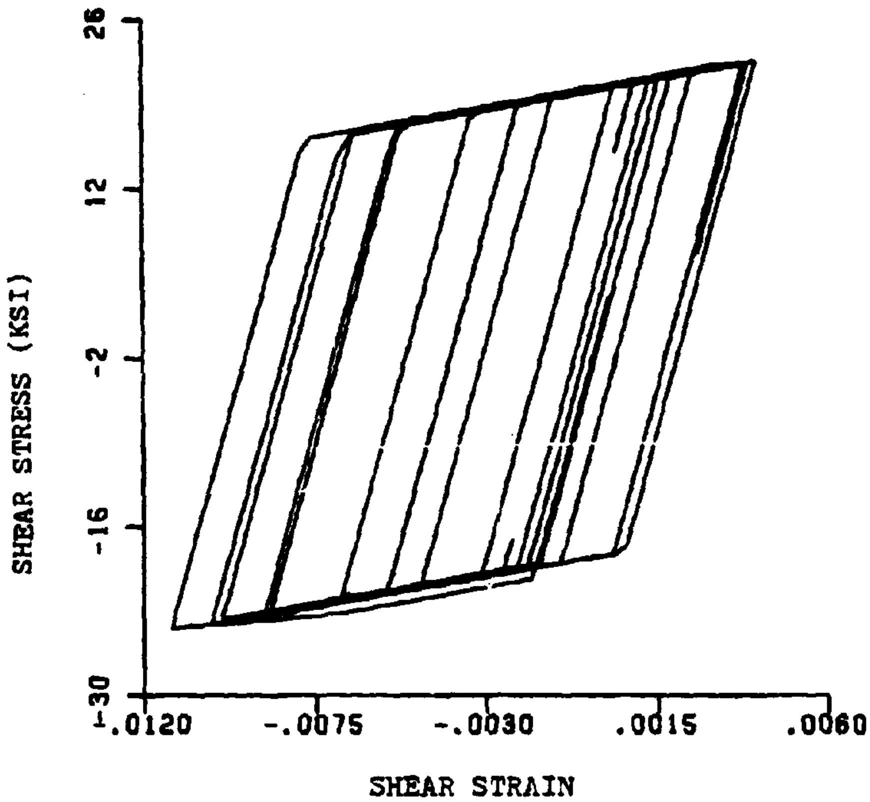

FIGURE 5.32- QKE 2

PANEL ZONE FOURTEEN HYSTERETIC BEHAVIOR

UNREINFORCED CONNECTION CASE

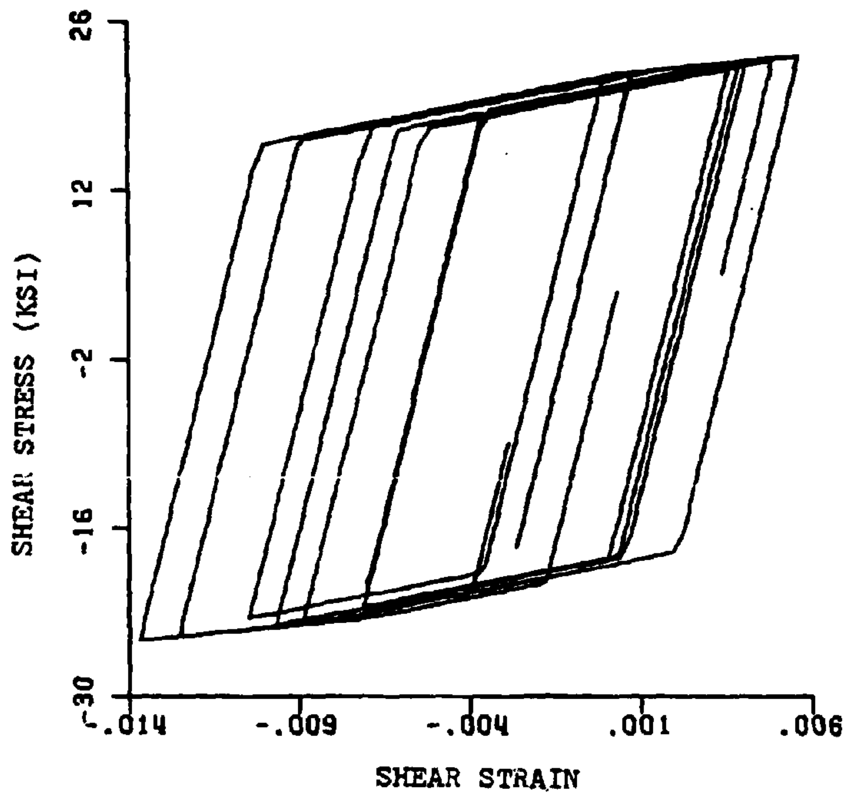

FIGURE 5.33- QKE 2

PANEL ZONE TEN HYSTERETIC BEHAVIOR

UNREINFORCED CONNECTION CASE

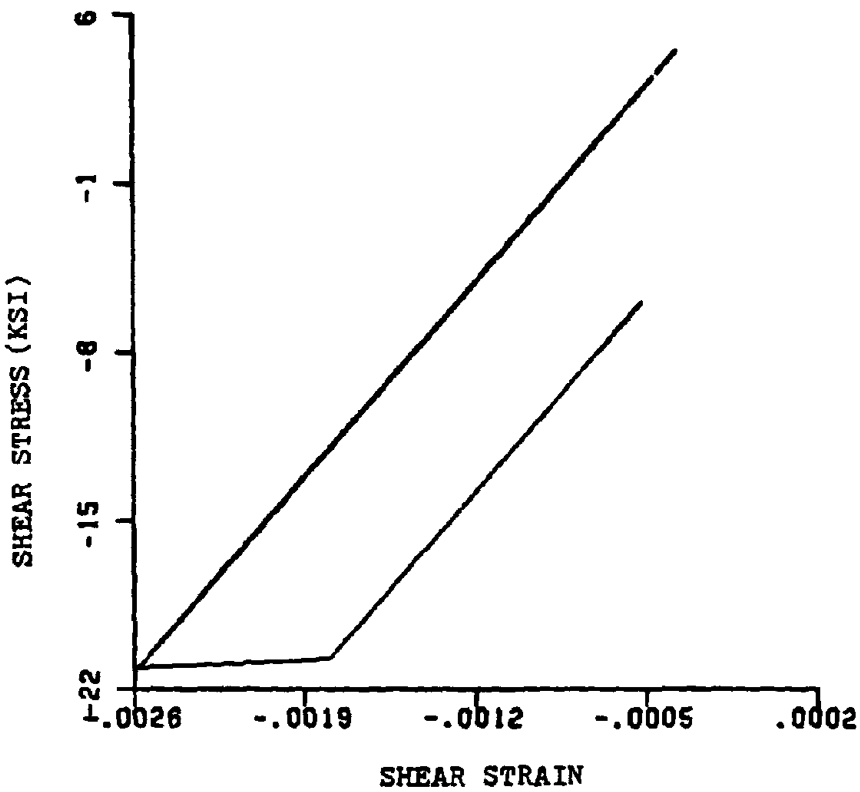

FIGURE 5.34- QKE 2

PANEL ZONE FOUR HYSTERETIC BEHAVIOR

UNREINFORCED CONNECTION CASE

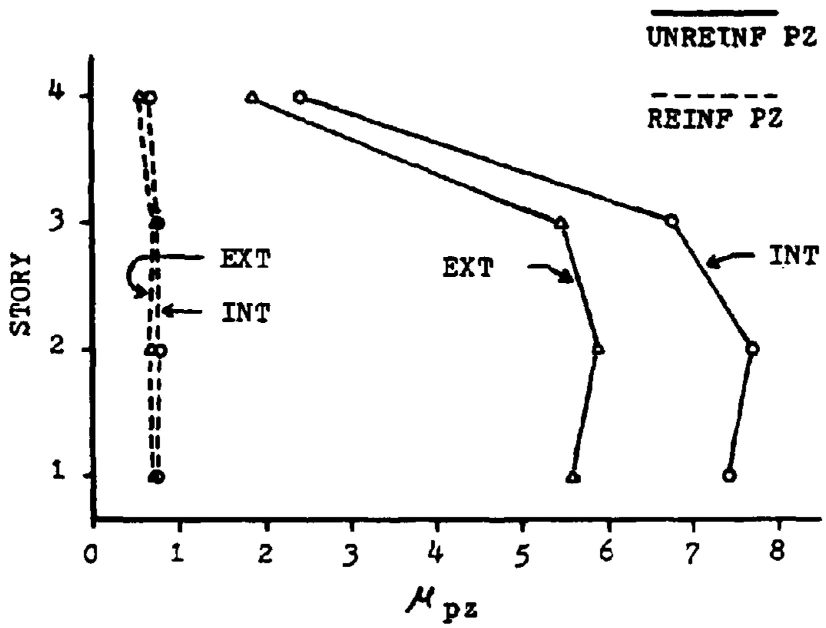

FIGURE 5.35- QKE 1, PZ DUCTILITY DEMAND

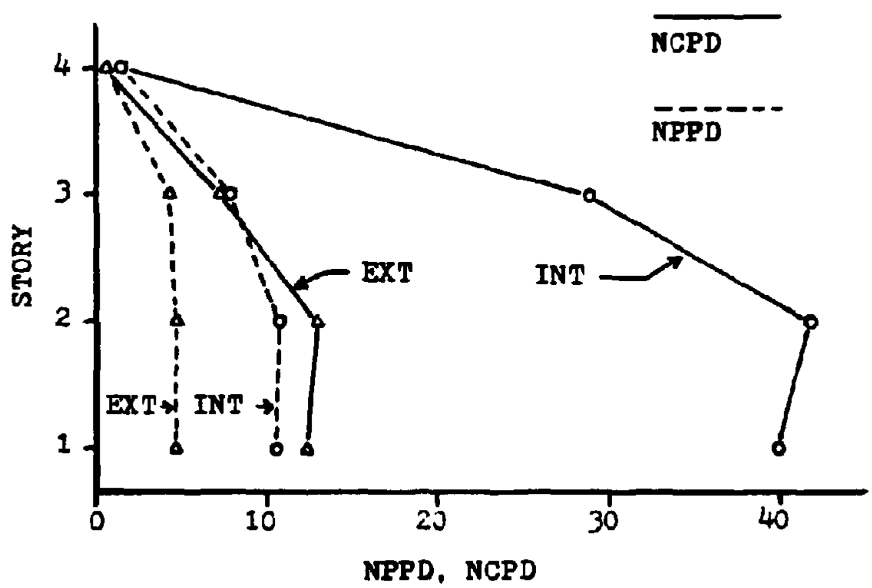

FIGURE 5.36- QKE 1, UNREINF PZ PLASTIC DEFORMATION

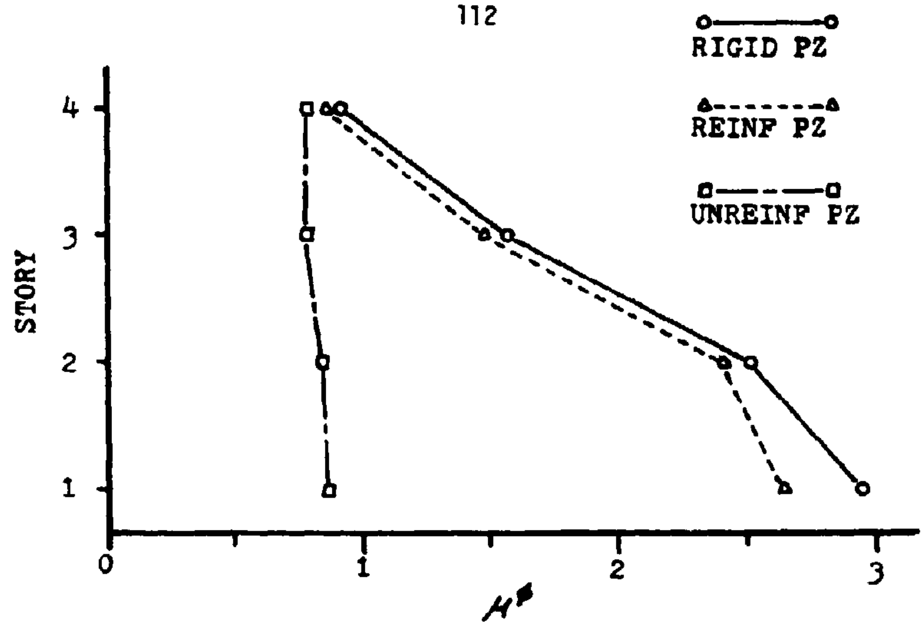

FIGURE 5.37- QKE 1
EXTERIOR BEAM CURVATURE DUCTILITY DEMAND

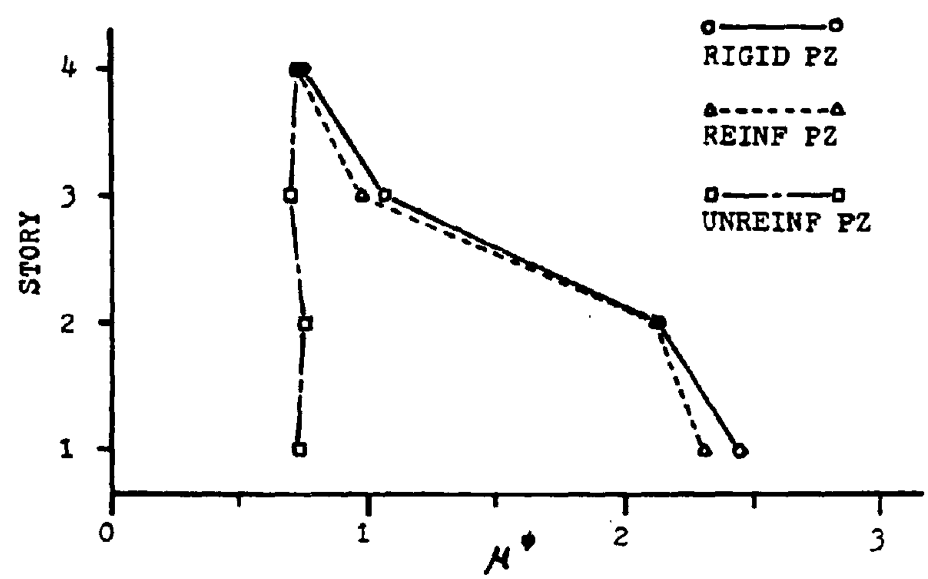

FIGURE 5.38- QKE 1
INTERIOR BEAM CURVATURE DUCTILITY DEMAND

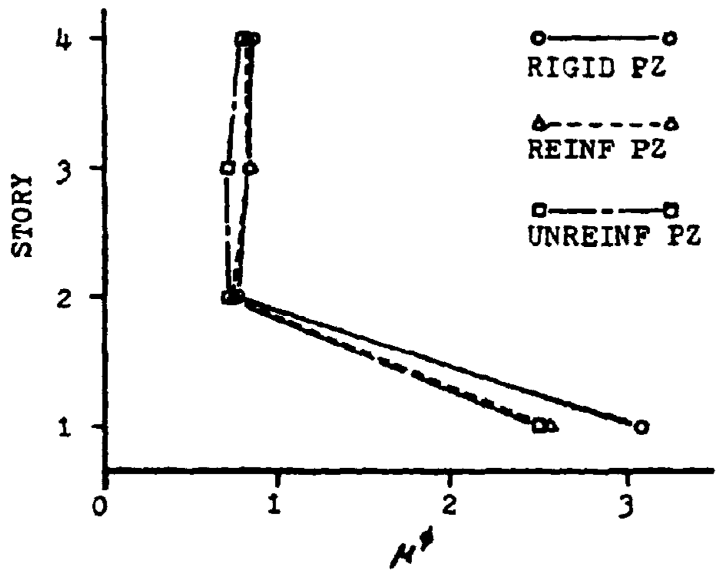

FIGURE 5.39- QKE 1

EXTERIOR COLUMN CURVATURE DUCTILITY DEMAND

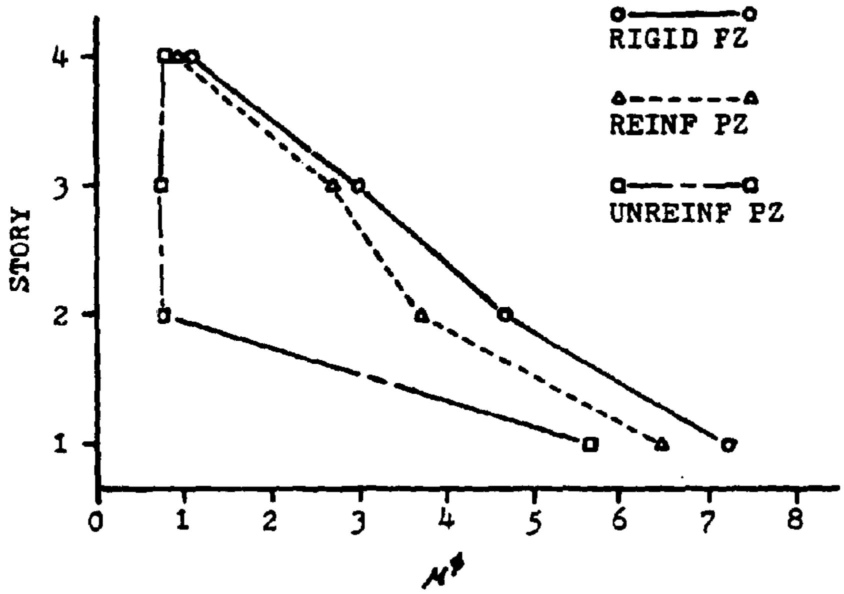

FIGURE 5.40- QKE 1

INTERIOR COLUMN CURVATURE DUCTILITY DEMAND

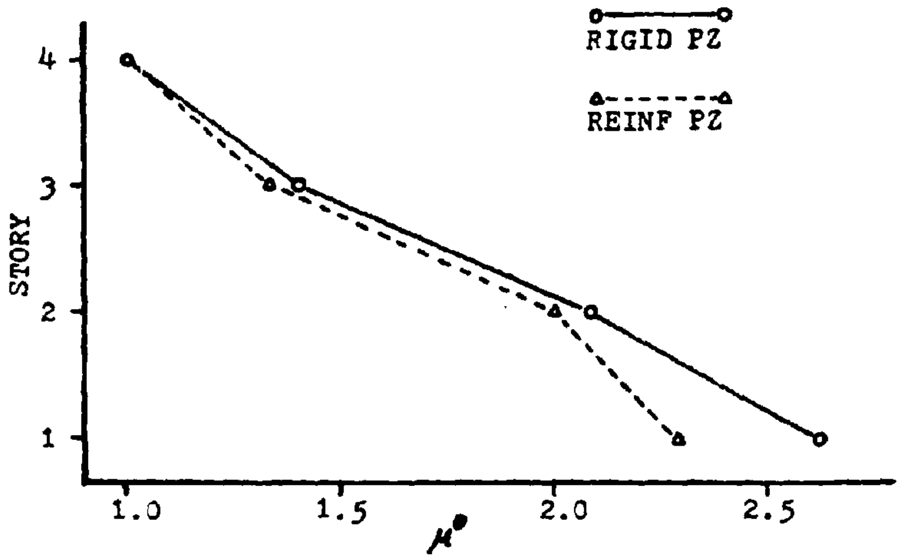

FIGURE 5.41- QKE 1

EXTERIOR BEAM ROTATION DUCTILITY DEMAND

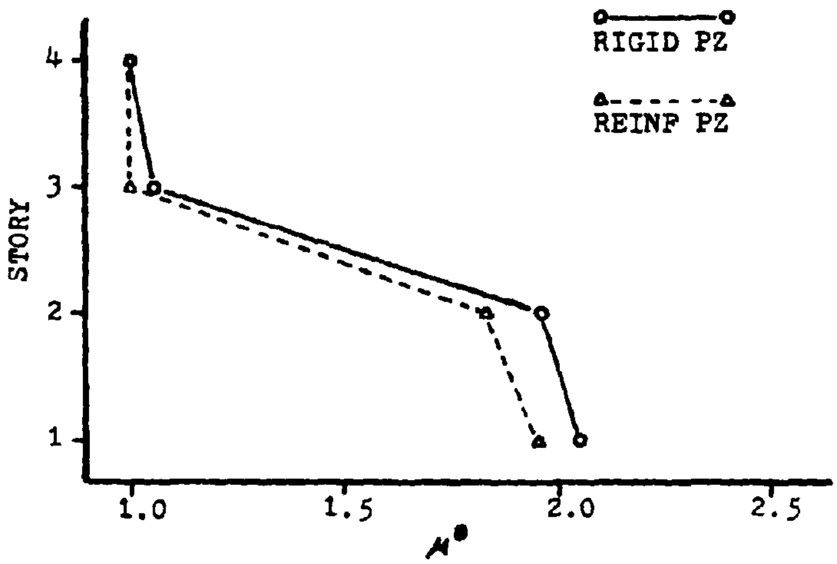

FIGURE 5.42- QKE 1

INTERIOR BEAM ROTATION DUCTILITY DEMAND

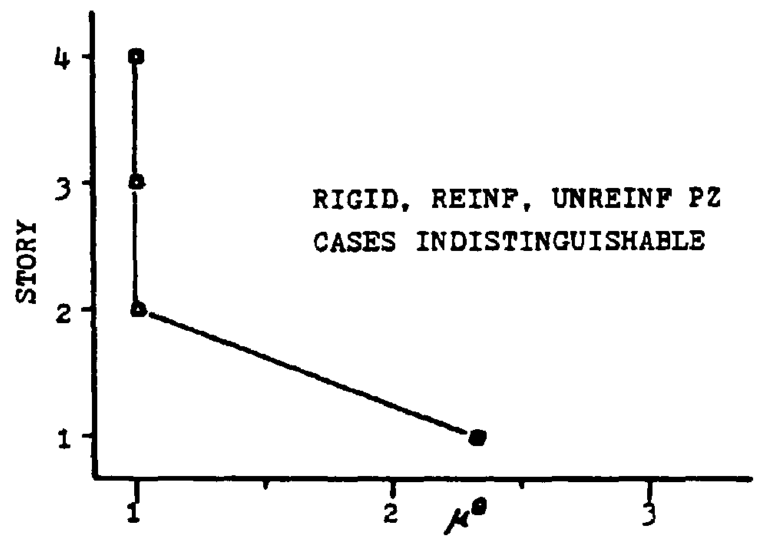

FIGURE 5.43- QKE 1

EXTERIOR COLUMN ROTATION DUCTILITY DEMAND

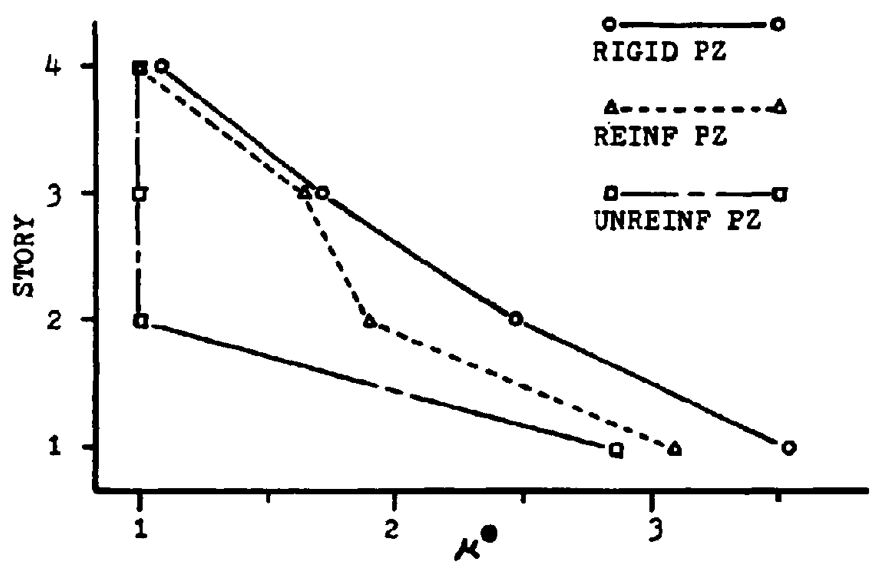

FIGURE 5.44- QKE 1

INTERIOR COLUMN ROTATION DUCTILITY DEMAND

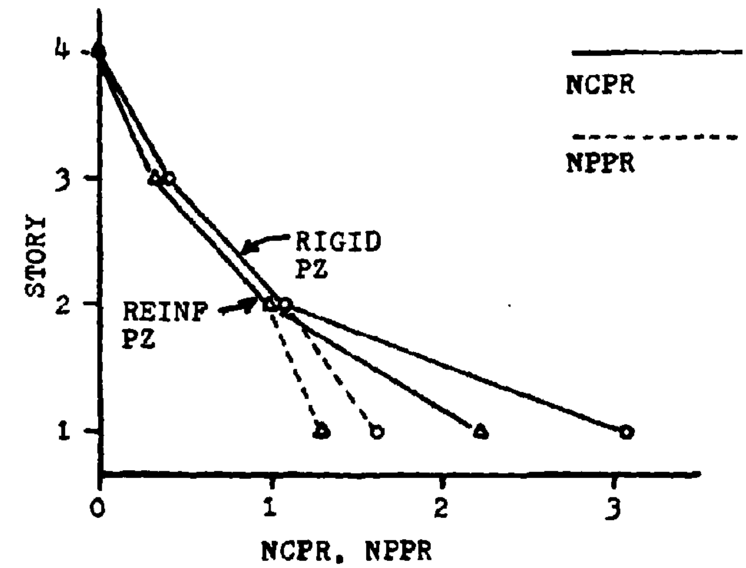

FIGURE 5.45- QKE 1

EXTERIOR BEAM NORMALIZED PLASTIC ROTATION

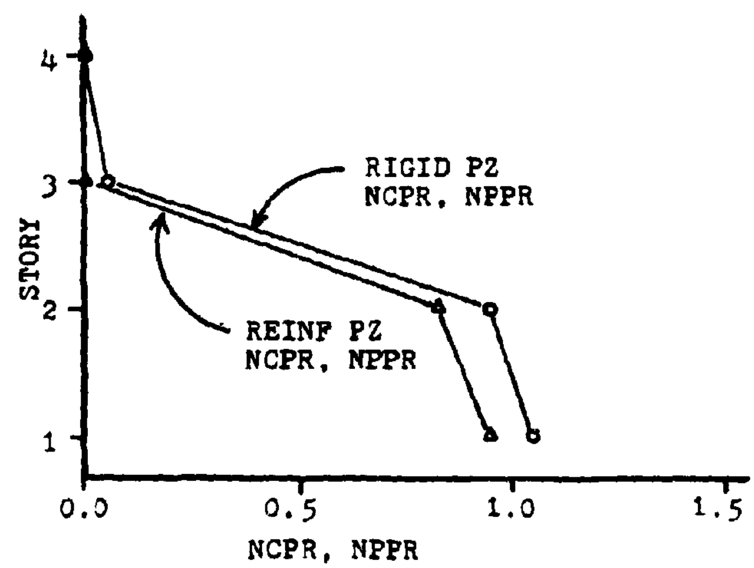

FIGURE 5.46- QKE 1

INTERIOR BEAM NORMALIZED PLASTIC ROTATION

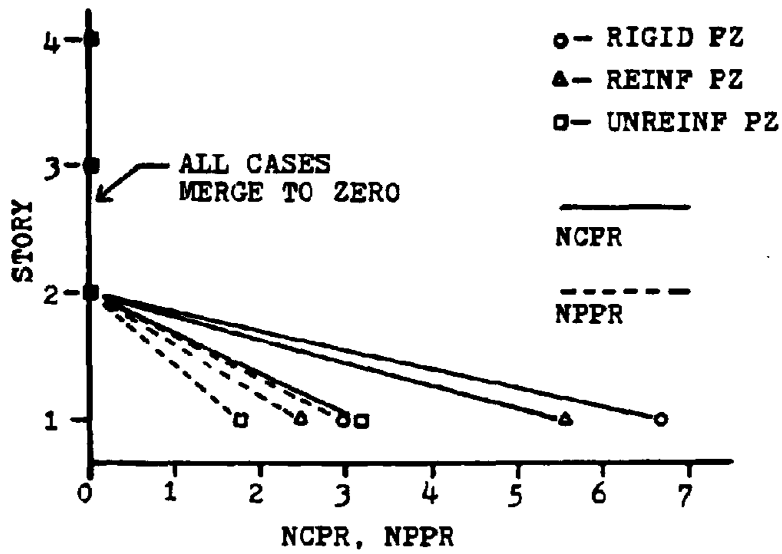

FIGURE 5.47- QKE 1

EXTERIOR COLUMN NORMALIZED PLASTIC ROTATION

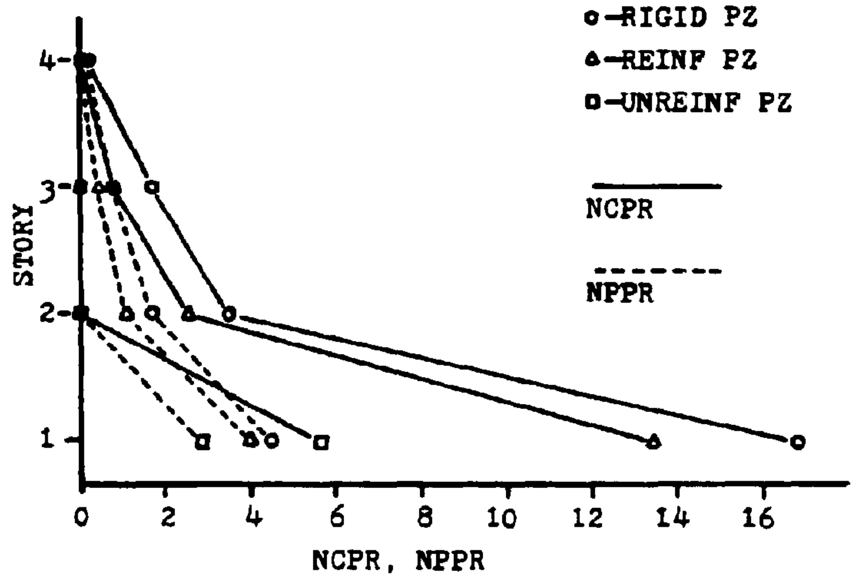

FIGURE 5.48- QKE 1

INTERIOR COLUMN NORMALIZED PLASTIC ROTATION

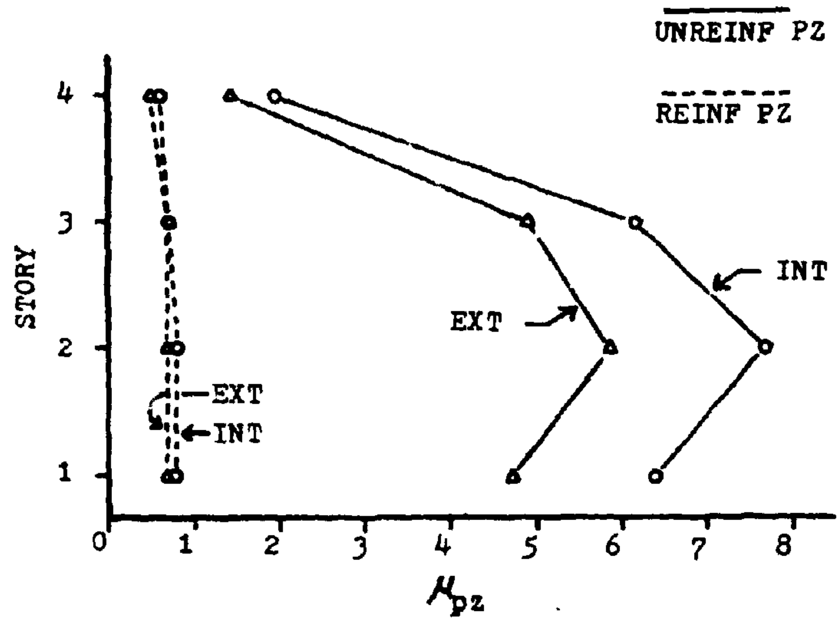

FIGURE 5.49- QKE 2, PZ DUCTILITY DEMAND

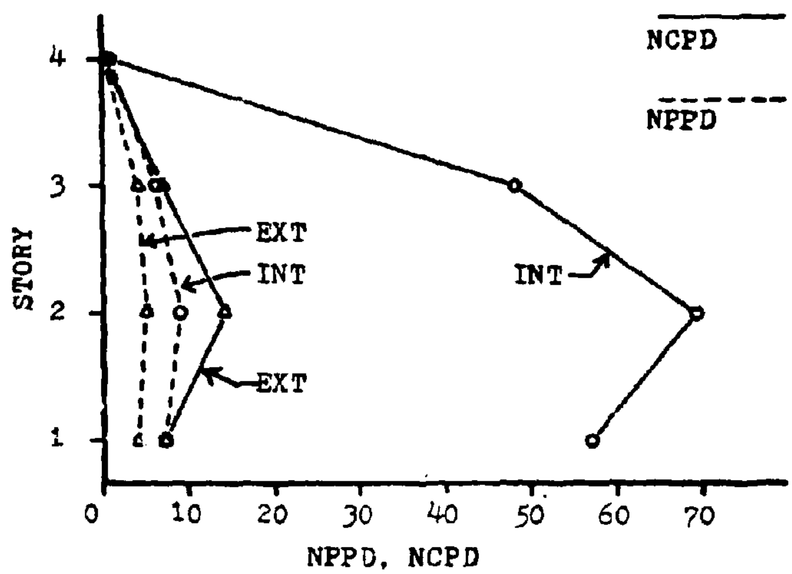

FIGURE 5.50- QKE 2, UNREINF PZ PLASTIC DEFORMATION

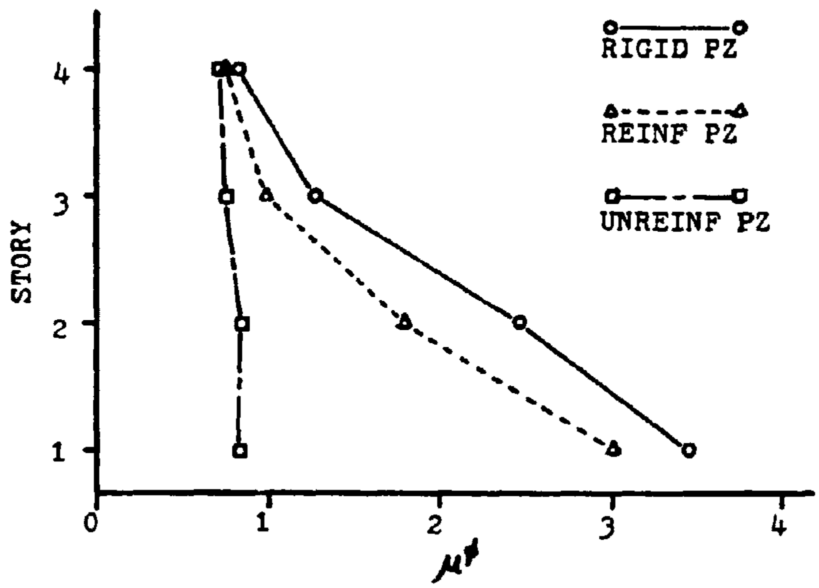

FIGURE 5.51- QKE 2

EXTERIOR BEAM CURVATURE DUCTILITY DEMAND

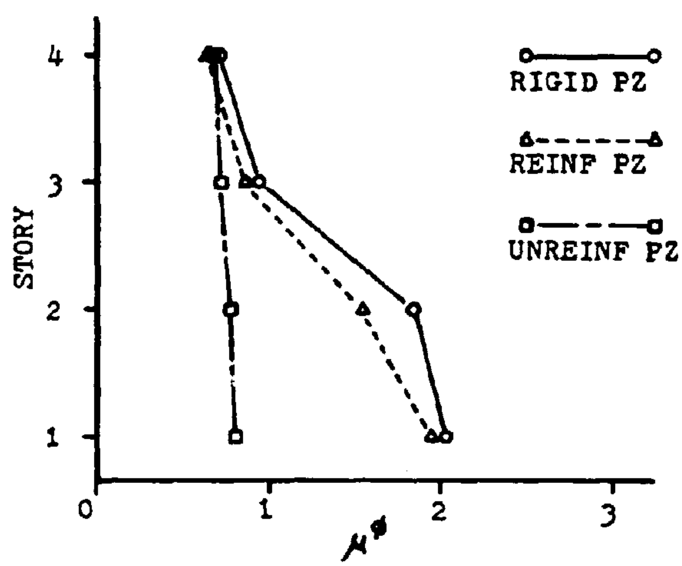

FIGURE 5.52- QKE 2

INTERIOR BEAM CURVATURE DUCTILITY DEMAND

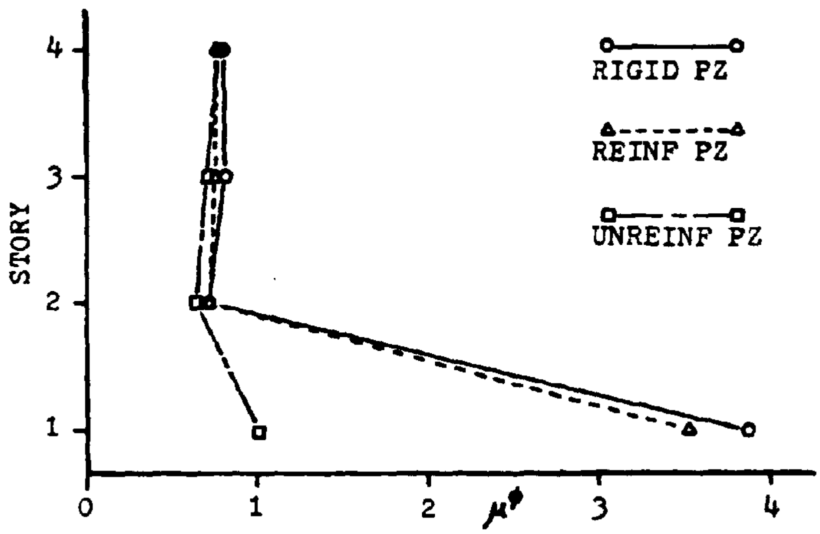

FIGURE 5.53- QKE 2

EXTERIOR COLUMN CURVATURE DUCTILITY DEMAND

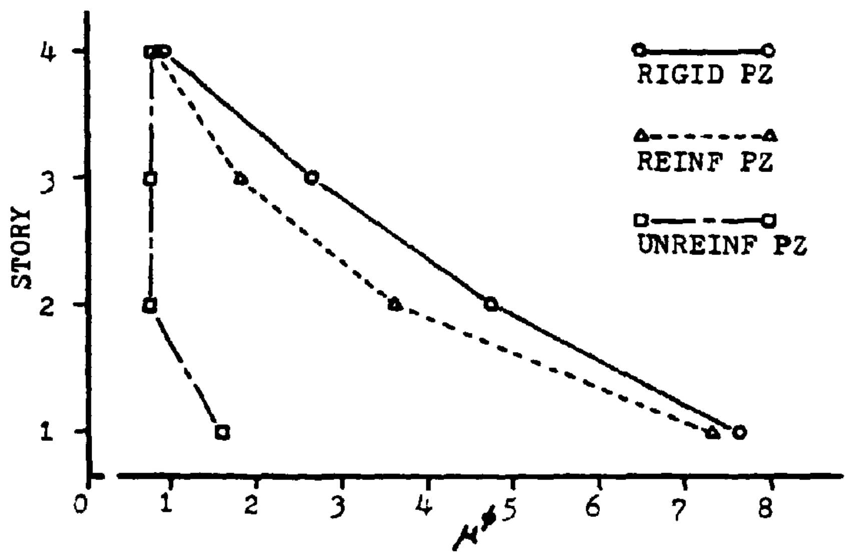

FIGURE 5.54- QKE 2

INTERIOR COLUMN CURVATURE DUCTILITY DEMAND

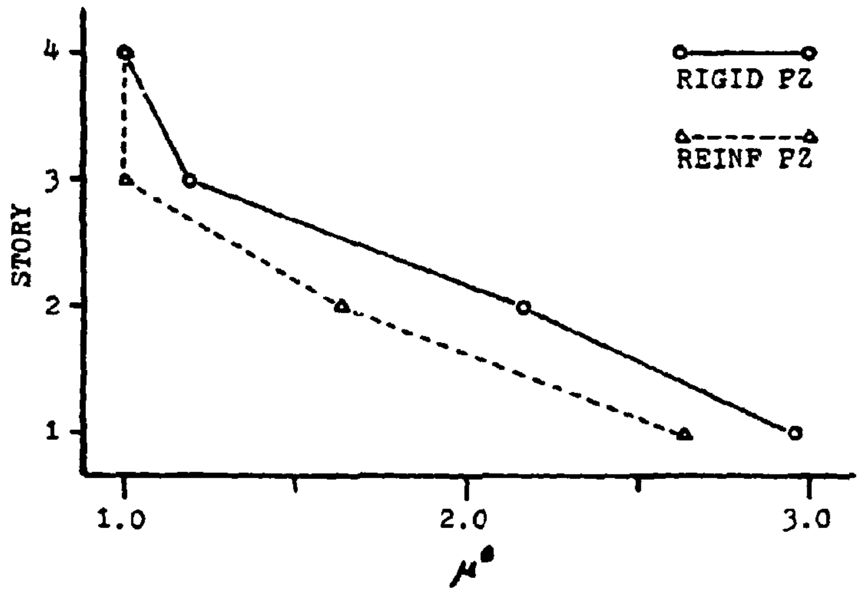

FIGURE 5.55- QKE 2
EXTERIOR BEAM ROTATION DUCTILITY DEMAND

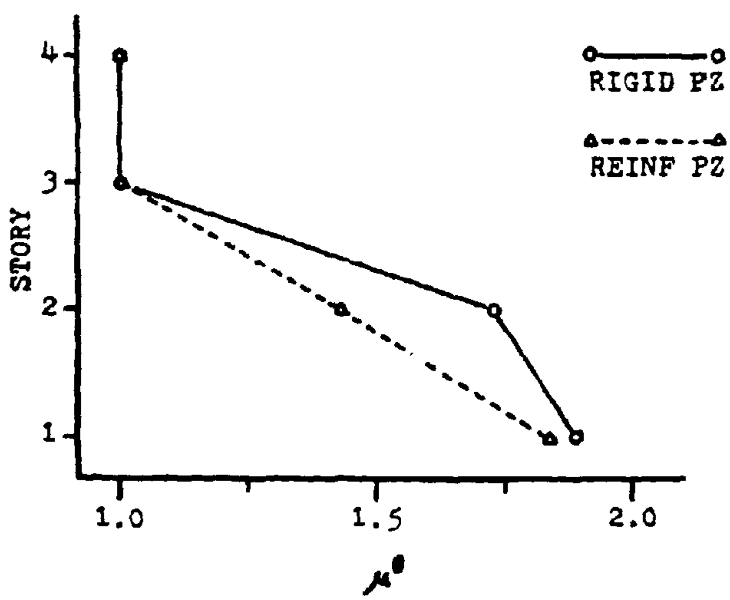

FIGURE 5.56- QKE 2
INTERIOR BEAM ROTATION DUCTILITY DEMAND

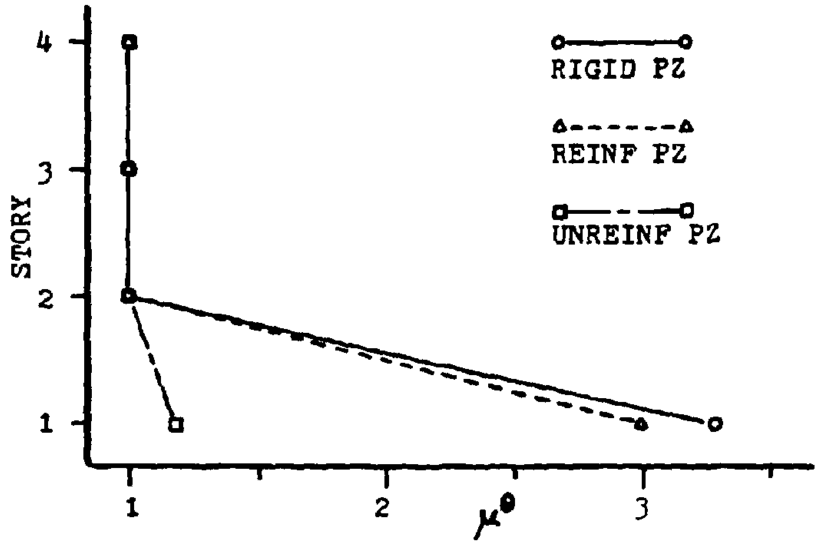

FIGURE 5.57- QKE 2

EXTERIOR COLUMN ROTATION DUCTILITY DEMAND

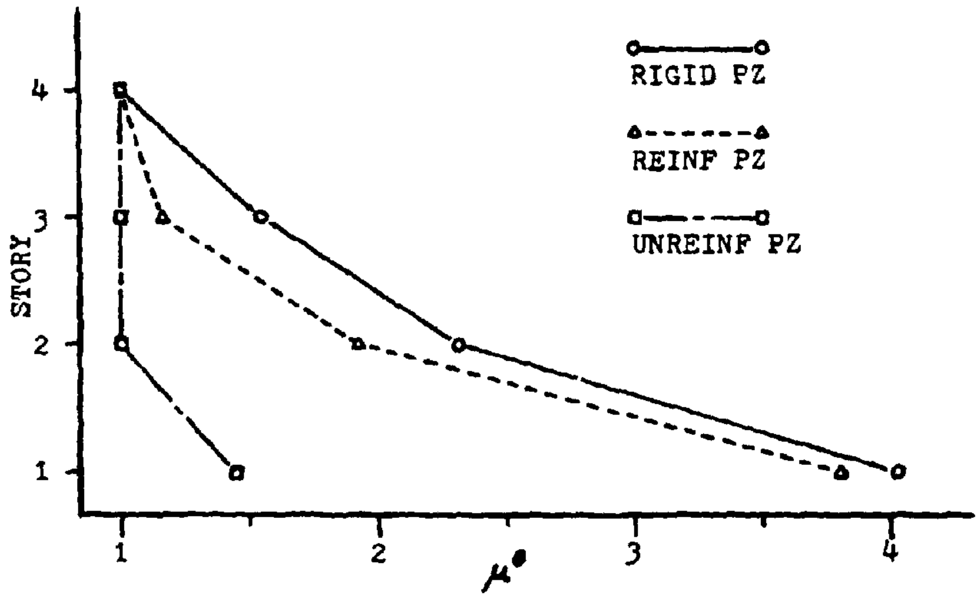

FIGURE 5.58- QKE 2

INTERIOR COLUMN ROTATION DUCTILITY DEMAND

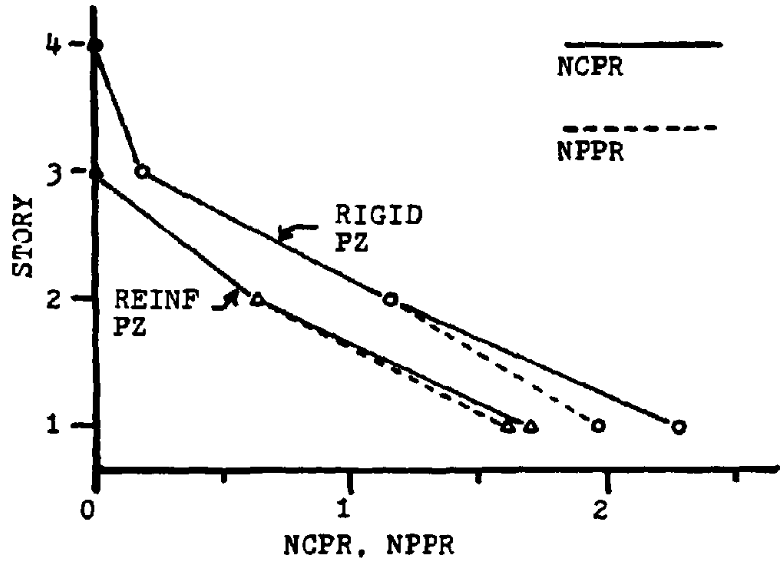

FIGURE 5.59- QKE 2

EXTERIOR BEAM NORMALIZED PLASTIC ROTATION

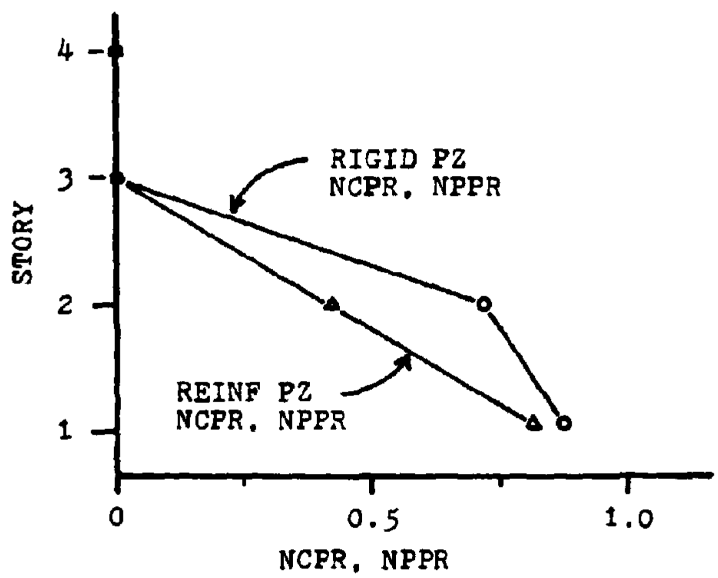

FIGURE 5.60- QKE 2

INTERIOR BEAM NORMALIZED PLASTIC ROTATION

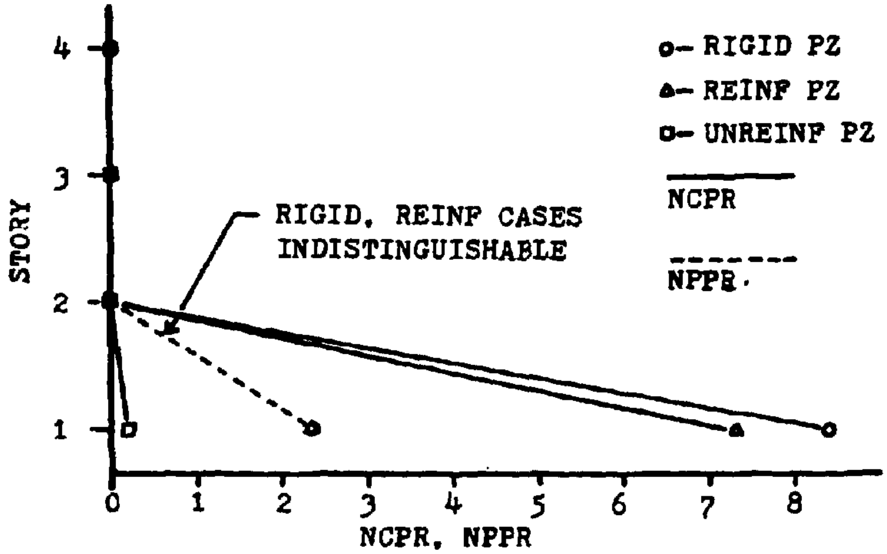

FIGURE 5.61- QKE 2

EXTERIOR COLUMN NORMALIZED PLASTIC ROTATION

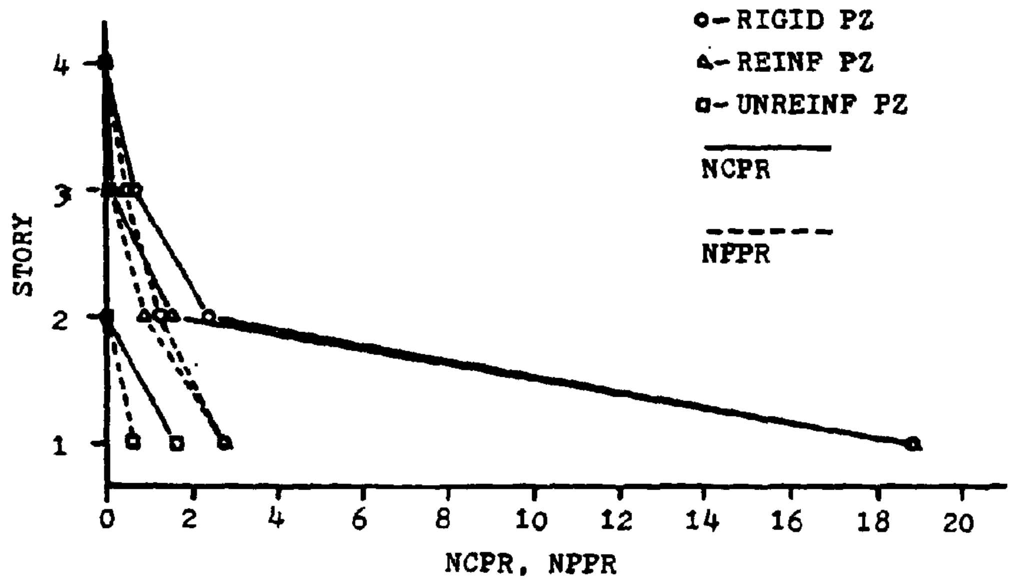

FIGURE 5.62- QKE 2

INTERIOR COLUMN NORMALIZED PLASTIC ROTATION

CHAPTER SIX - SUMMARY AND CONCLUSIONS

6.1 Principal Findings

This report has detailed an investigation into the effect that panel zone constitutive behavior has on the seismic response of welded moment-resisting steel frames. The results of elastic modal analysis suggest that connection flexibility will generally produce a structure of greater lateral flexibility—and period—than the common analysis procedure of ignoring connection size and flexibility would predict. Inelastic analysis has demonstrated that connection behavior has a great impact on the damage experienced by the beams and columns during an earthquake excitation.

The connection was modeled as a tri-linear shear mechanism, and a general matrix formulation was developed so that this effect can be included in a structure's stiffness matrix. This incorporation requires that:

1) An additional rotational degree of freedom be provided at each node in a structure's stiffness matrix where panel zone flexibility is to be modeled, and that

2) General matrix transformations be performed at each node in order to include the effect of finite connection size in the formulation.

Modal analysis of two example frames was performed, using this matrix formulation, which demonstrated that:

3) Ignoring connection flexibility and size in the analysis (i.e., by using only one rotational DOF at each node and by using the full c-c connection distance in calculation of the beam/column lengths) has a self-compensating effect that produced a good

estimate of the fundamental mode of vibration of the structures with heavily reinforced connections.

4) The structures without connection reinforcement were up to 14% more flexible in the fundamental mode of vibration than the simplified analysis as performed in 3) suggested.

5) An assumption that the connection was of finite size but of no flexibility lead to unrealistically stiff structures in the fundamental mode of vibration. However,

6) The assumption as stated in 5) leads to an accurate prediction of the highest modes of vibration.

The inelastic response of one of the example frames was examined by subjecting the structure to two records of artificial horizontal ground motion. Individual connections for this portion of the study were modeled by single finite elements constrained to have only shear deformation. The results of the analysis indicated that:

7) The frame with unreinforced connections dissipated energy through inelastic deformations in the panel zone and prevented plastic hinges from forming in the beams and columns at all locations other than at the fixed supports at the frame base. Reinforcing the connections so that they remained elastic forced the beams and columns into the role of energy dissipators.

8) Rigid connections produced the largest inelastic deformation demands on the beams and columns. This suggests that if a nonlinear dynamic analysis is performed in which panel zone flexibility is ignored but the physical connection size is modeled, the result will be a conservative estimation of the beam and column ductility demands.

9) For a connection designed to reman elastic, the most flexible design is the preferable one, implying that reinforcement in the

form of diagonal stiffeners is better than one employing doubler plates.

10) The maximum story displacements did not vary with the connection properties in a way that could be predicted from elastic analysis. Furthermore, no one set of connection properties produced appreciably larger lateral frame sway than another.

6.2 Recommendations for Future Research

The connection behavior for use in this study was assumed to be one of a simple shear mechanism, as this is the dominant form of connection deformation and the one that most significantly affects the beam and column moments. Other forms of deformation, however, also occur within a connection and should be included in the matrix formulation for a complete description of the physical frame behavior. This is particularly true for frames with bolted moment connections.

Panel zone flexibility implies that common analysis techniques will, to some extent, improperly predict the true distribution of forces in the structure under the design loads. Research is needed to determine the effect that connection flexibility has on the static load-carrying characteristics of open steel frames.

Most importantly, frames of various heights and configurations should be examined in greater detail under a larger variety of earthquake excitations, as this portion of the study was admittedly limited in scope. Finally, the inelastic models should be improved beyond the simple bi- and tri-linear formulations to more accurately emulate the full-range hysteretic behavior of the frame elements.

REFERENCES

1. American Institute of Steel Construction, Manual of Steel Construction, 7th Edition, AISC, New York, June 1973.

2. American Society of Civil Engineers, Plastic Design in Steel - A Guide and Commentary, Manual No. 41, WRC and ASCE, New York, 1971.

3. Becker, J.M. and Llorente, C., "The Seismic Response of Simple Precast Concrete Panel Walls," Proceedings of the 2nd U.S. Conference on Earthquake Engineering, EERI, Stanford University, Aug. 1979.

4. Beedle, L.S., Plastic Design of Steel Frames, John Wiley and Sons, London, 1958.

5. Bertero, V.V., Popov, E.P. and Krawinkler, H., "Beam-Column Subassemblages under Repeated Loading," Proceedings of the ASCE, Journal of the Structural Division, ST 5, May 1972.

6. Bertero, V.V., Krawinkler, H. and Popov, E.P., "Further Studies on Seismic Behavior of Beam-Column Subassemblages," Report No. EERC-73-27, Univ. of Calif., Berkeley, December 1973.

7. Biggs, J.M., Introduction to Structural Dynamics, McGraw-Hill, New York, 1964.

8. Clough, R.W. and Penzien, J., Dynamics of Structures, McGraw-Hill, New York, 1975.

9. Clough, R.W. and Tang, D.T., "Earthquake Simulator Study of a Steel Frame Structure, Vol. 1: Experimental Results," Report No. EERC 75-6, Univ. of Calif., Berkeley, April 1975.

10. Edelen, D.G.B. and Kydoniefs, A.D., An Introduction to Linear Algebra for Science and Engineering, American Elsevier, New York, 1975.

11. Giberson, M.F., "Two Nonlinear Beams with Definitions of Ductility," Proceedings of the ASCE, Journal of the Structural Division, ST. 2, February 1969.

12. Fielding, D.J., Chen, W.F., "Steel Frame Analysis and Connection Shear Deformation," Proceedings of the ASCE, Journal of the Structural Division, ST 1, January 1973.

13. Hsieh, Y.Y., Elementary Theory of Structures, Prentice-Hall, New Jersey, 1970.

14. Kaldjian, M.J., "Moment-Curvature of Beams as Ramberg-Osgood Functions," Proceedings of the ASCE, Journal of the Structural Division, ST 5, October 1967.

15. Kanaan, A.E. and Powell, G.H., "General Purpose Computer Program for Inelastic Dynamic Response of Plane Structures," Report No. EERC 73-6, Univ. of Calif., Berkeley, April 1973.

16. Kato, B. and Nakao, M., "The Influence of the Elastic Plastic Deformation of Beam-to-Column Connections on the Stiffness, Ductility, and Strength of Open Frames," Proceedings, 5th World Conference on Earthquake Engineering, Rome, Italy, June 1973.

17. Krawinkler, H., "Shear in Beam-Column Joints in Seismic Design of Steel Frames," Engineering Journal, AISC, Vol. 15, No. 3, Third Quarter, 1978.

18. Krawinkler, H., Bertero, V. and Popov, E., "The Influence of the Elastic Plastic Deformation of Beam-to-Column Connections on the Stiffness, Ductility and Strength of Open Frames," Proceedings 5th World Conference on Earthquake Engineering, Rome, Italy, June 1973.

19. Krawinkler, H., Bertero, V. and Popov, E., "Shear Behavior of Steel Frame Joints," Proceedings of the ASCE, Journal of the Structural Division, ST 11, November 1975.

20. Lionberger, S.R. and Weaver, W., "Dynamic Response of Frames with Nonrigid Connections," Proceedings of the ASCE, Journal of the Engineering Mechanics Division, EM1, February 1969.

21. Lionberger, S.R., "Statics and Dynamics of Building Frames with Nonrigid Connections," Thesis presented to Stanford Univ. in partial fulfillment of the requirements for the degree of Doctor of Philosophy, April 1967.

22. Naka, T., Kato, B. and Yamada, S., "Frame Analysis for Lateral Loading Considering the Shearing Distortion of Members," Proceedings of the Symposium on the External Forces and Structural Design of High-Rise and Long-Span Structures, J.S.C.E. and Arch. Inst. of Japan, Tokyo, Sept. 1965.

23. Petersson, H. and Popov, E.P., "Constitutive Relations for Generalized Loadings," Proceedings of the ASCE, Journal of the Engineering Mechanics Division, EM4, August 1977.

24. Petersson, H. and Popov, E.P., "Substructuring and Equation System Solutions in Finite Element Analysis," Computers and Structures, Vol. 7, 1977.

25. Pinkney, R.B., "Cyclic Plastic Analysis of Structural Steel Joints," Report No. EERC 73-15, Univ. of Calif., Berkeley, August 1973.

26. Piqué, J.R., "On the Use of Simple Models in Nonlinear Dynamic Analysis," Publication No. R76-43, M.I.T. Dept. of Civil Engineering, September 1976.

27. Popov, E.P., "Inelastic Behavior of Steel Braces under Cyclic Loading," Proceedings of the 2nd U.S. Conference on Earthquake Engineering, EERI, Stanford Univ., Aug. 1979.

28. Popov, E.P. and Betero, V.V., "Cyclic Loading of Steel Beams and Connections," Proceedings of the ASCE, Journal of the Structural Division, ST6, June 1973.

29. Popov, E.P. and Bertero, V.V., "Seismic Analysis of Some Steel Building Frames," Plastic Analysis of Civil Engineering Structural Systems: State-of-the-Art, 1979 ASCE Convention, Boston, April 1979.

30. Popov, E.P.and Bertero, V.V., "Seismic Analysis of Some Steel Building Frames," Proceedings of the ASCE, Journal of the Engineering Mechanics Division, February 1980.

31. Popov, E.P., Bertero, V.V. and Chandramouli, S., "Hysteretic Behavior of Steel Columns," Report No. EERC 75-11, Univ. of Calif., Berkeley, September 1975.

32. Popov, E.P. and Ortiz, M., "Macroscopic and Microscopic Cyclic Metal Plasticity," Proceedings Third Engineering Mechanics Specialty Conference, ASCE, Austin, Texas, September 1979.

33. Popov, E.P. and Pinkney, R.B., "Cyclic Yield Reversal in Steel Building Connections," Proceedings of the ASCE, Journal of the Structural Division, ST3, March 1969.

34. Popov, E.P. and Stephen, R.M., "Tensile Capacity of Partial Penetration Groove Welds," Proceedings of the ASCE, Journal of the Structural Division, ST 9, Septtember 1977.

35. Robinson, J.H., "Inelastic Dynamic Design of Steel Frames to Resist Seismic Loads," Publication No. R77-23, M.I.T. Dept. of Civil Engineering, July 1977.

36. Romstad, K.M. and Subramanian, C.V., "Analysis of Frames with Partial Connection Rigidity," Proceedings of the ASCE, Journal of the Structural Division, ST 11, November 1970.

37. Shepherd, R. and Le-Huu, D., "Some Cyclic Loading Characteristics of Steel Beam/Column Joints," 6th Australian Conference on the Mechanics of Structures and Materials, Christchurch, August 1977.

38. STRUDL OPERATION MANUAL, ICES, MBB and IUG, Germany, July 1976.

39. Tall, L., Structural Steel Design, Second Edition, Ronald Press, New York, 1974.

40. Tang, D.T., "Earthquake Simulator Study of a Steel Frame Structure, Vol. II: Analytical Results," Report No. EERC 75-36, Univ. of Calif., Berkeley, October 1975.

41. Tamizawa, M., "Extended Kani Method in Consideration of Both Axial Deformation of Columns and Shear Deformation of Joint Panels," Transactions, Arch. Inst. of Japan, Vol. 157, Sept. 1970.

42. Tang, P. and Rossettos, J.N., Finite Element Method, M.I.T. Press, Cambridge, Mass., 1977.

43. Uniform Building Code, International Association of Building Officials, 1973 and 1979 Editions, California.

44. Vasquez, J., Popov, E.P. and Bertero, V.V., "Earthquake Analysis of Steel Frames with Non-Rigid Joints," Proceedings of the 5th World Conference on Earthquake Engineering, Rome, Italy, June 1973.

45. Veneziano, D., Unpublished Class Notes for M.I.T. Course 1.571, Cambridge, Mass., September 1978.

APPENDIX A - PROGRAM JAN

JAN is an interactive computer program that will assemble the stiffness matrix of planar building frames with finite connection size and panel zone shear deformation. In addition, JAN will statically condense any degrees of freedom not specified in the DOF RETAIN COMMAND, thus permitting calculation of such properties as the frame's lateral stiffness matrix. The program is directly based upon the matrix formulation of Chapter Two. No claims are made as to the efficiency of the program—there is, for example, a distinctly poor utilization of storage space—but the cost of a single run is fairly low nonetheless. Being an interactive program, JAN does not require much explanation; what follows is a brief description of the program's numbering and dimensioning requirements.

JAN requires a node numbering sequence as shown in Fig. A.1. Nodes that are supported in any manner are not numbered. The size of the global stiffness matrix is calculated as:

$$\text{NELC} = 4(\text{ND}) \quad , \qquad \text{(A.1)}$$

where ND is the number of nodes in the structure. The program is peculiar in that it will not accept over-dimensioning of the stiffness matrix; hence the size of GMAT (in the MAIN and subroutine ADDRS) and AV (in subroutines PTAVC and SCON) must be carefully stipulated before each run. As illustrated in the program listing, JAN is set up for an 8-node structure. The specific dimensioning requirements of the program are summarized in Table A.1.

Provision has been made for structures that will undergo antisymmetric bending, as did the frames of this study during the modal analysis. The

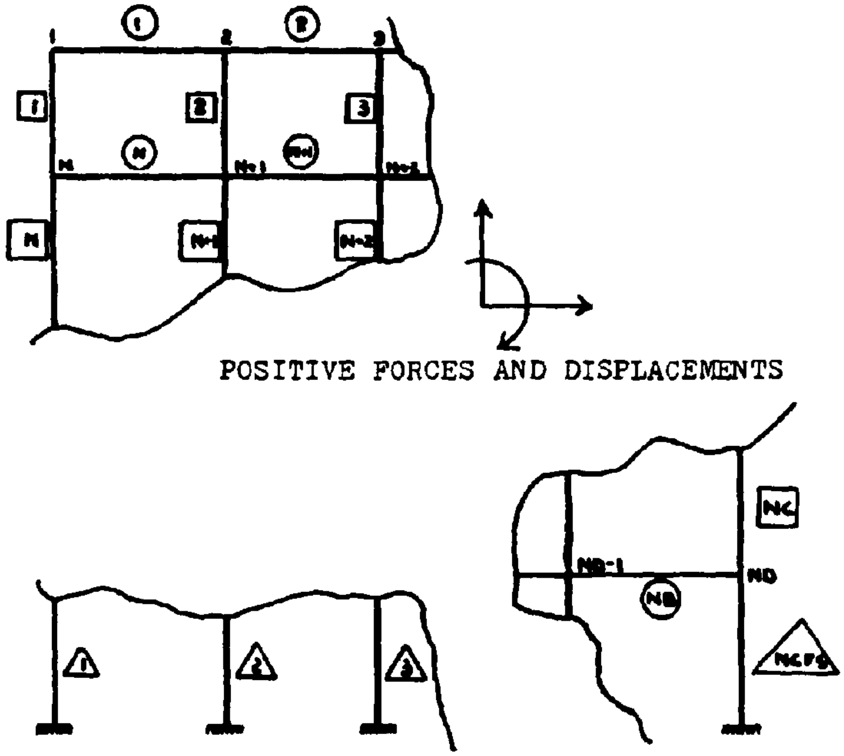

n = NODE NUMBER

(n) = INTERNAL BEAM NUMBER

[n] = INTERNAL COLUMN NUMBER

△n = COLUMN WITH FIXED SUPPORT NUMBER

FIGURE A.1- ELEMENT NUMBERING REQUIREMENTS

Description of Variable	Variable	Array	Required Dimension of Array
No. of basic stiffness types	NSTFT	AQ,AIQ, ALQ,ASQ	$\geq$ (NSTFT)
Total no. of beams and columns	JSFT	APRP,AIPRP ALPRP,ASPRP	$\geq$ (JSFT)
Size of global matrix	NELG	GMAT	= (NELG,NELG)
		NCON	$\geq$ (NELG)
		AV	= ($NELG^2$)
No. of nodes (PZ's)	ND	PZD	$\geq$ (ND,2)
		IGEOM	$\geq$ (ND,5)
No. of equal displacement commands	NEDC	NHOLD	$\geq$ (NEDC)

TABLE A.1 - DIMENSIONING REQUIREMENTS OF PROGRAM JAN structural idealization and numbering for frames of this type are shown in Fig. A.2.

Any members (including those with supports at an end) which differ in cross-sectional area, moment of inertia, effective shear area, or length must be specified as different STIFFNESS TYPES. Member lengths are taken as center-to-center connection distances, as the program automatically adjusts these lengths for the true connection size. The lengths of beams used to specify the antisymmetry condition (members 1, 2, 3, 4 in Fig. A.2) are again taken as their full c-c dimension.

Member numbering is illustrated in Figs. A.1 and A.2. Beams, Columns, Columns with Fixed Supports at the base, and Beams with Roller Supports are all numbered independently beginning with 1.

The Submatrix address of a beam is determined as the node number to the left of the beam followed by the node number to the right. The submatrix address of a column is determined as the node number above that column followed by the node number below.

JAN will prompt the user for the panel zone thickness of each node. No adjustment is made by the program for the effective PZ shear area; if adjustment is desired, Eq. (2.10) may be used to determine an appropriate thickness to be input. Specifying zero as the PZ thickness will result in a singular stiffness matrix.

The degrees of freedom in the stiffness matrix are arranged in accordance with the formulation of Sec. 2.2. The address of any degree of freedom (for use in the EQUAL DISPLACEMENT COMMAND and the DOF RETAIN COMMAND) may be found from:

$$AD_u = 4(i-1) + j \quad , \qquad \text{(A.2)}$$

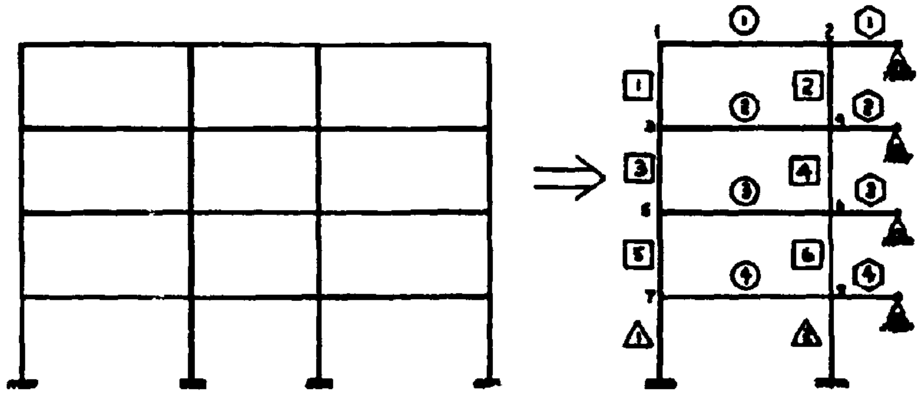

(n) = BEAM WITH ROLLER SUPPORT NUMBER

FIGURE A.2- IDEALIZATION OF SYMMETRIC STRUCTURE IN ANTI-SYMMETRIC BENDING

$$
\begin{bmatrix}
AV(1) & AV(3) & AV(6) & & & \\
 & AV(2) & AV(5) & & & \\
 & & AV(4) & & & \\
 & & & \cdot & & \\
 & & & & \ddots & \\
 & & & & & \cdot
\end{bmatrix}
\quad
\overset{\text{RETAINED DOF NO.}}{\overset{\downarrow}{\begin{bmatrix} 1 \\ 2 \\ 3 \\ \vdots \\ \\ NDFR \end{bmatrix}}}
$$

FIGURE A.3- OUTPUT SEQUENCE OF REDUCED UPPER-TRIANGULAR STIFFNESS MATRIX where: AD_u = Matrix address of degree of freedom u

i = Node number of degree of freedom u

$$j = \begin{cases} 1 & u = u_{bi} \\ 2 & u = v_{ci} \\ 3 & u = \theta_{ci} \\ 4 & u = \theta_{bi} \end{cases} .$$

Degrees of freedom may be stipulated as identical through the EQUAL DISPLACEMENT COMMAND; a rigid connection, for example, can be modeled by requiring the beam and column rotations at the node to be identical through this command. Only two degrees of freedom may be specified as equal in a single command; more than two degrees of freedom may be constrained through multiple commands. The first specified DOF is the location where the resulting superimposed equations are stored; the second location is eliminated from the system.

Degrees of freedom to be retained in the reduced stiffness matrix can be specified by the DOF RETAIN COMMAND. All other DOF's are eliminated by static condensation. The reduced upper-triangular stiffness matrix is output as a column vector corresponding to the order of the DOF's specified in this command, as illustrated in Fig. A.3.

```
      IMPLICIT REAL*8(A-H,O-Z)
C
C*********************************************************************
C*    JAN--     PROGRAM FOR STIFFNESS REDUCTION OF BUILDING          *
C*              FRAMES WITH FINITE CONNECTION SIZE AND PZ            *
C*              SHEAR DEFORMATION                                    *
C*                                                                   *
C*    DEVELOPED BY    R.W. GRAVES         DEPT. OF CIVIL ENGINEERING *
C*                    M.I.T.              CAMBRIDGE, MA.  02139      *
C*                    APRIL  1990                                    *
C*********************************************************************
C
      COMMON/STIFF/AQ(10),AIQ(10),ALQ(10),ASQ(10)
      COMMON/BCPRP/APRP(20),AIPRP(20),ALPRP(20),ASPRP(20)
      COMMON/CLR/G(4,4)
      COMMON/COND/NCON(50)
      COMMON/AD/GMAT(32,32)
      DIMENSION NHOLD(50),IGEOM(10,5),PZD(10,2)
C
      PRINT 5
    5 FORMAT(//,5X,'JAN-- PROGRAM FOR STIFFNESS REDUCTION OF BUILDING',/
     1,11X,'FRAMES WITH FINITE CONNECTION SIZE AND PZ DEFORMATION',//)
      PRINT 10
   10 FORMAT(//,5X,'ENTER SIZE OF GLOBAL MATRIX',/)
      READ(5,*) NELG
C
C     INITIALIZE WORK SPACE
C
      DO 20 I=1,NELG
      DO 20 J=1,NELG
      GMAT(I,J)=0.
   20 CONTINUE
      ND=NELG/4
      DO 30 I=1,ND
      DO 30 J=1,5
      IGEOM(I,J)=0
   30 CONTINUE
      JSFT=0
      ICCHK=0
C
C     INPUT BASIC STIFFNESS TYPES
C
      PRINT 40
   40 FORMAT(//,5X,'ENTER ELASTIC MODULUS, SHEAR MODULUS',/)
      READ(5,*) E, GS
      PRINT 50
   50 FORMAT(//,5X,'ENTER NO. OF STIFFNESS TYPES',/)
      READ(5,*) NSTFT
      DO 60 I=1,NSTFT
      PRINT 70, I
   70 FORMAT(//,5X,'ENTER A,I,L,ASHEAR, OF STIFFNESS TYPE',I3,/)
      READ(5,*) AQ(I),AIQ(I),ALQ(I),ASQ(I)
   60 CONTINUE
C
C     BEAM DATA INPUT
C
      PRINT 80
   80 FORMAT(///,5X,'ENTER NO. OF INTERNAL BEAM ELEMENTS',/)
      READ(5,*) NB
      IF(NB.EQ.0)GO TO 140
      DO 130 I=1,NB
      JSFT=JSFT+1
      PRINT 90, I
   90 FORMAT(//,5X,'ENTER SUBMATRIX ROW & COL OF BEAM',I3,/)
      READ(5,*) IR,IC
      PRINT 100, I
  100 FORMAT(//,5X,'ENTER STIFFNESS TYPE OF BEAM',I3,/)
      READ(5,*) ISTFT
      PRINT 110
  110 FORMAT(//,5X,'ENTER COL DEPTH ON LEFT & RIGHT',/)
      READ(5,*) DCL,DCR
```

```
C
C     SET UP BEAM GEOMETRY AND DETERMINE PZ DIMENSIONS
C
      IGEOM(IR,4)=JSFT
      IGEOM(IC,2)=JSFT
      PZD(IR,1)=DCL
      PZD(IC,1)=DCR
C
C     CALC BEAM SUBMATRIX AND LOAD INTO GLOBAL MATRIX
C
      CALL CLEAR
      CALL STFT (ISTFT,A,AI,AL,AS)
      CALL PROP (JSFT,A,AI,AL,AS,DCL,DCR,ICCHK)
      CALL BEAM (E,GS,A,AI,AL,AS,DCL,DCR)
      CALL ADDRS (IR,IC)
C
C     PRINT BEAM SUBMATRIX
C
      PRINT 120, IR,IC
  120 FORMAT(//,22X,'BEAM SUBMATRIX',I3,I3,/)
C
      CALL PTSUB
C
  130 CONTINUE
  140 CONTINUE
C
C     INPUT COLUMN DATA
C
      PRINT 150
  150 FORMAT(///,5X,'ENTER NO. OF INTERNAL COL. ELEMENTS',/)
      READ(5,*) NC
      IF(NC.EQ.0)GO TO 210
      DO 200 I1=1,NC
      JSFT=JSFT+1
      PRINT 160, I1
  160 FORMAT(//,5X,'ENTER SUBMATRIX ROW & COL OF COLUMN',I3,/)
      READ(5,*) IR,IC
      PRINT 170, I1
  170 FORMAT(//,5X,'ENTER STIFFNESS TYPE OF COLUMN',I3,/)
      READ(5,*) ISTFT
      PRINT 180
  180 FORMAT(//,5X,'ENTER BEAM DEPTH ON TOP & BOTTOM',/)
      READ(5,*) DBT,DBB
C
C     SET UP COLUMN GEOMETRY AND DETERMINE PZ DIMENSIONS
C
      IGEOM(IR,3)=JSFT
      IGEOM(IC,1)=JSFT
      PZD(IR,2)=DBT
      PZD(IC,2)=DBB
C
C     CALC COLUMN SUBMATRIX AND LOAD INTO GLOBAL MATRIX
C
      CALL CLEAR
      CALL STFT (ISTFT,A,AI,AL,AS)
      CALL PROP (JSFT,A,AI,AL,AS,DBT,DBB,ICCHK)
      CALL COLM (E,GS,A,AI,AL,AS,DBT,DBB)
      CALL ADDRS (IR,IC)
C
C     PRINT COLUMN SUBMATRIX
C
      PRINT 190, IR,IC
  190 FORMAT(///,22X,'COLUMN SUBMATRIX',I3,I3,/)
C
      CALL PTSUB
C
  200 CONTINUE
  210 CONTINUE
```

```
C
C     INPUT SYMMETRY CONDITIONS
C
      PRINT 220
  220 FORMAT(//,5X,'ENTER NO OF BEAMS WITH ROLLER SUPPORTS ON RIGHT',/)
      READ(5,*) NBRS
      IF(NBRS.EQ.0)GO TO 240
      ICCHK=1
      DO 240 IRS=1,NBRS
      JSFT=JSFT+1
      PRINT 230, IRS
  230 FORMAT(//,5X,'ENTER NODE TO LEFT OF ROLLER SUPPORTED BEAM',I4,
     1' AND STIFFNESS TYPE',/)
      READ(5,*) LN,ISTFT
C
C     ADJUST RS BEAM STIFFNESS PROPERTIES
C
      DC=PZD(LN,1)
C
      CALL STFT (ISTFT,A,AI,AL,AS)
      CALL PROP (JSFT,A,AI,AL,AS,DC,DC,ICCHK)
C
C     ESTABLISH GEOMETRY OF RS BEAM AND SET FLAG FOR CONDENSATION
C
      IGEOM(LN,4)=JSFT
      IGEOM(LN,5)=ICCHK
  240 CONTINUE
      ICCHK=0
C
C     INPUT FIXED SUPPORT CONDITIONS
C
      PRINT 250
  250 FORMAT(//,5X,'ENTER NO OF COLUMNS WITH FIXED SUPPORT AT BASE',/)
      READ(5,*) NCFS
      DO 270 IFS=1,NCFS
      JSFT=JSFT+1
      PRINT 260, IFS
  260 FORMAT (//,5X,'ENTER NODE ABOVE SUPPORTED COL',I4,'  AND STIFFNESS
     1 TYPE',/)
      READ(5,*) NA,ISTFT
C
C     ADJUST SUPPORTED COLUMN STIFFNESS PROPERTIES
C
      DB=PZD(NA,2)
      DMB=0.
C
      CALL STFT (ISTFT,A,AI,AL,AS)
      CALL PROP (JSFT,A,AI,AL,AS,DB,DMB,ICCHK)
C
C     ESTABLISH SUPPORTED COLUMN GEOMETRY
C
      IGEOM(NA,3)=JSFT
  270 CONTINUE
C
C     INPUT PANEL ZONE THICKNESS
C
      DO 340 IRD=1,ND
      PRINT 280, IRD
  280 FORMAT(//,5X,'ENTER PANEL ZONE THICKNESS OF NODE',I3,/)
      READ(5,*) T
C
C     RECALL PZ DIMENSIONS
C
      DC=PZD(IRD,1)
      DB=PZD(IRD,2)
C
      CALL CLEAR
```

```
C
C
C     CALC NODE SUBMATRIX
C
C
C     BRANCH IF NO COLUMN EXISTS ABOVE NODE
C
      IF(IGEOM(IRD,1).EQ.0)GO TO 290
      JSFT=IGEOM(IRD,1)
C
C     CALC ABV COLUMN COMPONENT OF NODE SUBMATRIX
C
      CALL NASM (JSFT,A,AI,AL,AS)
      CALL NCOLA (E,GS,A,AI,AL,AS,DC,DS)
C
  290 CONTINUE
C
C     BRANCH IF NO BEAM EXISTS TO LEFT OF NODE
C
      IF(IGEOM(IRD,2).EQ.0)GO TO 300
      JSFT=IGEOM(IRD,2)
C
C     CALC LEFT BEAM COMPONENT OF NODE SUBMATRIX
C
      CALL NASM (JSFT,A,AI,AL,AS)
      CALL NBML (E,GS,A,AI,AL,AS,DC,DB)
C
  300 CONTINUE
C
C     CALC BELOW COLUMN COMPONENT OF NODE SUBMATRIX
C
      JSFT=IGEOM(IRD,3)
C
      CALL NASM (JSFT,A,AI,AL,AS)
      CALL NCOLB (E,GS,A,AI,AL,AS,DC,DB)
C
C     BRANCH IF NO BEAM EXISTS TO RIGHT OF NODE
C
      IF(IGEOM(IRD,4).EQ.0)GO TO 320
C
C     BRANCH IF NO SYMMETRY CONDITION IS SPECIFIED
C
      IF(IGEOM(IRD,5).EQ.0)GO TO 310
C
C     CALC CONDENSED BEAM COMPONENT OF NODE SUBMATRIX
C
      JSFT=IGEOM(IRD,4)
C
      CALL NASM (JSFT,A,AI,AL,AS)
      CALL BMCON (E,GS,A,AI,AL,AS,DC,DB)
C
      GO TO 320
  310 CONTINUE
C
C     CALC RIGHT BEAM COMPONENT OF NODE SUBMATRIX
C
      JSFT=IGEOM(IRD,4)
C
      CALL NASM (JSFT,A,AI,AL,AS)
      CALL NBMR (E,GS,A,AI,AL,AS,DC,DB)
C
  320 CONTINUE
C
C     ADD PANEL ZONE STIFFNESS TO NODE SUBMATRIX
C
      ZD=GS*T*DB*DC
      G(3,3)=G(3,3)+ZD
      G(3,4)=G(3,4)-ZD
      G(4,4)=G(4,4)+ZD
```

```
      G(2,1)=G(1,2)
      G(3,1)=G(1,3)
      G(4,1)=G(1,4)
      G(3,2)=G(2,3)
      G(4,2)=G(2,4)
      G(4,3)=G(3,4)
C
C     LOAD NODE SUBMATRIX INTO GLOBAL MATRIX
C
      CALL ADDRS (IRD,IRD)
C
C     PRINT NODE SUBMATRIX
C
      PRINT 330, IRD
 330  FORMAT(//,21X,'NODE',I3,'  SUBMATRIX',//)
C
      CALL PTSUB
C
 340  CONTINUE
C
C
C
C     INPUT EQUAL DISPLACEMENT COMMANDS
C
      PRINT 350
 350  FORMAT(//,5X,'ENTER NO. OF EQUAL DISPL. COMMANDS',/)
      READ(5,*) NEDC
      IF(NEDC.EQ.0)GO TO 410
      DO 400 I=1,NEDC
      PRINT 360, I
 360  FORMAT(//,5X,'ENTER DOFS FOR COMMAND',I3,/)
      READ(5,*) LD1,LD2
C
C     SUPERIMPOSE ROWS AND COLS OF COMMAND, PLACE IN LD1
C
      DO 370 J=1,NELG
      GMAT(LD1,J)=GMAT(LD1,J)+GMAT(LD2,J)
 370  CONTINUE
      DO 380 K=1,NELG
      GMAT(K,LD1)=GMAT(K,LD1)+GMAT(K,LD2)
 380  CONTINUE
      NHOLD(I)=LD2
C
C     PLACE ZEROS IN ELIMINATED DOF, LD2
C
      DO 390 II=1,NELG
      GMAT(II,LD2)=0.
      GMAT(LD2,II)=0.
 390  CONTINUE
 400  CONTINUE
 410  CONTINUE
C
C     INPUT DEGREES OF FREEDOM TO BE RETAINED,
C     OTHERS ARE ELIMINATED
C
      PRINT 420
 420  FORMAT(//,5X,'ENTER NO. OF DOFS TO BE RETAINED',/)
      READ(5,*) NDFR
      IF(NDFR.EQ.NELG)GO TO 480
      DO 470 J2=1,NDFR
      PRINT 430, J2
 430  FORMAT(//,5X,'ENTER DOF OF COMMAND',I3,/)
      READ(5,*) IDFR
C
C     REORGANIZE MATRIX SO RETAINED DOFS ARE FIRST ENTRIES
C
```

```
      DO 440 ICHK=1,NEDC
      IF(J2.EQ.NHOLD(ICHK))NHOLD(ICHK)=IDFR
 440  CONTINUE
      DO 450 KCEX=1,NELG
      CRET=GMAT(KCEX,J2)
      GMAT(KCEX,J2)=GMAT(KCEX,IDFR)
      GMAT(KCEX,IDFR)=CRET
 450  CONTINUE
      DO 460 KREX=1,NELG
      RRET=GMAT(J2,KREX)
      GMAT(J2,KREX)=GMAT(IDFR,KREX)
      GMAT(IDFR,KREX)=RRET
 460  CONTINUE
 470  CONTINUE
 480  CONTINUE
C
C     PLACE ZERO ROWS AND COLUMNS TO END OF MATRIX
C
      NCLEG=NELG-NEDC+1
      IF(NEDC.EQ.0)GO TO 530
      DO 520 J3=NCLEG,NELG
      JCNT=J3-NCLEG+1
      NLCEX=NHOLD(JCNT)
      DO 490 ICHK2=1,NEDC
      IF(J3.EQ.NHOLD(ICHK2))NHOLD(ICHK2)=NHOLD(JCNT)
 490  CONTINUE
      DO 500 J4=1,NELG
      CHLD=GMAT(J4,NLCEX)
      GMAT(J4,NLCEX)=GMAT(J4,J3)
      GMAT(J4,J3)=CHLD
 500  CONTINUE
      DO 510 J5=1,NELG
      RHLD=GMAT(NLCEX,J5)
      GMAT(NLCEX,J5)=GMAT(J3,J5)
      GMAT(J3,J5)=RHLD
 510  CONTINUE
 520  CONTINUE
 530  CONTINUE
C
C     PREPARE MATRIX FOR CONDENSATION
C
      NMAX=NELG-NEDC
      NAVE=0
      DO 540 I=1,NMAX
      NAVE=NAVE+I
 540  CONTINUE
      IC=1
      IR=1
      DO 550 J=1,NELG
      DO 550 I=1,NELG
      GMAT(I,J)=GMAT(IR,IC)
      IR=IR-1
      IF(IR.NE.0)GO TO 550
      IC=IC+1
      IF(IC.GT.NMAX)GO TO 560
      IR=IC
 550  CONTINUE
 560  CONTINUE
C
C     PRINT NO OF ENTRIES IN UPPER TRIANGULAR
C     UNCONDENSED STIFFNESS MATRIX
C
      PRINT 570, NAVE
 570  FORMAT(///,5X,'NO. OF ENTRIES IN UNCONDENSED A-VECTOR=',I5,//)
C
C     SET FLAG FOR DOF ELIMINATION AND CONDENSE MATRIX
C
```

```
      DO 580 I12=1,NMAX
      NCON(I12)=0
      IF(I12.GT.NOFR)NCON(I12)=1
  580 CONTINUE
C
      CALL SCON (NMAX)
C
C     PRINT UPPER TRIANGULAR CONDENSED MATRIX
C
      PRINT 590
  590 FORMAT(//,12X,'UPPER TRIANGULAR',/,12X,'CONDENSED MATRIX',//)
C
      CALL PTAVC (NDFR)
C
      END
```

```
C
C
C     ----------------------------------------------------------------
C        SUBROUTINE FOR STORING BASIC STIFFNESS TYPES
C     ----------------------------------------------------------------
      SUBROUTINE STFT (ISTFT,A,AI,AL,AS)
      IMPLICIT REAL*8(A)
      COMMON/STIFF/AQ(10),AIQ(10),ALQ(10),ASQ(10)
      A=AQ(ISTFT)
      AI=AIQ(ISTFT)
      AL=ALQ(ISTFT)
      AS=ASQ(ISTFT)
      RETURN
      END
```

```
C
C     ----------------------------------------------------------------
C        SUBROUTINE FOR ASSEMBLING BEAM AND COLUMN PROPERTIES
C        AND ADJUSTING C-C DIMENSIONS
C     ----------------------------------------------------------------
      SUBROUTINE PROP (JSFT,A,AI,AL,AS,DM1,DM2,ICCHK)
      IMPLICIT REAL*8(A-H,O-Z)
      COMMON/BCPRP/APRP(20),AIPRP(20),ALPRP(20),ASPRP(20)
      APRP(JSFT)=A
      AIPRP(JSFT)=AI
      ASPRP(JSFT)=AS
      IF(ICCHK.EQ.1)GO TO 10
      ALPRP(JSFT)=AL-(DM1+DM2)/2.
      GO TO 20
   10 ALPRP(JSFT)=(AL-DM1)/2.
   20 AL=ALPRP(JSFT)
      RETURN
      END
```

```
C                                                                       JAN04560
C     ------------------------------------------------------------------JAN04570
C        SUBROUTINE FOR RECALLING PROPERTIES OF BEAMS AND               JAN04580
C        COLUMNS FRAMING INTO NODE                                      JAN04590
C     ------------------------------------------------------------------JAN04600
      SUBROUTINE NASM (JSFT,A,AI,AL,AS)                                 JAN04610
      IMPLICIT REAL*8(A)                                                JAN04620
      COMMON/BCPRP/APRP(20),AIPRP(20),ALPRP(20),ASPRP(20)               JAN04630
      A=APRP(JSFT)                                                      JAN04640
      AI=AIPRP(JSFT)                                                    JAN04650
      AS=ASPRP(JSFT)                                                    JAN04660
      AL=ALPRP(JSFT)                                                    JAN04670
      RETURN                                                            JAN04680
      END                                                               JAN04690
```

```
C                                                                       JAN04700
C     ------------------------------------------------------------------JAN04710
C        SUBROUTINE TO CLEAR SUBMATRIX WORK SPACE                       JAN04720
C     ------------------------------------------------------------------JAN04730
      SUBROUTINE CLEAR                                                  JAN04740
      IMPLICIT REAL*8(G)                                                JAN04750
      COMMON/CLR/G(4,4)                                                 JAN04760
      DO 10 I=1,4                                                       JAN04770
      DO 10 J=1,4                                                       JAN04780
      G(I,J)=0.                                                         JAN04790
   10 CONTINUE                                                          JAN04800
      RETURN                                                            JAN04810
      END                                                               JAN04820
```

```
C                                                                       JAN04830
C     ------------------------------------------------------------------JAN04840
C        SUBROUTINE FOR LOADING SUBMATRIX INTO GLOBAL MATRIX            JAN04850
C     ------------------------------------------------------------------JAN04860
      SUBROUTINE ADDRS (IR,IC)                                          JAN04870
      IMPLICIT REAL*8(G)                                                JAN04880
      COMMON/CLR/G(4,4)                                                 JAN04890
      COMMON/AD/GMAT(32,32)                                             JAN04900
      IROW=4*(IR-1)+1                                                   JAN04910
      ICOL=4*(IC-1)+1                                                   JAN04920
      IRM=IROW+3                                                        JAN04930
      ICM=ICOL+3                                                        JAN04940
      DO 10 K1=IROW,IRM                                                 JAN04950
      DO 20 K2=ICOL,ICM                                                 JAN04960
      IRG=K1-IROW+1                                                     JAN04970
      ICG=K2-ICOL+1                                                     JAN04980
      GMAT(K1,K2)=G(IRG,ICG)                                            JAN04990
      GMAT(K2,K1)=GMAT(K1,K2)                                           JAN05000
   20 CONTINUE                                                          JAN05010
   10 CONTINUE                                                          JAN05020
      RETURN                                                            JAN05030
      END                                                               JAN05040
```

```
C                                                                       JAN05050
C     ------------------------------------------------------------------JAN05060
C        SUBROUTINE FOR PRINTING SUBMATRIX                              JAN05070
C     ------------------------------------------------------------------JAN05080
      SUBROUTINE PTSUB                                                  JAN05090
      IMPLICIT REAL*8 (G)                                               JAN05100
      COMMON/CLR/G(4,4)                                                 JAN05110
      DO 10 K3=1,4                                                      JAN05120
      PRINT 20, (G(K3,K4),K4=1,4)                                       JAN05130
   10 CONTINUE                                                          JAN05140
   20 FORMAT(/,4(5X,E10.3))                                             JAN05150
      RETURN                                                            JAN05160
      END                                                               JAN05170
```

```
C                                                                       JAN05180
C     ------------------------------------------------------------------JAN05190
C        SUBROUTINE FOR PRINTING CONDENSED STIFFNESS MATRIX             JAN05200
C     ------------------------------------------------------------------JAN05210
      SUBROUTINE PTAVC (NDFR)                                           JAN05220
      IMPLICIT REAL*8(A)                                                JAN05230
      COMMON/AO/AV(1024)                                                JAN05240
      JDEX=0                                                            JAN05250
      DO 10 I=1,NDFR                                                    JAN05260
      INDX=NDFR-I+1                                                     JAN05270
      DO 20 J=INDX,NDFR                                                 JAN05280
      JDEX=JDEX+1                                                       JAN05290
      PRINT 30, JDEX, AV(JDEX)                                          JAN05300
   20 CONTINUE                                                          JAN05310
   10 CONTINUE                                                          JAN05320
   30 FORMAT(10X,'A(',I2,')=',E14.7)                                    JAN05330
      PRINT 40                                                          JAN05340
   40 FORMAT(///)                                                       JAN05350
      RETURN                                                            JAN05360
      END                                                               JAN05370
```

```
C                                                                       JAN05380
C     ------------------------------------------------------------------JAN05390
C        SUBROUTINE TO DETERMINE BEAM ELEMENT SUBMATRIX                 JAN05400
C     ------------------------------------------------------------------JAN05410
      SUBROUTINE BEAM (E,GS,A,AI,AL,AS,DCL,DCR)                         JAN05420
      IMPLICIT REAL*8(A-H,O-Z)                                          JAN05430
      COMMON/CLR/G(4,4)                                                 JAN05440
      PHI=12.*E*AI/AS/GS/AL/AL                                          JAN05450
      PHI1=PHI+1.                                                       JAN05460
      G(1,1)=-1.*E*A/AL                                                 JAN05470
      G(2,2)=-12.*E*AI/PHI1/AL**3.                                      JAN05480
      G(2,3)=-6.*E*AI*DCR/PHI1/AL**3.                                   JAN05490
      G(3,2)=-1.*G(2,3)*DCL/DCR                                         JAN05500
      G(2,4)=-6.*E*AI/PHI1/AL/AL                                        JAN05510
      G(4,2)=-1.*G(2,4)                                                 JAN05520
      G(3,3)=3.*E*AI*DCL*DCR/PHI1/AL**3.                                JAN05530
      G(3,4)=3.*E*AI*DCL/PHI1/AL/AL                                     JAN05540
      G(4,3)=G(3,4)*DCR/DCL                                             JAN05550
      G(4,4)=(2.-PHI)*E*AI/PHI1/AL                                      JAN05560
      RETURN                                                            JAN05570
      END                                                               JAN05580
```

```
C
C     ------------------------------------------------------------------
C        SUBROUTINE TO DETERMINE COLUMN ELEMENT SUBMATRIX
C     ------------------------------------------------------------------
      SUBROUTINE COLM (E,GS,A,AI,AL,AS,DBT,DBB)
      IMPLICIT REAL*8(A-H,O-Z)
      COMMON/CLR/G(4,4)
      PHI=12.*E*AI/GS/AS/AL/AL
      PHI1=PHI+1
      G(1,1)=-12.*E*AI/PHI1/AL**3.
      G(2,2)=-1.*E*A/AL
      G(1,3)=-6.*E*AI/PHI1/AL/AL
      G(3,1)=-1.*G(1,3)
      G(1,4)=-6.*E*AI*DBB/PHI1/AL**3.
      G(4,1)=-1.*G(1,4)*DBT/DBB
      G(3,3)=(2.-PHI)*E*AI/PHI1/AL
      G(3,4)=3.*E*AI*DBB/PHI1/AL/AL
      G(4,3)=G(3,4)*DBT/DBB
      G(4,4)=3.*E*AI*DBT*DBB/PHI1/AL**3.
      RETURN
      END
C
C     ------------------------------------------------------------------
C        SUBROUTINE TO DETERMINE NODE SUBMATRIX COMPONENT
C        OF COLUMN ABOVE NODE
C     ------------------------------------------------------------------
      SUBROUTINE NCOLA (E,GS,A,AI,AL,AS,DC,DB)
      IMPLICIT REAL*8(A-H,O-Z)
      COMMON/CLR/G(4,4)
      PHI=12.*E*AI/GS/AS/AL/AL
      PHI1=PHI+1.
      G(1,1)=12.*E*AI/PHI1/AL**3.
      G(2,2)=E*A/AL
      G(1,3)=6.*E*AI/PHI1/AL/AL
      G(1,4)=6.*E*AI*DB/PHI1/AL**3.
      G(3,3)=(4.+PHI)*E*AI/PHI1/AL
      G(3,4)=3.*E*AI*DB/PHI1/AL/AL
      G(4,4)=3.*E*AI*DB*DB/PHI1/AL**3.
      RETURN
      END
C
C     ------------------------------------------------------------------
C        SUBROUTINE TO DETERMINE NODE SUBMATRIX COMPONENT
C        OF BEAM TO LEFT OF NODE
C     ------------------------------------------------------------------
      SUBROUTINE NBML (E,GS,A,AI,AL,AS,DC,DB)
      IMPLICIT REAL*8(A-H,O-Z)
      COMMON/CLR/G(4,4)
      PHI=12.*E*AI/AS/GS/AL/AL
      PHI1=PHI+1.
      G(1,1)=G(1,1)+E*A/AL
      G(2,2)=G(2,2)+12.*E*AI/PHI1/AL**3.
      G(2,3)=G(2,3)+6.*E*AI*DC/PHI1/AL**3.
      G(2,4)=G(2,4)+6.*E*AI/PHI1/AL/AL
      G(3,3)=G(3,3)+3.*E*AI*DC*DC/PHI1/AL**3.
      G(3,4)=G(3,4)+3.*E*AI*DC/PHI1/AL/AL
      G(4,4)=G(4,4)+(4.+PHI)*E*AI/PHI1/AL
      RETURN
      END
```

```
C
C     ------------------------------------------------------------------
C        SUBROUTINE TO DETERMINE NODE SUBMATRIX COMPONENT
C        OF COLUMN BELOW NODE
C     ------------------------------------------------------------------
      SUBROUTINE NCOLB (E,GS,A,AI,AL,AS,DC,DB)
      IMPLICIT REAL*8(A-H,O-Z)
      COMMON/CLR/G(4,4)
      PHI=12.*E*AI/AS/GS/AL/AL
      PHI1=PHI+1.
      G(1,1)=G(1,1)+12.*E*AI/PHI1/AL**3.
      G(2,2)=G(2,2)+E*A/AL
      G(1,3)=G(1,3)-6.*E*AI/PHI1/AL/AL
      G(1,4)=G(1,4)-6.*E*AI*DB/PHI1/AL**3.
      G(3,3)=G(3,3)+(4.+PHI)*E*AI/PHI1/AL
      G(3,4)=G(3,4)+3.*E*AI*DB/PHI1/AL/AL
      G(4,4)=G(4,4)+3.*E*AI*DB*DB/PHI1/AL**3.
      RETURN
      END
```

```
C
C     ------------------------------------------------------------------
C        SUBROUTINE TO DETERMINE NODE SUBMATRIX COMPONENT
C        OF SYMMETRY BEAM TO RIGHT OF NODE
C     ------------------------------------------------------------------
      SUBROUTINE BMCON (E,GS,A,AI,AL,AS,DC,DB)
      IMPLICIT REAL*8(A-H,O-Z)
      COMMON/CLR/G(4,4)
      PHI=12.*E*AI/AS/GS/AL/AL
      PHI1=PHI+1.
      PHI2=(1.-(2.-PHI)/(4.+PHI))
      PHI3=(1.-3./(4.+PHI))
      PHIS=(1.-((2.-PHI)/(4.+PHI))**2.)
      G(2,2)=G(2,2)+12.*E*AI*PHI3/PHI1/AL**3.
      G(2,3)=G(2,3)-6.*E*AI*DC*PHI3/PHI1/AL**3.
      G(2,4)=G(2,4)-6.*E*AI*PHI2/PHI1/AL/AL
      G(3,3)=G(3,3)+3.*E*AI*DC*DC*PHI3/PHI1/AL**3.
      G(3,4)=G(3,4)+3.*E*AI*DC*PHI2/PHI1/AL/AL
      G(4,4)=G(4,4)+(4.+PHI)*E*AI*PHIS/PHI1/AL
      RETURN
      END
```

```
C
C     ------------------------------------------------------------------
C        SUBROUTINE TO DETERMINE NODE SUBMATRIX COMPONENT
C        OF BEAM TO RIGHT OF NODE
C     ------------------------------------------------------------------
      SUBROUTINE NBMR (E,GS,A,AI,AL,AS,DC,DB)
      IMPLICIT REAL*8(A-H,O-Z)
      COMMON/CLR/G(4,4)
      PHI=12.*E*AI/AS/GS/AL/AL
      PHI1=PHI+1.
      G(1,1)=G(1,1)+E*A/AL
      G(2,2)=G(2,2)+12.*E*AI/PHI1/AL**3.
      G(2,3)=G(2,3)-6.*E*AI*DC/PHI1/AL**3.
      G(2,4)=G(2,4)-6.*E*AI/PHI1/AL/AL
      G(3,3)=G(3,3)+3.*E*AI*DC*DC/PHI1/AL**3.
      G(3,4)=G(3,4)+3.*E*AI*DC/PHI1/AL/AL
      G(4,4)=G(4,4)+(4.+PHI)*E*AI/PHI1/AL
      RETURN
      END
```

```
C
C     ------------------------------------------------------------------
C        SUBROUTINE FOR STATIC CONDENSATION OF STIFFNESS MATRIX
C     ------------------------------------------------------------------
      SUBROUTINE SCON (NMAX)
      IMPLICIT REAL*8(A-H,O-Z)
      COMMON/AD/AV(1024)
      COMMON/COND/NCON(50)
      DO 10 N=1,NMAX
      NC=NCON(N)*N
      IF(NC.EQ.0)GO TO 10
      IIA=NC*(NC-1)/2+1
      DO 20 I=1,NMAX
      KK=NCON(I)*I
      IF(KK.EQ.I.AND.KK.LE.NC)GO TO 20
      ID=I*(I-1)/2+1
      IK=IIA+NC-I
      IF(ID.GT.IIA)IK=ID+I-NC
      G1=AV(IK)/AV(IIA)
      ID=I
      DO 30 J=ID,NMAX
      IF(J.EQ.NC)GO TO 30
      JD=J*(J-1)/2+1
      JK=IIA+NC-J
      IF(JD.GT.IIA)JK=JD+J-NC
      JJ=JD+J-I
      AV(JJ)=AV(JJ)-G1*AV(JK)
   30 CONTINUE
   20 CONTINUE
   10 CONTINUE
      RETURN
      END
```

APPENDIX B - DECOMPOSITION OF N-LINEAR RELATIONSHIP TO N-1 BI-LINEAR SUPERPOSITIONS

As illustrated by Fig. B.1, a general softening load-deflection relationship of n segments can be expressed as the sum of (n-1) bi-linear relationships. At any level of deformation the force—and stiffness—of the (n-1) parallel springs add directly to create the desired n-linear result. The bi-linear relationships represent 2(n-1) unknowns related through only n equations, hence the system is underspecified by n-2. Energy requirements of each inelastic spring, however, provide the additional requirements that:

$$\begin{aligned} S_1^i &\geq S_2^i && 1 \leq i \leq n-1 \\ S_1^i &\geq 0 && 1 \leq i \leq n-1 \qquad \text{(B.1)} \\ S_2^i &\geq 0 && 1 \leq i \leq n-1 \end{aligned}$$

If the third of these requirements is taken as an equality for the last n-2 superpositions (i.e., $S_2^i = 0,\ 2 \leq i \leq n-1$), then all of the requirements will automatically be satisfied and the system will have a unique solution. This assumption implies that $S_n = S_2^1$ and:

$$\underset{\sim}{S}^* = \underline{Z}\,\underset{\sim}{S} + S_n\,\underset{\sim}{e} \qquad \text{(B.2)}$$

where: $\underset{\sim}{S}^* = (S_1 \;\; S_2 \;\; S_3 \;\; \ldots\ldots \;\; S_{n-2} \; S_{n-1})^T$

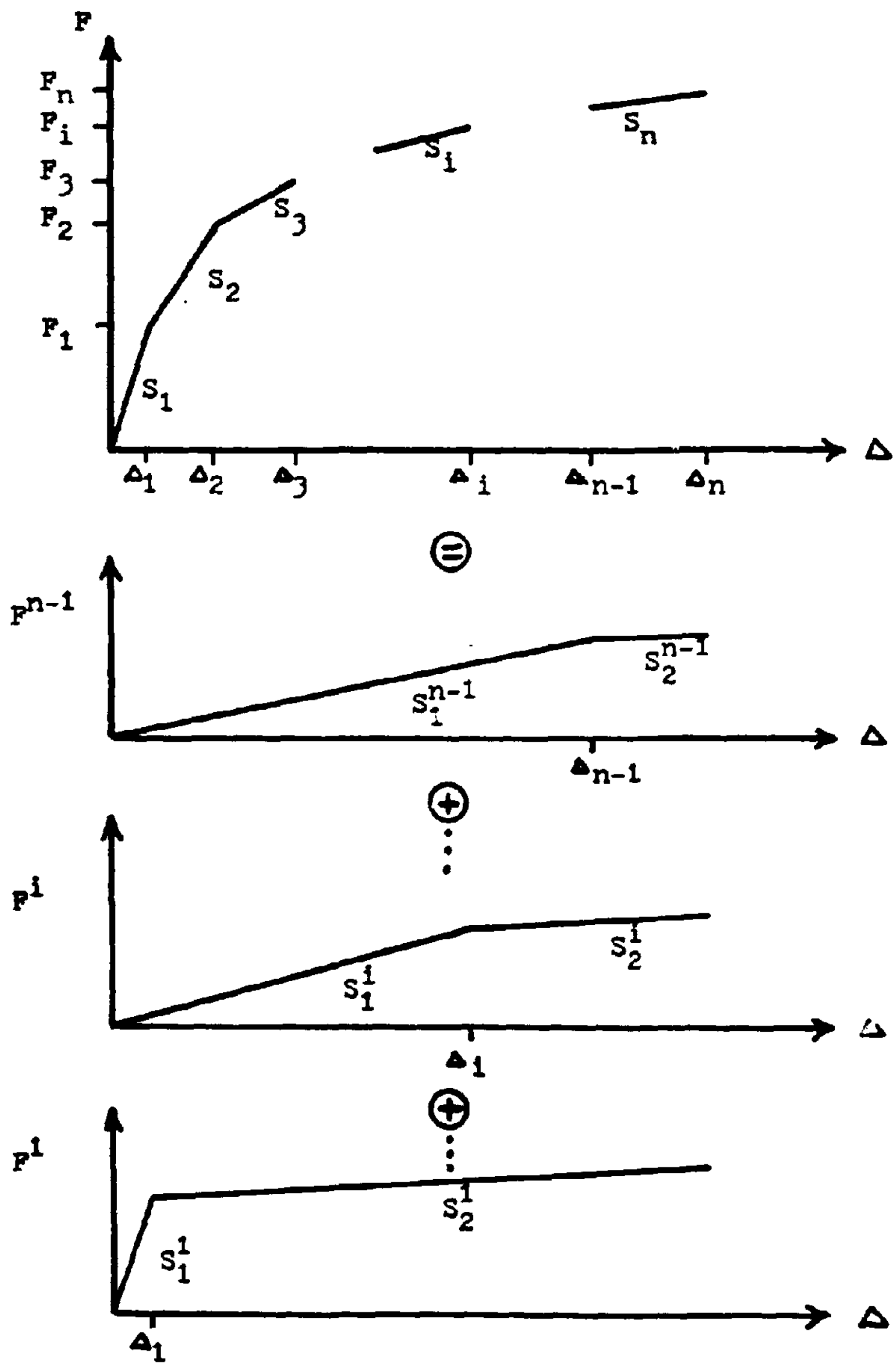

FIGURE B.1-(N-1) BI-LINEAR SUPERPOSTIONS
TO CREATE N-LINEAR RESULT

$$\underline{Z} = \begin{bmatrix} 1 & 1 & 1 & \cdots & 1 & 1 \\ 0 & 1 & 1 & \cdots & 1 & 1 \\ 0 & 0 & 1 & \cdots & 1 & 1 \\ \vdots & & & \ddots & \vdots & \\ 0 & 0 & 0 & \cdots & 1 & 1 \\ 0 & 0 & 0 & \cdots & 0 & 1 \end{bmatrix}$$

$$\underset{\sim}{S} = (S_1^1 \;\; S_1^2 \; S_1^3 \; \cdots \; S_1^{n-2} \; S_1^{n-1})^T$$

$$\underset{\sim}{e} = (0 \quad 1 \quad 1 \; \cdots \; 1 \quad 1)^T \quad .$$

Solving Eq. (B.2) for $\underset{\sim}{S}$, the desired bi-linear slopes are found:

$$\underset{\sim}{S} = \underline{Z}^{-1} \underset{\sim}{S}^{*} - \underline{Z}^{-1} \underset{\sim}{e} \; S_n \qquad \text{(B.3)}$$

where

$$\underline{Z}^{-1} = \begin{bmatrix} 1 & -1 & 0 & 0 & \cdots & 0 & 0 \\ 0 & 1 & -1 & 0 & \cdots & 0 & 0 \\ 0 & 0 & 1 & -1 & \cdots & 0 & 0 \\ \vdots & & & & \vdots & & \\ 0 & 0 & 0 & 0 & \cdots & 1 & -1 \\ 0 & 0 & 0 & 0 & \cdots & 0 & 1 \end{bmatrix}$$

Equation (B.3) can be expanded and combined with the initial assumption used to remove the underspecification to achieve the total solution:

$$S_2^i = 0 \qquad\qquad 2 \le i \le n-1$$

$$S_2^1 = S_n$$

$$S_1^1 = S_1 - S_2 + S_n \qquad\qquad (B.4)$$

$$S_1^i = S_i - S_{i+1} \qquad 2 \le i \le n-1$$

As a result of the softening nature of the load-deflection relationship, $S_i > S_{i+1}$, $1 \le i \le n-1$, hence the energy requirements of Eq. (B.1) will be satisfied.